Channel Estimation Architectures for Mobile Reception in Emerging DVB Standards

Lorena Martínez Jiménez

Supervisors:

Mikel Mendicute Errasti

and

Jon Altuna Iraola

MONDRAGON
UNIBERTSITATEA

A thesis submitted for the degree of

Doctor por Mondragon Unibertsitatea

Department of Electronics and Computer Science

Mondragon Goi Eskola Politeknikoa

Mondragon Unibertsitatea

May 2012

Para aita, ama e Iker

Y para Gaizka

Strive for perfection in everything you do
Take the best that exists and make it better
When it does not exist, design it.

Frederick Henry Royce

Agradecimientos

A lo largo de estos ya casi cinco años, he tenido la oportunidad de conocer un montón de gente que ha contribuido de diferentes formas al desarrolo de este trabajo. Por su ayuda y ánimo en los momentos más difíciles y por su compañía en los buenos momentos, me gustaría expresarles a todos ellos mi más profundo agradecimiento.

Me gustaría agradecer a mis directores de tesis, **Mikel Mendicute** y **Jon Altuna**, por el apoyo y la ayuda que me han prestado a lo largo de estos años. A **Mikel Mendicute**, por los buenos consejos que me ha dado, por su paciencia y por el tiempo que ha dedicado en todo el proceso de elaboración de esta tesis, con sus opininones, correcciones, comentarios, el seguimiento y supervisión continua de este trabajo y su buena disposición en cualquier momento, que me han ayudado a llevar esta tesis a buen término. A **Jon Altuna**, por haberme brindado la oportunidad de realizar la tesis en **Mondragon Goi Eskola Politeknikoa**, a la cual agradezco la financiación y los medios que me ha brindado durante todos estos años.

Quisiera agradecer muy especialmente a **Ulrich Reimers** por haberme acogido en el *Institut für Nachrichtentechnik* de la *Technische Universität Braunschweig*, hacerme partícipe de su grupo y darme la oportunidad de poder colaborar con ellos. También a todos los compañeros con los que coincidí allí, **Patrick Bauer**, **Teodor Buburuzan**, **Arnd Eden**, **Philipp Hasse**, **Martin Jacob**, **Marcos Liso**, **Moritz Schack**, **Peter Schlegel**, **Jan Sonnenberg**, **Philipp Steckel**, **Suhadi Suhadi**, **Nina Wahnschaffe**, y muy especialmente a **Jörg Robert**, **Marius Spika** y **David Scheler**, por acogerme tan cálidamente y hacerme partícipe de todos los eventos y excursiones de la universidad.

También me gustaría expresar mi gratitud a mis compañeros doctorandos, por amenizar esos ratos de cafés y por todos los buenos momentos de risas y bromas que hemos compartido juntos. A **Joxe Aixpurua**, **Maitane Barrenechea**, **Maite Beamurgia**, **Lorea Belategui**, **Enaitz Ezpeleta**, **Iñaki Garitano**, **Keldor Gerrikagoitia**, **Idoia Jiménez**, **Aritz Legarda**, **Igor Ordoñez**, **Alain Pérez**, **Iker Pérez**, **Alexander Salor** e **Iker Zuriarrain**; También a **Pello Ochandiano** e **Iker Sobrón** con los cuales he compartido tantísimas conversaciones y quebraderos de cabeza sobre la televisión digital.

Finalmente, me gustaría agradecer a mis **amigas**, por compartir tantos buenos momentos

inolvidables y por ayudarme a desconectar cuando lo necesitaba. A mi familia, a mis **padres**, mi **hermano** y mis **abuelos** por su apoyo, sus consejos, su comprensión y en definitiva por animarme siempre a seguir adelante y confiar plenamente en mi. Y a **Gaizka** por estar siempre ahí, por escucharme, aconsejarme y ayudarme siempre que lo necesitaba, por hacerme reir y por compartir tantos y tantos buenos momentos conmigo.

Acknowledgments

Throughout these nearly five years, I have had the opportunity to meet lots of people who have contributed in different ways to the development of this work. For their help and encouragement in difficult times and his company in good times, I would like to express all my gratitude.

I would like to thank my thesis supervisors, **Mikel Mendicute** and **Jon Altuna**, for the support and assistance they have given me over the years. To **Mikel Mendicute**, for the good advice, his patience and the time he invested in the whole process of this thesis, with his opinions, corrections, comments and the continuous monitoring and supervision of this work, and specially for his willingness at any now, which have helped me bring this thesis to fruition. To **Jon Altuna**, for having given me the opportunity to carry out the thesis in **Mondragon Goi Eskola Politeknikoa**, to which I thank the funding and resources given to me during all these years.

I would like to extend special thanks to **Ulrich Reimers** for receiving me in the *Institut für Nachrichtentechnik* of the *Technische Universität Braunschweig*, for letting me join his group and for giving me the chance of collaborating with them. Also to all the colleagues with whom I met there, **Patrick Bauer**, **Teodor Buburuzan**, **Arnd Eden**, **Philipp Hasse**, **Martin Jacob**, **Marcos Liso**, **Moritz Schack**, **Peter Schlegel**, **Jan Sonnenberg**, **Philipp Steckel**, **Suhadi Suhadi**, **Wahnschaffe Nina**, and particularly to **Jörg Robert**, **Marius Spika** and **David Scheler**, for welcoming me so warmly and make me a partaker of all events and tours of the university.

I would also like to express my gratitude to my fellow colleagues, for the enjoyable coffee breaks and all the great moments of laughter and jokes we shared together. To **Joxe Aixpurua**, **Maitane Barrenechea**, **Maite Beamurgia**, **Lorea Belategui**, **Enaitz Ezpeleta**, **Iñaki Garitano**, **Keldor Gerrikagoitia**, **Idoia Jiménez**, **Aritz Legarda**, **Igor Ordoñez**, **Alain Pérez**, **Iker Pérez**, **Alexander Salor** and **Iker Zuriarrain**; Also to **Pello Ochandiano** and **Iker Sobrón** with whom I shared so many conversations and headaches on digital television.

Finally, I would like to thank my **friends**, for sharing so many unforgettable good times

with me. To my **family**, my **parents**, my **brother** and **grandparents**, for their support, advice, understanding and ultimately for always encouraging me to go ahead and rely on me. And to **Gaizka**, for always being there for me, for listening to me, for his advise and help whenever I needed it, for making me laugh and for sharing so many good times with me.

Abstract

Throughout this work, channel estimation techniques have been analyzed and proposed for moderate and very high mobility DVB (digital video broadcasting) receivers, focusing on the DVB-T2 (Digital Video Broadcasting - Terrestrial 2) framework and the forthcoming DVB-NGH (Digital Video Broadcasting - Next Generation Handheld) standard. Mobility support is one of the key features of these DVB specifications, which try to deal with the challenge of enabling HDTV (high definition television) delivery at high vehicular speed.

In high-mobility scenarios, the channel response varies within an OFDM (orthogonal frequency-division multiplexing) block and the subcarriers are no longer orthogonal, which leads to the so-called ICI (inter-carrier interference), making the system performance drop severely. Therefore, in order to successfully decode the transmitted data, ICI-aware detectors are necessary and accurate CSI (channel state information), including the ICI terms, is required at the receiver.

With the aim of reducing the number of parameters required for such channel estimation while ensuring accurate CSI, BEM (basis expansion model) techniques have been analyzed and proposed for the high-mobility DVB-T2 scenario. A suitable clustered pilot structure has been proposed and its performance has been compared to the pilot patterns proposed in the standard. Different reception schemes that effectively cancel ICI in combination with BEM channel estimation have been proposed, including a Turbo scheme that includes a BP (belief propagation) based ICI canceler, a soft-input decision-directed BEM channel estimator and the LDPC (low-density parity check) decoder. Numerical results have been presented for the most common channel models, showing that the proposed receiver schemes allow good reception, even in receivers with extremely high mobility (up to 0.5 of normalized Doppler frequency).

Resumen

Esta tesis doctoral analiza y propone diferentes técnicas de estimación de canal para receptores DVB (*Digital Video Broadcasting*) con movilidad moderada y alta, centrándose en el estándar de segunda generación DVB-T2 (*Digital Video Broadcasting - Terrestrial 2*) y en el próximó estándar DVB-NGH (*Digital Video Broadcasting - Next Generation Handheld*). La movilidad es una de las principales claves de estas especificaciones, que tratan de lidiar con el reto de permitir la recepción de señal HDTV (*high definition television*) en receptores móviles.

En escenarios de alta movilidad, la respuesta del canal varía dentro de un símbolo OFDM (*orthogonal frequency-division multiplexing*) y las subportadoras ya no son ortogonales, lo que genera la llamada ICI (*inter-carrier interference*), deteriorando el rendimiento de los receptores severamente. Por lo tanto, con el fin de decodificar correctamente los datos transmitidos, detectores capaces de suprimir la ICI y una precisa CSI (*channel state information*), incluyendo los términos de ICI, son necesarios en el receptor.

Con el objetivo de reducir el número de parámetros necesarios para dicha estimación de canal, y al mismo tiempo garantizar una CSI precisa, la técnica de estimación BEM (*basis expansion model*) ha sido analizada y propuesta para identificar el canal con ICI en receptores DVB-T2 de alta movilidad. Además se ha propuesto una estructura de pilotos basada en clústers, comparando su rendimiento con los patrones de pilotos establecidos en el estándar. Se han propuesto diferentes sistemas de recepción que cancelan ICI en combinación con la estimación BEM, incluyendo un esquema Turbo que incluye un detector BP (*belief propagation*), un estimador BEM *soft* y un decodificador LDPC (*low-density parity check*). Se han presentado resultados numéricos para los modelos de canal más comunes, demostrando que los sistemas de recepción propuestos permiten la decodificación correcta de la señal incluso en receptores con movilidad muy alta (hasta 0,5 de frecuencia de Doppler normalizada).

Laburpena

Doktoretza tesi honetan, hainbat kanal estimazio teknika ezberdin aztertu eta proposatu dira mugikortasun ertain eta handiko DVB (*Digital Video Broadcasting*) hartzaileentzat, bigarren belaunaldiko Lurreko Telebista Digitalean DVB-T2 (*Digital Video Broadcasting - Terrestrial 2*) eta hurrengo DVB-NGH (*Digital Video Broadcasting - Next Generation Handheld*) estandarretan oinarrututa. Mugikortasuna bigarren belaunaldiko telebista estandarrean funtsezko ezaugarri bat da, HDTV (*high definition television*) zerbitzuak abiadura handiko hartzaileetan ahalbidetzeko erronkari aurre egiteko nahian.

Baldintza horietan, kanala OFDM (*ortogonalak maiztasun-zatiketa multiplexing*) sinbolo baten barruan aldatzen da, eta subportadorak jada ez dira ortogonalak, ICI-a (*inter-carrier interference*) sortuz, eta sistemaren errendimendua hondatuz. Beraz, transmititutako datuak behar bezala deskodeatzeko, ICI-a ekiditeko gai diren detektagailuak eta CSI-a (*channel state information*) zehatza, ICI osagaiak barne, ezinbestekoak egiten dira hartzailean.

Kanalaren estimazio horretarako beharrezkoak diren parametro kopurua murrizteko eta aldi berean CSI zehatza bermatzeko, BEM (*basis expansion model*) teknika aztertu eta proposatu da ICI kanala identifikatzeko mugikortasun handiko DVB-T2 eszenatokitan. Horrez gain, pilotu egitura egokia proposatu da, estandarrean proposatutako pilotu ereduekin alderatuz BEM estimazioan oinarritua. ICI-a baliogabetzen duten hartzaile sistema ezberdin proposatu dira, Turbo sistema barne, non BP (*belief propagation*) detektagailua, *soft* BEM estimazioa eta LDPC (*low-density parity check*) deskodetzailea uztartzen diren. Ohiko kanal ereduak erabilita, simulazio emaitzak aurkeztu dira, proposatutako hartzaile sistemak mugikortasun handiko kasuetan harrera ona dutela erakutsiz, 0.5 Doppler maiztasun normalizaturaino.

Declaration of Originality

I hereby declare that the research recorded in this thesis and the thesis itself were developed entirely by myself at the Signal Theory and Communications Area, Department of Electronics and Computer Science, at the University of Mondragon.

The software used to perform the simulations was developed entirely by myself, with the following exceptions:

- The implementation of the basic transmission-reception chain of the DVB-T2 simulator has been jointly designed by Iker Sobrón, Pello Ochandiano and myself.
- The Matlab implementation of the BP ICI canceler has been developed by Pello Ochandiano.

Lorena Martínez Jiménez
Department of Electronics and Computer Science
Mondragon Goi Eskola Politeknikoa
Mondragon Unibertsitatea
May, 2012

Contents

List of Figures

List of Tables

Acronyms

CFR	channel frequency response
APP	*a posteriori* probability
AR	autoregressive
ARMA	autoregressive-moving-average
AWGN	additive white Gaussian noise
BCH	Bose-Chaudhuri-Hocquenghem
BEM	basis expansion model
BER	bit error rate
BICM	bit interleaved coded modulation
BLE	block linear equalizer
BP	belief propagation
CD3	coded decision directed demodulation
CE-BEM	complex exponential BEM
CIR	channel impulse response
CP	cyclic prefix
CR	code rate
CSI	channel state information
DD	decision-directed

DDSF	delay-Doppler spread function
DFT	discrete Fourier transform
DTV	digital television
DVB	Digital Video Broadcasting
DVB-C	Digital Video Broadcasting - Cable
DVB-H	Digital Video Broadcasting - Handheld
DVB-NGH	Digital Video Broadcasting - Next Generation Handheld
DVB-S	Digital Video Broadcasting - Satellite
DVB-S2	Digital Video Broadcasting - Satellite 2
DVB-T2	Digital Video Broadcasting - Terrestrial 2
DVB-T	Digital Video Broadcasting - Terrestrial
FDKD	frequency-domain Kronecker delta
FDM	frequency-division multiplexing
FEC	forward error correction
FFT	fast Fourier transform
FG	factor graph
GCE-BEM	General Complex Exponential BEM
GI	guard interval
GS	generic streams
HDTV	high definition television
ICI	inter-carrier interference
IDFT	inverse discrete Fourier transform
IDSF	input delay spread function
IFFT	inverse fast Fourier transform
ISI	inter-symbol interference

LDPC	low-density parity check
LLR	log-likelihood ratio
LOS	line-of-sight
LS	least squares
MAP	maximum a-posteriori
MHP	multimedia home platform
MIMO	multiple-input multiple-output
MISO	multiple-input single-output
ML	maximum likelihood
MMSE	minimum mean squared error
MRC	maximum ratio combining
MSE	mean squared error
NLOS	non line-of-sight
NMSE	normalized mean square error
ODSF	output Doppler spread function
OFDM	orthogonal frequency-division multiplexing
PAPR	peak-to-average power ratio
P-BEM	Polynomial BEM
PDF	probability density function
PIC	parallel interference cancellation
PLP	physical layer pipe
PSAM	pilot-symbol aided modulation
QAM	quadrature amplitude modulation
QEF	quasi-error free
RA6	Rural Area channel - 6 paths

RF	radio-frequency
RS	Reed-Solomon
SD	sphere decoder
SFN	single frequency networks
SIC	serial interference cancellation
SIMO	single-input multiple-output
SISO	single-input single-output
SLE	serial linear equalizer
SNR	signal to noise ratio
SOS	sum of sinusoids
SPA	sum-product algorithm
STBC	space-time block codes
STC	space-time coding
STTC	space-time Trellis codes
TB	training based
TPS	transmission parameter signaling
TS	transport stream
TVTF	time-varying transfer function
TU6	Typical Urban channel - 6 paths
ZF	zero forcing

List of Symbols

$\mathbf{B}$	A matrix that collects the BEM basis functions
b_c	The first position of each cluster
B_c	Smoothing parameter used to control the amount of interference taken into account for channel estimation
B_{wc}	Coherence bandwidth
B_{ws}	Bandwidth of the signal
C	Number of pilot clusters in the model
$\gamma_{m,k}$	Equalized QAM symbols in OFDM symbol m at subcarrier position k
$\mathbf{\Delta}_q$	Diagonal matrix whose diagonal is the frequency response of the BEM coefficients for the q-th basis function
$\mathbf{D}_q$	Circulant matrix that contains the frequency response of the q-th basis function as it first column
$\mathbf{D}_{q,c}^{(d)}$	Submatrix of $\mathbf{D}_q$ that contains information concerning the relationship between the position of the data carriers and the received samples for cluster c
$\mathbf{D}_{q,c}^{(p)}$	Submatrix of $\mathbf{D}_q$ that contains information concerning the relationship between the position of the pilot carriers and the received samples for cluster c
$\mathbf{F}$	discrete Fourier transform (DFT) matrix
f	Frequency
F_d	Absolute Doppler frequency
f_d	Normalized Doppler frequency

$\mathbf{F}_L$	Submarix of $\mathbf{F}$ that contains the first L columns of the matrix $\sqrt{N}\mathbf{F}$
$\mathbf{H}^{\dagger}$	Pseudoinverse of matrix H_{MIMO}
$\mathbf{H}$	Frequency-domain channel matrix
$\overline{\mathbf{h}}_l$	A time-domain vector that contains the channel coefficients for the l-th channel tap
$\mathbf{H}_m$	Frequency-domain channel matrix for each OFDM symbol m
$\mathbf{h}_m$	Main diagonal of the matrix $\mathbf{H}_m$
$\mathbf{H_{MIMO}}$	Complex MIMO channel matrix
$h_{m,k}$	Channel frequency response in OFDM symbol m at subcarrier position k
$\hat{h}_{m,k}$	Estimated channel frequency response in OFDM symbol m at subcarrier position k
$\mathbf{h}^p$	Estimated channel frequency response vector at the pilot positions
$\overline{\overline{\mathbf{H}}}$	Time-domain channel matrix
$\mathbf{h}_u$	A vector that contains the BEM coefficients for all the channel taps
$\mathbf{h}_{u,l}$	A vector that contains the BEM coefficients for the l-th channel tap
$\boldsymbol{I}_N$	$N \times N$ identity matrix
L	Number of taps of a multi-path channel
L_p	Length of each pilot cluster
$\mathbf{m}$	A vector that contains the soft data estimates
M_{ant}	Number of transmitting antennas
N	Number of subcarriers
N_{ant}	Number of receiving antennas
$P(a)$	Probability of event a
$Q+1$	Number of basis functions
$\mathbf{r}$	Received signal vector in time-domain
$\mathbf{R}_{\hat{\overline{\mathbf{h}}}_l}$	Channel autocorrelation function

$\mathbf{R}_{\mathbf{h}_u}$	Covariance matrix of BEM coefficients
$\mathbf{R}_w^{(p)}$	Covariance matrix of the noise corresponding to the pilot positions
$\mathbf{s}$	Transmitted signal vector in time-domain
T_c	Coherence time
T_s	Sampling period
$\mathbf{W}$	Additive white Gaussian noise matrix in MIMO receiver
$\mathbf{w}$	Frequency-domain additive white Gaussian noise vector
$\mathbf{w}_c$	Frequency-domain additive white Gaussian noise vector for the c-th cluster
$\mathbf{W}_{\mathbf{coeff}}$	Wiener filter coefficients
$w_{m,k}$	Noise term in frequency-domain at OFDM symbol m and subcarrier position k
σ^2	Noise variance
$\mathbf{X}$	Transmitted MIMO signal matrix
$\mathbf{x}$	Transmitted signal vector in frequency-domain
$\mathbf{x}_c^{(p)}$	Transmitted signal vector for the pilot positions at c-th pilot cluster
x_{min}	Threshold value for the improved decision-directed algorithm
$x_{m,k}$	Transmitted signal in frequency-domain at OFDM symbol m and subcarrier position k
$\mathbf{x}^{(p)}$	Transmitted signal vector for the pilot positions
$\mathbf{Y}$	Received MIMO signal matrix
$\mathbf{y}$	Received signal vector in frequency-domain
$y_{m,k}$	Received signal in frequency-domain in OFDM symbol m at subcarrier position k
$\mathbf{y}^{(p)}$	Received signal vector for the pilot positions
$\mathbf{z}$	Time-domain additive white Gaussian noise vector

Capítulo 1

Introducción

La posiblilidad de disponer de información en cualquier momento y lugar, ha transformado los hábitos de consumo y ha dado lugar a nuevas posibilidades de comunicación. En cuanto a la transmisión de señal de televisión, la evolución de la electrónica y el procesamiento digital de la señal ha dado lugar a la demanda de servicios de mayor capacidad y a nuevos escenarios de alta definición, tanto en equipos portátiles como móviles.

En este sentido, uno de los sistemas inalámbricos más populares para la difusión de contenidos sigue siendo la televisión terrestre, la cual es ya exclusivamente digital en España debido al apagón analógico de abril de 2010, siendo DVB-T (*Digital Video Broadcasting - Terrestrial*) el estándar adoptado. La television digital aporta numerosas ventajas frente a la analógica, mejorando notablemente la calidad en la recepción y siendo más inmune a interferencias. Además, se pueden transmitir un mayor número de programas en el mismo canal, hasta 4 de definición sencilla SDTV (*standard-definition television*) por cada canal analógico, y es posible disponer de servicios adicionales tales como subtítulos, información meteorológica, emisoras de radio o servicios interactivos.

Con el objetivo de proporcionar una mayor capacidad, en 2009 surge DVB-T2 (*Digital Video Broadcasting - Terrestrial 2*), extensión natural de DVB-T, el cual fue inicialmente diseñado con el fin de proporcionar televisión de alta definición HDTV (*high definition television*) para dispositivos fijos y portátiles. Para hacer frente a estos nuevos servicios, DVB-T2 incorpora una serie de herramientas que permiten un aumento de la capacidad y una mejora sustancial de la robustez. En concreto, la corrección de errores mediante códigos LDPC (*low-density parity check*), la incorporación de nuevos patrones de pilotos, nuevos intervalos de guarda, mayores longitudes de FFT (*fast Fourier transform*), mayores órdenes de modulación y la introducción de múltiples tuberías de capa física o PLPs (*physical layer pipe*), hacen posible que el estándar se adapte a los requisitos de diversos modos de transmisión, dando como resultado un sistema mucho más flexible. Sin embargo, la movilidad en el receptor se ha convertido en una cuestión clave y por lo tanto de cara a futuros estándares, tales como DVB-NGH (*Digital Video Broadcasting - Next Generation Handheld*), el reto es permitir la recepción en sistemas portátiles y especialmente móviles.

1.1 Motivación y Objetivos

El principal problema derivado de los requerimientos de movilidad de DVB-T2 y DVB-NGH es la interferencia interportadora o ICI (*inter-carrier interference*), la cual destruye la ortogonalidad entre las subportadoras de datos y degrada el rendimiento del sistema. Actualmente en Reino Unido se está utilizando la modalidad de 32K para maximizar la tasa de datos para HDTV en receptores estacionarios. Aunque la configuración elegida sea más robusta frente a la interferencia intersimbólica o ISI (*inter-symbol interference*) en redes de frecuencia única SFN (*single frequency network*) y en última instancia ofrezca una mayor cobertura, también supone desventajas. En concreto, implica una mayor vulnerabilidad frente a la ICI debido al menor espaciado entre las subportadoras, lo que significa que los receptores móviles no pueden recibir la señal de forma tan fiable.

Sin embargo, DVB-T2 permite proporcionar servicios con diferente protección mediante múltiples PLPs, que permiten que los servicios tengan diferente modulación, tasa de codificación o entrelazado temporal. Así, recientemente se ha creado un nuevo pérfil, DVB-T2 Lite, que permite emitir con niveles de protección distintos y mediante los FEFs (*future extension frame*), permite combinar DVB-T2 con futuras tecnologías en un mismo múltiplex mediante una multiplexación por división en el tiempo. Además, de esta forma es posible la convergencia entre redes fijas y móviles sin necesidad de desplegar una red específica para los servicios móviles.

Por todo ello, la movilidad en el receptor se ha convertido en una cuestión clave. Dicha movilidad provoca ICI, y esto afecta negativamente al sistema. Por lo tanto, para decodificar correctamente los datos transmitidos, es necesaria una adecuada estimación de la ICI y del propio canal, para contrarestar la distorsión introducida. Ésta estimación es más complicada en canales altamente variantes en el tiempo, lo que hace necesario diseñar algoritmos eficientes y de baja complejidad. En consecuencia, esta tesis se centrará en la estimación del canal, incluyendo el término de ICI y en el diseño de receptores que permitan un buen rendimiento del sistema a altas velocidades.

Por lo tanto, los objetivos principales de esta tesis son:

- Análisis comparativo de los estándares DVB-T y DVB-T2 con canal perfectamente conocido en diferentes escenarios de movilidad.

- Estudio del efecto de los diferentes modos de DVB-T2 en escenarios móviles, analizando especialmente la robustez ofrecida por los nuevos entrelazadores y los nuevos patrones pilotos.

- Análisis y evaluación del rendimiento de técnicas de estimación de canal en diferentes escenarios, especialmente en canales de alta movilidad.

- Analizar las diferentes estructuras de patrones piloto de DVB-T2 y comparar los rendimientos conseguidos para diferentes estimadores de canal.

- Proponer arquitecturas de recepción, compuestos por estimadores de canal y cancelladores de ICI, para DVB-T y DVB-T2 en escenarios de movilidad.

- Proponer receptores capaces de funcionar en escenarios severos de movilidad, ej. hasta $f_d = 0.5$ de frecuencia de Doppler normalizada.

1.2 Contribuciones de la Tesis

En esta sección se describen las contribuciones principales del trabajo de investigación desarrollado. Asimismo, se indican las publicaciones asociadas a las diferentes aportaciones:

- Análisis del rendimiento de diferentes esquemas de estimación e interpolación de canal sobre la cadena de transmisión-recepción de DVB-T2 en escenarios de recepción fija y móvil. Además se ha evaluado el efecto de la estimación de canal frente a la profundidad del entrelazado temporal comparando diferentes longitudes de bloque. Este trabajo ha sido publicado en [Martínez10b].

- Análisis del comportamiento de diferentes técnicas de estimación e interpolación de canal para transmisiones MISO (*multiple-input single-output*), tanto para canales fijos como móviles. Este trabajo ha sido publicado en [Martínez10b, Mendicute10].

- Propuesta de un algoritmo optimizado de estimación de canal guiada por decisiones para DVB-T2, basado en el algoritmo CD3 (*coded decision directed demodulation*) [Mignone96]. Dicho algoritmo mejora el original propuesto para DVB-T, empleando el esquema de pilotos PP8 de DVB-T2. El algoritmo propuesto supera notablemente a la estimación de canal basada exclusivamente en pilotos, mientras que introduce pérdidas aceptables en canales poco variantes en el tiempo. Este trabajo ha sido publicado en [Martínez10a].

- Análisis de diferentes agrupaciones de pilotos en escenarios de alta movilidad para DVB-T2, comparando resultados con los patrones de pilotos propuestos en los estándares de televisión digital terrestre.

- Se ha analizado el rendimiento de la capa física de DVB-T2 en condiciones de alta movilidad y para bloques OFDM (*orthogonal frequency-division multiplexing*) largos, conluyendo que no se puede obtener una recepción libre de errores a frecuencias de Doppler elevadas, es decir, mayores que $f_d = 0.3$ de frecuencia de Doppler normalizada.

- Propuesta de un receptor que combina la estimación de canal BEM (*basis expansion model*) con la cancelación MAP (*maximum a-posteriori*) de ICI, proporcionando buenos resultados y eliminando el suelo de error a frecuencias medias de Doppler. Sin embargo, se demuestra que, a medida que la frecuencia de Doppler aumenta, son necesarios métodos más adecuados para mejorar la estimación de canal y eliminar la ICI residual. Este trabajo ha sido publicado en [Martínez11].

- Se ha propuesto un novedoso esquema que combina un estimador de canal BEM con un detector BP (*belief propagation*). El citado modelo sustituye el ecualizador MAP de ICI por un detector BP y mantiene el entrelazador de tiempo [Ochandiano12].

- Se ha propuesto una arquitectura de receptor iterativo, que consta de un estimador BEM y un detector BP. El esquema propuesto elimina el entrelazador de tiempo e incorpora un receptor turbo con el objetivo de mantener una complejidad similar. Este esquema cancela la ICI con muy buenos resultados en alta movilidad y longitudes de bloque FFT elevados. El buen funcionamiento del algoritmo se ha probado a través de simulaciones que muestran una mejora del BER (*bit error rate*) en canales como TU6 (*Typical Urban channel - 6 paths*) y RA6 (*Rural Area channel - 6 paths*). Se han mostrado resultados para un sistema BICM-OFDM (*bit interleaved coded modulation-OFDM*) genérico.

- Se ha analizado el receptor trubo en el marco de DVB-T2. Se ha combinado un estimador CE-BEM (*complex exponential BEM*), el detector BP y el decodificador LDPC de una forma iterativa para obtener buenos resultados en alta movildiad. Además se ha propuesto una estructura de pilotos adecuada para identificar el canal afectado por ICI en DVB-T2, obteniendo buenos resultados en canales TU6 y RA6 a frecuencias Doppler normalizadas de hasta $f_d = 0.5$. El receptor propuesto se puede aplicar para mejorar el rendimiento de los estándares móviles terrestres, así como al próximo estándar DVB-NGH, en entornos exigentes de alta movilidad [Martínez12, Ochandiano12].

1.3 Estructura de la Tesis

La memoria de la tesis consta de 6 capítulos. En el primero de ellos se introduce la temática de la tesis y se presenta la motivación que ha llevado a la realización de este trabajo. Además, se exponen los principales objetivos de este trabajo de investigación y se resumen brevemente las contribuciones del mismo.

El capítulo 2 realiza una descripción general de los estándares de televisión digital terrestre de primera y segunda generación, DVB-T y DVB-T2, haciendo hincapié en las mejoras más significativas introducidas por este último en comparación con su predecesor. Además

analiza la idoneidad de DVB-T2 en sistemas de movilidad. Por otro lado, se analizan los modelos de sistema y de canal escogidos realizando un breve repaso de los sistemas variantes en el tiempo. A su vez se describe brevemente la transmisión MISO en DVB-T2.

El capítulo 3 examina las principales técnicas de estimación de canal existentes para canales OFDM inalámbricos, poniendo especial énfasis en la estimación basada en portadoras piloto. Se han analizado diferentes técnicas de estimación de canal, presentando resultados en diferentes escenarios y con diferentes profundidades de entrelazado. En cuanto a las técnicas semi-ciegas, se ha propuesto un método de estimación de canal dirigida por decisiones o DD (*decision directed*) para DVB-T2, bajo el supuesto de un canal con desvanecimiento lento. Dicho algoritmo mejora el rendimiento del algoritmo CD3, obteniendo mejores resultados para canales fijos.

El capítulo 4 propone la utilización de la estimación BEM en DVB-T2 y propone dos esquemas de recepción que combinan la estimación del canal y la cancelación de ICI. El primero es un sistema que combina la estimación BEM y la detección MAP, eliminando eficazmente el suelo de error que surge en sistemas de movilidad con frecuencias de Doppler del orden de $f_d = 0.045$, en canales TU6. El segundo esquema propuesto consiste en un estimador de canal BEM y un detector BP, eliminando completamente el suelo de error incluso para frecuencias normalizadas de Doppler de $f_d = 0.5$. El comportamiento de los algoritmos propuestos se ha probado para diferentes frecuencias de Doppler y diferentes modelos de canal.

El capítulo 5 evalúa el rendimiento de la capa física de DVB-T2 en alta movilidad, concluyendo que no es capaz de proporcionar una recepción libre de errores en altas frecuencias Doppler, especialmente cuando se utilizan bloques OFDM largos. Con el fin de resolver este problema, se ha analizado la utilización de la arquitectura más eficiente propuesta en el capítulo 4, es decir, BEM más BP. Haciendo uso de la selectividad frecuencial y temporal de los canales doblemente selectivos, se han propuesto dos esquemas de recepción diferentes. El primero (PS1), emplea el detector BP y mantiene el entrelazador de tiempo, mientras que el segundo (PS2), elimina el entrelazador e incorpora el principio turbo, de tal manera que la complejidad total se mantiene. Finalmente, se ha analizado el rendimiento sobre canales TU6 y RA6 para diferentes frecuencias normalizadas de Doppler.

Chapter 2
Background and system model

2.1 Introduction

In recent years there has been a noteworthy growth in the demand of wireless communications. Smartphones, laptops and other communications devices have become essential in our daily lives.

Considering television broadcasting, there have not been many revolutionary advances until the end of the late 1990s. However, with the age of digitalization, and after the analog switchover in Europe, it was necessary to develop new terrestrial digital television standards, leading to the Digital Video Broadcasting - Terrestrial (DVB-T) specification. Currently, with the deployment almost finished in most European countries, a second generation standard Digital Video Broadcasting - Terrestrial 2 (DVB-T2) has been developed due to the need for new services that require greater capacity, such as high definition television (HDTV), and improved coverage.

This chapter provides a theoretical background of DVB-T and DVB-T2, as well as a general comparison between them. In addition, special emphasis is done on the improvements introduced by the new standard, since it is the specification that has been taken as a reference for the implementation of the case studies and simulation results presented in this thesis. Propagation channel characteristics and channel models are then analyzed, specially focusing on mobile environments. Since multiple-input single-output (MISO) transmission is one of the novelties of DVB-T2, it will be also considered in Chapter 3 for the channel estimation review, and basic concepts will also be explained.

2.2 First generation digital terrestrial television: DVB-T

Digital Video Broadcasting (DVB) is the agency responsible for creating and submitting standardization procedures for digital television, with more than 270 members all over the world including broadcasters, network operators, software developers and regulatory bod-

ies. The following digital video broadcasting techniques have been defined: Digital Video Broadcasting - Cable (DVB-C), adopted in 1994 [ETSI94b], Digital Video Broadcasting - Satellite (DVB-S), in 1995 [ETSI94a], and DVB-T [ETSI97], in 1997. DVB has also developed an adaptation of the DVB-T standard for handheld (portable) devices, named Digital Video Broadcasting - Handheld (DVB-H) [ETSI04], which reduced battery consumption by 90%. Subsequently, enhanced versions of these systems, such as DVB-C2 [ETSI10], DVB-S2 [ETSI05], DVB-T2 [ETSI09] or DVB-SH [ETSI07], have been developed.

Both terrestrial DVB specifications have adopted orthogonal frequency-division multiplexing (OFDM), which is recognized as one of the most efficient modulation schemes and has been widely developed in wireless communications. With the joint use of OFDM and channel coding, the main problems of analog television, such as poor use of the spectrum and noise effects, are solved. For example, in DVB-T, it is possible to broadcast multiple programs (4 in Spain) simultaneously in the same bandwidth used by a traditional analog channel (8 MHz). Moreover, digital television enjoys a better picture and sound quality, access to new digital services, such as digital radio, and interactive applications accessible through the multimedia home platform (MHP) technology, namely weather forecast, contests or surveys.

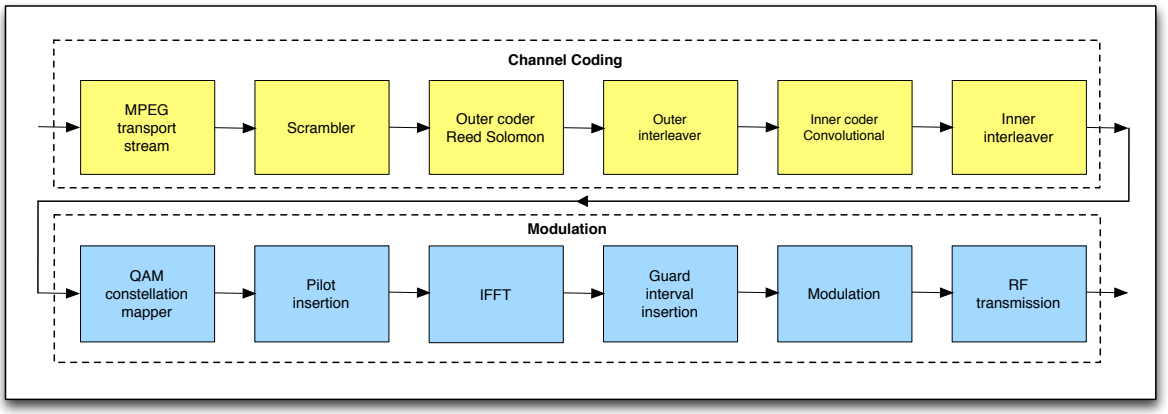

Figure 2.1: Block diagram of a DVB-T transmitter.

Fig. 2.1 shows the DVB-T transmission scheme, where it can be seen that the data bit stream is scrambled and then processed by an outer Reed-Solomon (RS) coder, an interleaver and an inner convolutional coder. The RS code removes the error floor at high signal to noise ratio (SNR) values and the convolutional code reduces the bit error rate (BER) at the receiver by including redundant information. The coded information is again interleaved and thereafter, the input bits from channel coding stage are mapped onto a quadrature amplitude modulation (QAM) constellation and modulated using OFDM, which will be briefly explained in the next section.

While the deployment of DVB-T is still ongoing in some countries, the industry and the scientific community have already published its second generation specification. DVB-T2,

which was published in 2009, will be explained in the following section.

2.3 Second generation digital terrestrial television: DVB-T2

The development of DVB-T2 has been given by the need for new services that require greater capacity, such as HDTV. A single HDTV channel or service in DVB-T would occupy the bandwidth of a multiplex of 8 MHz. Nevertheless, DVB-T2 improves this and enables simultaneous transmission of multiple high-definition services in a terrestrial multiplex, thus improving its predecessor. The first regular transmissions already started in the UK at the end of 2009, showing a significant performance increase compared to DVB-T. DVB-T2 is compatible with its predecessor in some physical-layer aspects, since the signal has to be received with existing DVB-T equipment.

2.3.1 DVB-T2 chain

The block diagram of a DVB-T2 transmitter is depicted in Fig. 2.2. As it can be seen, it is divided into four main parts; input processing, bit interleaved coded modulation (BICM), frame builder and OFDM generation.

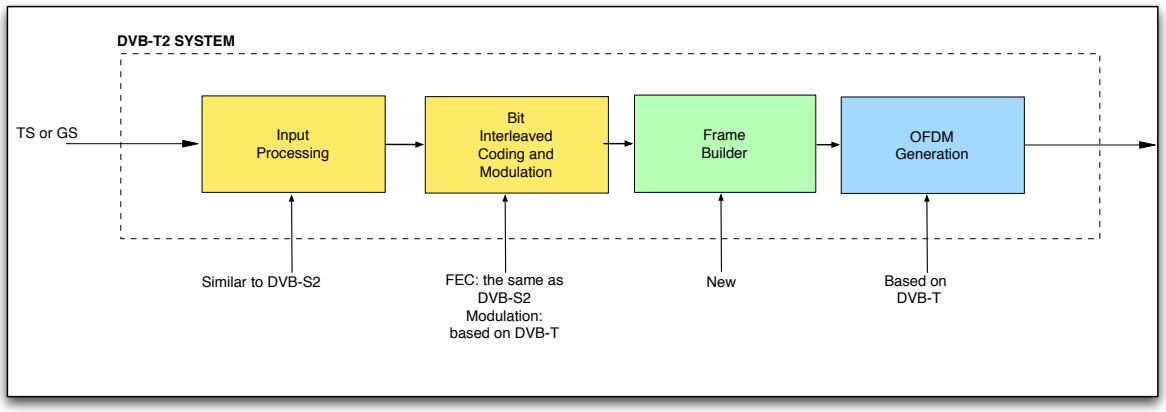

Figure 2.2: High level DVB-T2 block diagram.

This dissertation focuses on the physical layer of DVB-T2 standard, leaving aside input processing and signaling. The entrance to the system consists of randomly generated bits while the output is a radio frequency signal. Regarding frame architecture, DVB-T2 implements a very flexible time interleaving and, in this case, the simplest frame scheme defined in the standard was chosen. The model considers all frames as data regardless of the different types of existing signaling frames. Furthermore, DVB-T2 includes the concept of physical

layer pipe (PLP), that is to say, parallel streams with different parameters, so that it is possible to have different services in the same frequency channel. In order to simplify the simulations, a single PLP was considered in this research work.

In Fig. 2.3, the system block diagram at the transmitter side is shown in detail, being the reverse process performed at the receiver side. These blocks will be briefly described in the following subsections.

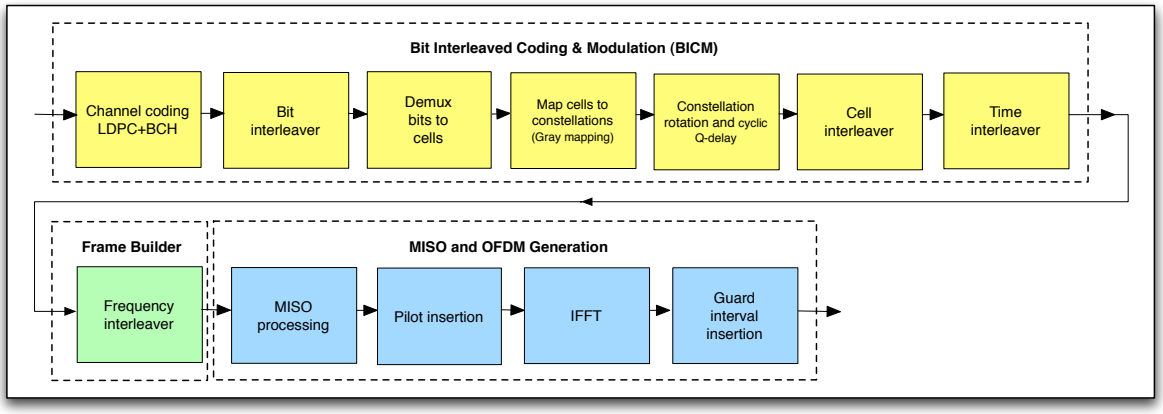

Figure 2.3: Block diagram of a DVB-T2 transmitter.

The most important blocks of the model are the following:

2.3.1.1 Channel Coding

The purpose of the channel encoder is to introduce redundancy in the information sequence that can be used in the receiver to overcome the effects of noise and interference, therefore improving the transmission reliability. DVB-T2 has to face the challenge of increasing the capacity without increasing the power and bandwidth consumption, in order to be compatible with its predecessor. This enhanced capacity is mainly obtained from the inclusion of channel codes with higher correction error capability. DVB-T2 uses a powerful coding scheme based on the combination of low-density parity check (LDPC) and Bose-Chaudhuri-Hocquenghem (BCH) error correcting codes.

2.3.1.2 Interleavers

Interleaving is used to combat signal fading by spreading out adjacent data over multiple blocks and subcarriers. This way, error bursts do not affect consecutive bits and can be easier corrected by the channel decoder. DVB-T2 has three different interleavers: bit, time and frequency. Frequency-interleaving ensures that symbols that have suffered deep fading are spread out across frequency subcarriers. Likewise, time-interleaving ensures that several consecutive bits are transmitted separately. The latter is very advantageous and achieves

significant performance improvements in fast fading channels, where the variations of the channel can provide diversity through interleaving and coding. Finally, the bit interleaver avoid burst errors within a code word.

2.3.1.3 OFDM Generation

OFDM is a frequency-division multiplexing (FDM) scheme used as a digital multi-carrier modulation method. OFDM is very robust against multi-path, frequency selective fading and radio-frequency (RF) interference. As it is well-known, OFDM divides the available bandwidth into many narrow bands and the data is modulated over multiple parallel subcarriers, each of which transmits at a lower rate. The subcarriers used for transmission are chosen so they are orthogonal to each other (see Fig. 2.4), allowing to perform the modulation easily by means of an inverse fast Fourier transform (IFFT). OFDM has been recognized as one of the most efficient modulation schemes and has been widely adopted in wireless communication standards, including DVB-T and DVB-T2. As can be seen in the last part of Fig. 2.3, OFDM involves an IFFT operation and the addition of a cyclic prefix (CP) in order to provide time spacing between symbols to prevent inter-symbol interference (ISI). Thus, the CP introduced in OFDM allows the deployment of single frequency networks (SFN), where several transmitters and repeaters can operate in the same frequencies, improving the spectral efficiency and coverage.

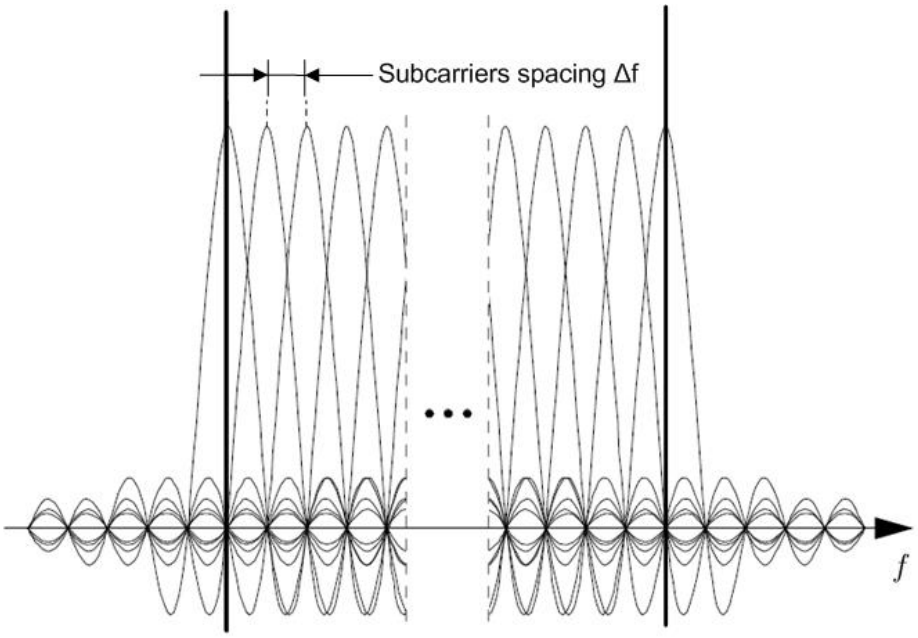

Figure 2.4: Simplified diagram of OFDM subcarriers

2.3.2 Improvements over DVB-T

The DVB-T2 specification includes several new features and improvements with respect to its predecessor DVB-T. Most of these enhancements concentrate on the physical and transport layers, providing a capacity improvement of 30%, greater efficiency in the use of the spectrum, improved robustness against interference and greater flexibility over the former DVB-T specification.

As it has been previously stated, the capacity enhancement is mainly due to the LDPC codes that provide higher performance than convolutional codes. Furthermore, DVB-T2 offers higher-order modulation schemes, lower code rates, longer fast Fourier transform (FFT) modes (16K and 32K) and 8 different pilot patterns (form PP1 to PP8) to adapt channel estimation to system requirements. Table 2.1 summarizes the main features that have been changed at the physical layer.

	DVB-T	**DVB-T2**
FEC	Convolutional + Reed-Solomon 1/2, 2/3, 3/4, 5/6, 7/8	LDPC + BCH 1/2, 3/5, 2/3, 3/4, 4/5, 5/6
Modes	QPSK, 16QAM, 64QAM	QPSK, 16QAM, 64QAM, 256QAM
Guard intervals	1/4, 1/8, 1/16, 1/32	1/4, 19/256, 1/8, 19/128 1/16, 1/32, 1/128
FFT size	2K, 8K	1K, 2K, 4K, 8K, 16K, 32K
Scattered pilots	8% of total	1%, 2%, 4% and 8% of total
Continual pilots	2.6% of total	0.35% of total

Table 2.1: Available modes in DVB-T and DVB-T2.

Another important difference lies in the input formats. While DVB-T only supported MPEG transport stream (TS), the second generation also includes generic ways to transport variable length packets, known as generic streams (GS), which were first introduced in Digital Video Broadcasting - Satellite 2 (DVB-S2) to improve IP transport, aiming at carrying data sequences without specifying time restrictions.

Furthermore, DVB-T2 includes novel functions within the frame builder module, offering the possibility of working with several PLPs so that each of the PLPs can be modulated and encoded differently to meet the needs of each service, and hence increase the robustness and flexibility of the system.

While in DVB-T external encoding (RS) and inner encoding (convolutional) were carried out, this has changed in DVB-T2 and the same encoding schemes that were selected for DVB-S2 are being used. Therefore, once the adaptation frame has been made, the data is sent to the BICM module responsible for linking the external encoding BCH with the

inner, LDPC. The latter offer better performance in the presence of high levels of noise and interference although encoding schemes for DVB-T2 require more processing power at the receiver. Thanks to the forward error correction (FEC) capability of LDPCs, in addition to the three modulation schemes that are also available at DVB-T (QPSK, 16QAM and 64QAM), DVB-T2 provides a higher order modulation scheme, 256QAM.

After FEC encoding, the interleaving processes are carried out (bit, time and frequency interleaver) that make transmission more robust against burst errors. In terms of efficiency and flexibility of DVB-T2, another important change is the introduction of 8 different patterns of scattered pilot carriers that give rise to a greater flexibility. Regarding the improvement on robustness, DVB-T2 added new optional techniques such as peak-to-average power ratio (PAPR) reduction and constellation rotation. These two techniques have been omitted in the model considered in this research work.

DVB-T2 also specifies a transmit diversity method, known as the Alamouti coding, which improves the coverage in single frequency networks and is explained in more detail in Section 2.6.2. This technique is optional, allowing the network to adapt to different environments.

Fig. 2.5 shows the BER performance over additive white Gaussian noise (AWGN) and Typical Urban channel - 6 paths (TU6) channels for DVB-T and DVB-T2, using identical modulation schemes and coding rates. It can be seen that the second generation standard has a much better performance mainly due to the LDPC codes.

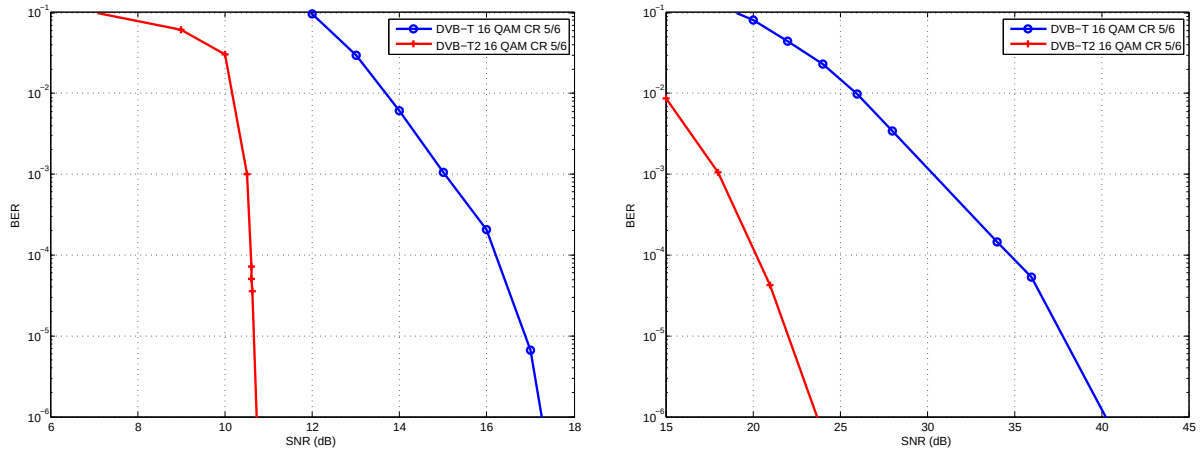

(a) (b)

Figure 2.5: BER performance for DVB-T and DVB-T2 for AWGN (a) and TU6 (b) channels.

It can also be seen that the gain of DVB-T2 over DVB-T is larger with a TU6 channel, where a 14 dB gap is achieved at BER of 10^{-4}, while for the AWGN channel, the improvement is of 5 dB. This is mainly due to the combination of the LDPC decoder and the interleavers, whose effects are negligible in the case of AWGN.

2.4 The suitability of DVB-T2 to mobile reception

DVB-T2 was initially designed to provide increased capacity in terrestrial transmissions, in order to allow HDTV services for fixed and portable receivers. However, the convergence of the fixed and mobile paradigms, and the significant changes that have taken place in the delivery and consumption of multimedia content in recent years, have prompted the simultaneous distribution of the same content in different formats. In order to target mobile scenarios, the technical requirements for the upcoming Digital Video Broadcasting - Next Generation Handheld (DVB-NGH) specification have been constituted, encompassing the following key issues:

- Wide coverage: in order to allow a user to access services across an entire territory.
- Robust reception: to make reception possible in all possible scenarios: indoor or outdoor, stationary, walking or traveling at speed.
- Responsive: quick to start up and to access audio-visual or interactive services, enabling fast channel change times.
- System end to end delay: important for Live events; e.g. use of the NGH system during sports events.

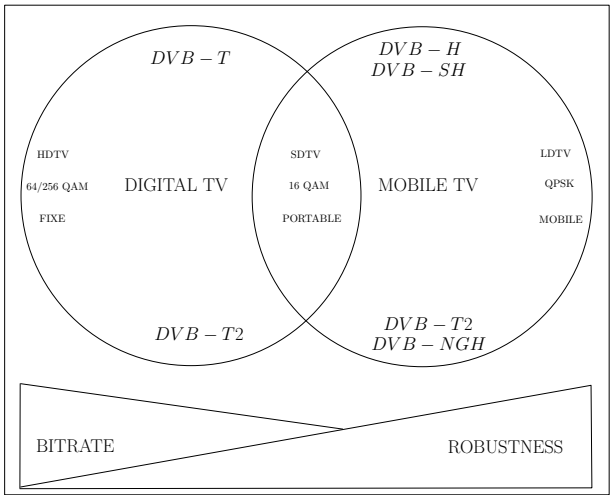

Figure 2.6: Dilema: bitrate vs robustness

DVB-T2 offers the possibility of transmitting multiple PLPs, assigning a specific robustness, and provides flexibility with a great amount of different configurations in order to satisfy different commercial requirements. Therefore, DVB-T2 is emerging as a strong candidate to become the starting point for DVB-NGH. One of these configuration has to do with the use of long OFDM blocks, as considered in Chapters 4 and 5, which makes the system more

robust against ISI in SFN networks, which ultimately provides wide coverage. In addition, the throughput is maximized and also allows networks convergence of fixed and mobile services, since 32K-length symbols are being used for fixed terrestrial digital television (DTV) in UK.

The use of long OFDM blocks entails challenging disadvantages as well. On one hand, the effects of inter-carrier interference (ICI) become greater, and that restricts the use of higher constellations. On the other hand, long OFDM blocks can due to a smaller subcarrier spacing, cause increased latency in the receiver. In any case, it is all about getting a trade-off between larger bitrates and robustness as is depicted in Fig. 2.6.

2.5 System and channel models

This section presents the system model that has been considered throughout this dissertation. Likewise, a brief overview on multi-path channels is carried out, selecting the channel models with which to work. In addition, time-varying models and the ICI channel model are considered.

2.5.1 System model

Let us consider a single-input single-output (SISO) system with one transmit and one receive antenna. The system model that has been considered, which focuses on the physical layer of DVB-T2, is the following one. Considering OFDM blocks of length N are transmitted, the effects of multi-path propagation in the received signal after the removal of the CP can be represented in matrix form as

$$\mathbf{r} = \overline{\mathbf{H}}\mathbf{F}^H\mathbf{x} + \mathbf{z}, \tag{2.1}$$

where $\mathbf{z}$ is the $N \times 1$ AWGN noise vector with zero mean and covariance $E\left\{\mathbf{z}\mathbf{z}^H\right\} = \sigma^2\mathbf{I}_N$, while $\mathbf{r}$ and $\mathbf{x}$ are the $N \times 1$ received and transmitted vectors in time and frequency domains, respectively. The N-point discrete Fourier transform (DFT) matrix $\mathbf{F}$, which is also used at the receiver to translate the symbols into frequency, is defined as

$$[\mathbf{F}]_{p,q} = \frac{1}{\sqrt{N}} \cdot exp(-j2\pi pq/N), \tag{2.2}$$

where $[\mathbf{F}]_{p,q}$ indicates the (p,q)th entry of matrix $\mathbf{F}$. The $N \times N$ time-domain channel matrix $\overline{\mathbf{H}}$ has $N \times L$ nonzero elements, being L the length of the channel impulse response (CIR), and is given by

$$\overline{\mathbf{H}} = \begin{bmatrix} \overline{h}_{0,0} & 0 & \cdots & \overline{h}_{0,2} & \overline{h}_{0,1} \\ \overline{h}_{1,1} & \overline{h}_{1,0} & \cdots & \overline{h}_{1,3} & \overline{h}_{1,2} \\ \vdots & \ddots & \ddots & \vdots & \vdots \\ \overline{h}_{L-1,L-1} & \overline{h}_{L-1,L-2} & \cdots & 0 & 0 \\ 0 & \overline{h}_{L,L-1} & \cdots & 0 & 0 \\ \vdots & \ddots & \ddots & \vdots & \vdots \\ 0 & 0 & \cdots & \overline{h}_{N-2,0} & 0 \\ 0 & 0 & \cdots & \overline{h}_{N-1,1} & \overline{h}_{N-1,0} \end{bmatrix}. \tag{2.3}$$

where the CIR at lag l and time sample n corresponds to $\overline{h}_{n,mod(n+l,N)}$, with $0 \leq l \leq L-1$ and $0 \leq n \leq N-1$. Applying the DFT to the received symbol vector leads to the frequency-domain received symbols

$$\mathbf{y} = \mathbf{Fr} = \mathbf{F}\overline{\mathbf{H}}\mathbf{F}^H\mathbf{x} + \mathbf{Fz} = \mathbf{Hx} + \mathbf{w}, \tag{2.4}$$

where $\mathbf{H} = \mathbf{F}\overline{\mathbf{H}}\mathbf{F}^H$ is the $N \times N$ frequency-domain channel matrix for each OFDM symbol m, and $\mathbf{w} = \mathbf{Fz}$ is the frequency-domain noise vector which has the same statistics as the time-domain vector $\mathbf{z}$. If the channel is considered time-invariant, it does not change during the transmission of one OFDM symbol and the receiver is able to compensate for the effects of the channel by a single tap equalizer, since $\overline{\mathbf{H}}$ is a circulant matrix and, hence, $\mathbf{H}$ becomes diagonal. Considering each transmitted OFDM symbol, the channel frequency response (CFR) matrix for each OFDM symbol m is represented as $\mathbf{H}_m$, and the main diagonal of this matrix is represented by means of the vector $\mathbf{h}_m = \text{diag}(\mathbf{H}_m)$.

2.5.2 Multi-path channel

The path between the transmitting and receiving antennas is the so-called communication channel. Free-space transmission occurs when the received signal is only the result of the direct path propagation. This is not the case for real transmissions, since it does not take into account many terrestrial effects that lead to multi-path propagation and affect the quality of communications. The channel may experience different effects like absorption, attenuation, Doppler effect and ISI.

When it comes to a mobile multi-path channel, the complexity of the system increases due to the presence of obstacles and movement of the receiver. There are three basic mechanisms that impact signal propagation in a mobile communication system: reflection, diffraction, and scattering. The most important effects that may occur are time and frequency dispersion. The transmitted signal generally propagates to the receiver antenna through many different paths, thus, due to reflectors and scatterers as cars, buildings, trees, the receiver antenna will receive multiple delayed and scaled copies of the transmitted signal leading to

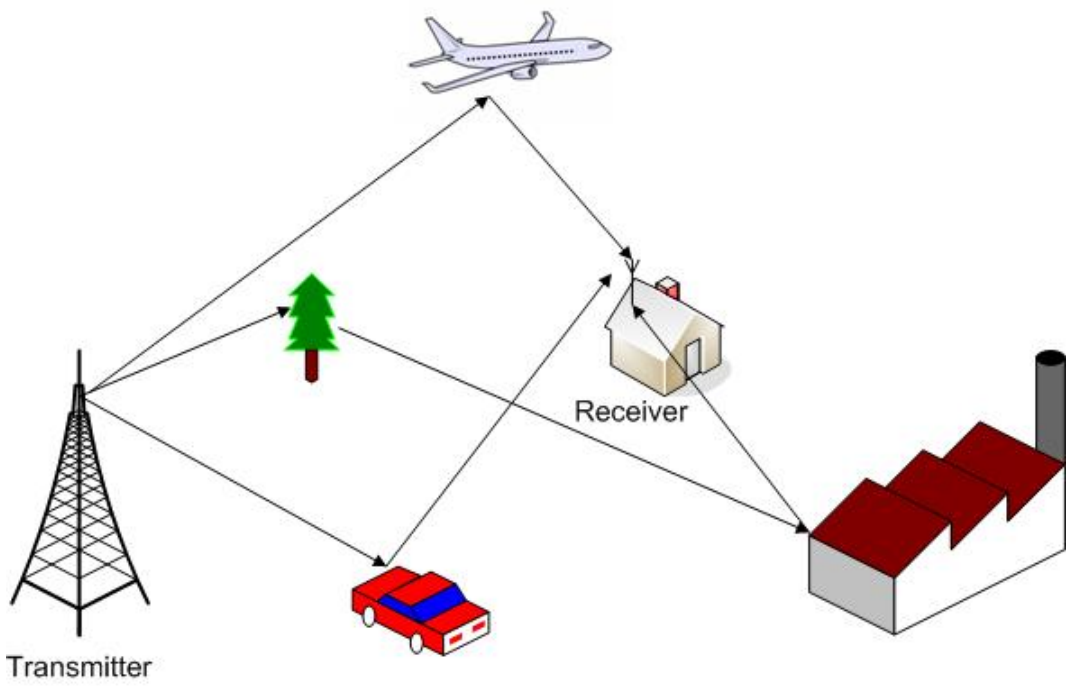

Figure 2.7: Multi-path transmission in a broadcasting application.

temporary dispersion. On the other hand, the movement at the receiver produces frequency dispersion. These effects lead to frequency and time-domain selectivity, respectively. In order to determine the effects that are present in the signal, it is necessary to consider their characteristics and the ones of the channel, such as the coherence time and bandwidth. In general terms, two types of fading effects that characterize mobile communications can be distinguished: large-scale and small-scale fading.

1. Large-scale fading:

   Explains the behavior of the signal at distances much greater than the wavelength (km). Large-scale fading represents the average signal power attenuation or path loss due to motion over large areas. The normal distribution is the one that best fits this fading and for this reason is also called "log-normal fading".

2. Small-scale fading:

   Explains the behavior of the signal at distances as small as a half-wavelength (m). Small-scale fading refers to the fluctuations in the received signal envelope that can be experienced as a result of scattering (small changes) from surrounding objects. Numerous studies have shown [Liu01, Gross05] that the multi-path channel is statistically described by a Rayleigh probability density function (PDF) when there is non line-of-sight (NLOS) between the transmitting and receiving antennas, whereas, in cases which there is line-of-sight (LOS), is consistent with Rice statistical distribution [Rappaport96].

Within the small-scale fading, different types can be distinguished according to the multi-path dispersion:

(a) According to the delay spread (multi-path)

i. Flat fading: This fading occurs when the channel frequency response is flat comparing with the frequency of the transmitted signal, i.e., the coherence bandwidth (B_{wc}) is greater than the bandwidth of the signal (B_{ws}), i.e. (B_{wc}> B_{ws}). If this happens, the channel multi-path characteristics preserve the quality of the signal at the receiver. All the frequency components of the received signal undergo almost the same attenuation and delay, therefore the channel is said to be non-selective in frequency and the effects of ISI does not appear.

ii. Frequency-selective fading: The channel is said selective in frequency if B_{ws} is smaller or comparable to B_{wc}. This means that the frequency components of the received signal separated by more than the coherence bandwidth can suffer significantly different levels of attenuation and delay. Thus generating ICI.

(b) According to the temporal variance (movement on the receiver)

i. Fast Fading: This fading is characterized by fast fluctuations on the envelope of the signal for short distances when the coherence time of the channel is small relative to the delay constraint of the channel. The channel is said to be selective in time if the coherence time (T_c) is smaller or comparable to the sampling time (T_s).

ii. Slow Fading: This fading is characterized by slow variations in the average signal value. The coherence time is long relative to the channel delay, i.e., the signal can be assumed stationary within one or more transmitted pulses, hence non selective in time.

To reduce the effects of multi-path, equalization, diversity and channel coding techniques are used. In order to identify the radio channel modeling is necessary to consider first the propagation area and mobility models with which to work. There are multiple models in the literature depending on the propagation environment, either in free space, indoors or in environments with small or large scale fading [Kim02].

2.5.2.1 TU6 and RA6 channel models

These channel models have been chosen to analyze the performance of the proposed schemes throughout this work, as they reproduce the terrestrial propagation in certain areas for mobile reception [COST207]. Additionally, these channel profiles have been adopted as reference

both in DVB-T and DVB-T2 standards. The Rural Area channel - 6 paths (RA6) channel profile consists of 6 paths having relatively short delay and small power, aiming at reproducing a rural area with LOS and NLOS, and hence, following a Ricean or Rayleigh channel model, respectively. TU6 profile consists of 6 paths having wide dispersion in delay and relatively strong power, reproducing an urban environment with NLOS, and consequently, following a Rayleigh model.

Since mobile reception will be one of the key aspects of this thesis, the time-varying channel model will be analyzed in the following section.

2.5.3 Time-varying channel models

A lot of literature has been published on mobile channels [Pätzold02, Proakis95, Jakes74, Matz06]. In a time-varying and frequency selective channel, there are four variables: time (t), denoting variability in the channel, the transmitted and received signals, the delay (τ), the frequency (f) and the Doppler shift (θ).

The two classical functions of time-invariant channels (impulse response and transfer function), are transformed into four when combined with the variables mentioned above. These functions are called system functions or Bello functions [Bello63]. The four functions are the following ones: input delay spread function (IDSF): $h(t,\tau)$, time-varying transfer function (TVTF): $T(f,t)$, delay-Doppler spread function (DDSF): $S(\tau,\theta)$ and output Doppler spread function (ODSF): $H(f,\theta)$. These functions are linked together through DFT and inverse discrete Fourier transform (IDFT). Fig. 2.8 shows the relationship between these variables:

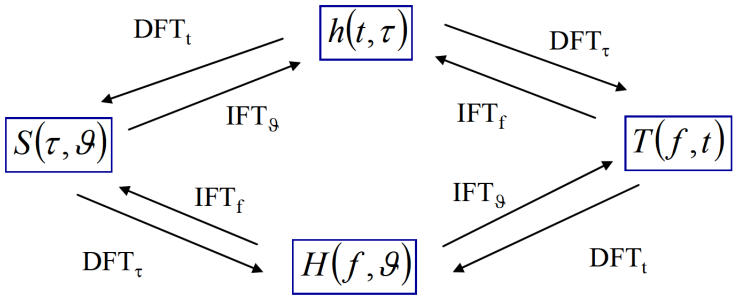

Figure 2.8: Fourier relations between the system functions.

In order to simulate time-variant Rayleigh fading channels, different models are usually considered in the literature. The most widely used ones are Clarke's fading model [Clarke68], or a simplified version known as Jakes spectrum [Jakes74], but there are also different versions of these models like sum of sinusoids (SOS) [Xiao06, Zheng03], autoregressive (AR) [Baddour05] and autoregressive-moving-average (ARMA) [Turin01, Schafhuber01] schemes.

If the receiver is moving at a constant velocity and the omnidirectional antenna receives an infinite number of reflected waves, with a uniformly distributed angle of arrival, the received signal will have a spectrum known as the Jakes spectrum, represented by the autocorrelation in time

$$R_c(\Delta t) = J_0(2\pi v \Delta t \frac{f_c}{c}), \tag{2.5}$$

where J_0 is the zero-order Bessel function of the first kind, f_c is the carrier frequency and c is the speed of light. The corresponding Doppler spectrum is given by

$$S_c(f) = \frac{1}{\pi F_d \sqrt[2]{1 - (\frac{f}{F_d})^2}}, \qquad |f| \leq F_d \tag{2.6}$$

where $F_d = v\frac{f_c}{c}$, is the maximum Doppler frequency and v denotes the vehicle velocity.

2.5.3.1 ICI channel model

Following the model previously described in Section 2.5.1, the ICI channel model will be introduced here. In a time-varying channel the orthogonality among subcarriers is destroyed and therefore, the resulting channel matrix in the frequency-domain is no longer diagonal. As the Doppler Frequency F_d increases or the subcarrier spacing is smaller, the ICI becomes more important and these off-diagonal terms must be taken into account in order to have an accurate estimate of the channel. Therefore, it is crucial to estimate and cancel that interference in order to obtain a good performance of the system. To do so, appropriate detectors and channel estimation methods able to counteract this effect are needed. The input-output relation for the k-th subcarrier is obtained as

$$y_k = h_{k,k}x_k + \underbrace{\sum_{n=0,n\neq k}^{N-1} h_{k,n}x_n}_{\text{ICI term}} + w_k. \tag{2.7}$$

The term on the left of the condition in (2.7) is the desired signal, while the term on the right is the interference signal. This loss of orthogonality seriously degrades the system performance, hence suitable techniques to estimate and remove ICI are needed. Furthermore, the estimation techniques that were used effectively in time invariant channels are no longer appropriate as they do not take into account the off-diagonal terms of the channel matrix $\mathbf{H}$, and more accurate techniques to keep the performance are necessary. Furthermore, as the Doppler frequency increases, these terms become more relevant and the channel estimation is more challenging. The ICI power is obtained through the following formula [Speth99]

$$P_{ICI} = (\pi^2/6) f_d^2, \tag{2.8}$$

and depends on the normalized Doppler frequency f_d as well as on the subcarrier spacing Δ_f as given in this formula: $f_d = F_d/\Delta_f$.

With respect to the number of non-zero off-diagonal elements that should be considered for equalization purposes, a limit must also be set, since taking the entire matrix is not affordable (for complexity reasons) and a trade-off between complexity and performance must be accomplished. Examples where the channel is considered strictly banded can be found in [Kannu05, Schniter04, Rugini05a].

Fig. 2.9 depicts a portion of the channel matrix **H** in order to show that the main diagonal is expanded and the terms in the off-diagonals are no longer negligible. Many research works have been published about this topic [Russell95, Diggavi97, Robertson99]. On one hand, some works ignore the ICI completely and take into account only the main diagonal of the channel matrix. Thus, there are many components of the signal that are obviated, and therefore generate detection errors. Some others view this channel matrix as banded, that is to say, the power is mostly concentrated in the main diagonal, but some other neighboring diagonals are also taken into account for the purpose of ICI cancellation and channel estimation. The simulation results in this thesis are obtained by taking into account two adjacent diagonals (the firsts to both sides of the main diagonal).

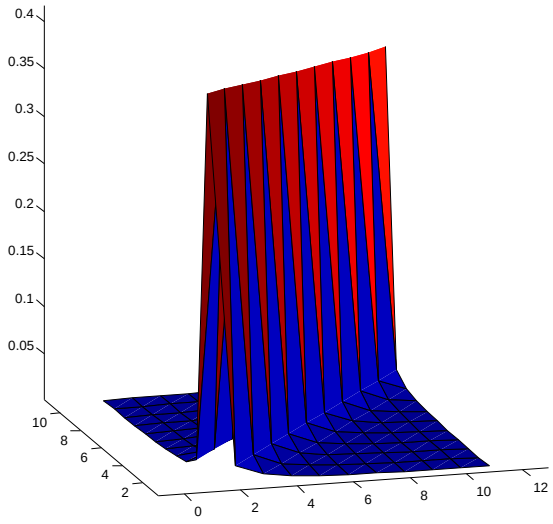

Figure 2.9: First 11×11 values of the **H** matrix.

2.6 MISO transmission in DVB-T2

Although it has not been the cornerstone of the thesis, MISO transmission has been considered in the first chapters, in order to analyze the full potential offered by the standard. In addition, it has also been considered in the channel estimation review results in Section 3.3.

2.6.1 Introduction to multi-antenna systems

Fig. 2.10 shows a M_{ant}xN_{ant} multiple-input multiple-output (MIMO) system, where M_{ant} is the number of transmitting antennas and N_{ant} is the number of receiving antennas. The channel matrix $\mathbf{H}_{MIMO}$ represent the path gains measured between different antenna gains, whose element h_{ij} represents the complex transfer function between the transmitter antenna j and receiver antenna i. Therefore, a flat fading MIMO system can be expressed by using the following equation

$$\mathbf{Y} = \mathbf{H}_{MIMO}\mathbf{X} + \mathbf{W}, \tag{2.9}$$

where $\mathbf{Y}$ is the set of received signals in the N_{ant} antennas, $\mathbf{X}$ is the set of transmitted signals and $\mathbf{H}_{MIMO}$ is the channel matrix of dimensions M_{ant}xN_{ant}.

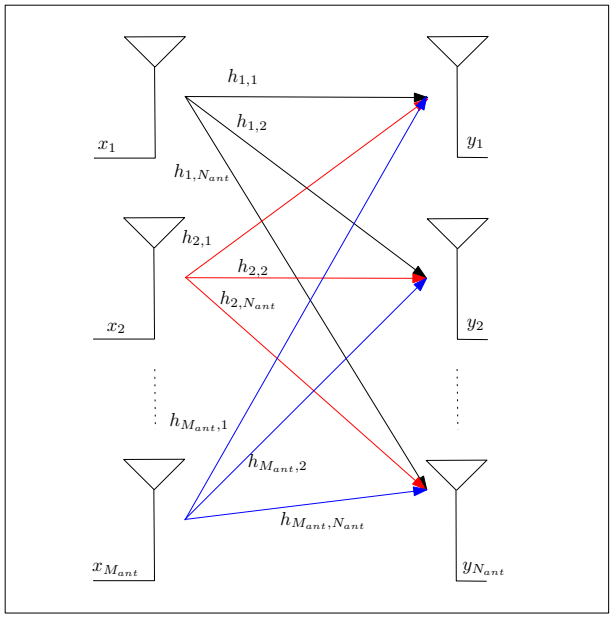

Figure 2.10: $M_{ant} \times N_{ant}$ MIMO channel scheme.

Thus, a new dimension, space, comes into play offering diversity and multiplexing gains without increasing the transmitted power nor the bandwidth. Generally, multi-path propagation experienced by the signals passing through the medium impair the signal due to reflections, solid objects (obstacles such as buildings) and weather, and hence, it has been considered negative because it causes fading. However, if this feature is used efficiently, by deploying multiple antennas at both transmitter and receiver side, the capacity of wireless channels can be greatly increased. Thus, the multi-path propagation provides spatial diversity and allows the combination at the receiver side of several signals that have experienced different fadings. Multi-antenna systems can be classified in single-input multiple-output (SIMO), MISO and finally MIMO.

MIMO systems offer a number of gains compared to conventional systems: diversity, array and multiplexing gains. The diversity gain in a MIMO system represents an improvement in the slope of the SNR, and corresponds to the average number of independently faded paths a symbol passes through. Therefore, in a system of M_{ant} transmission and N_{ant} reception antennas, the diversity gain is the product of M_{ant}xN_{ant}, being necessary to encode the signals to obtain this gain at the transmitter without the knowledge of the channel. Regarding the array gain, it is obtained through signal processing in the transmitter and the receiver side. Since the transmitted and received signals are weighted on each antenna, the array gain is also known as *beamforming*.

An implementation of multi-antenna MIMO communications is the spatial multiplexing system [Foschini96, Wolniansky98], which is effective to increase the data transmission rate. Thus, the signal is divided into several lower bandwidth flows where each signal is spread over different transmit antennas. Such flows are recovered at the receiver using different decoding techniques.

Another implementation is the so-called space-time coding (STC) architecture [Vucetic03, Liu01], in which the coding is done both in space and time domains in order to introduce correlation between transmitted signals from multiple antennas in different temporary periods [Berenguer03]. This space-time correlation is used to make the most of MIMO channel fadings in order to minimize the errors introduced by the channel. The most important STC approach are the space-time Trellis codes (STTC) [Tarokh98, Tarokh99], and the space-time block codes (STBC) proposed by Alamouti [Alamouti98]. The following section will explain in more detail the Alamouti STBC code, which is the unique multi-antenna technique included in DVB-T2.

2.6.2 Alamouti

This space-time coding scheme introduced by Alamouti, and generalized by Tarockh, is known for its simplicity and effectiveness and for that reason, it has been used in the second generation digital television standard, and is explained in detail below. Alamouti proposed a transmit diversity scheme for channels with flat fading where no inter-symbol interference occurs assuming the channel does not vary between two consecutive symbols. The Alamouti matrix is the following one

$$X_{al} = \begin{bmatrix} x_1 & -x_2^* \\ x_2 & x_1^* \end{bmatrix}, \tag{2.10}$$

where x_1 and x_2 are the two symbols transmitted in the codeword X_{al}, and $(^*)$ denotes the complex conjugate operation. The rows correspond to the items sent by the first and second antennas, respectively, and each column corresponds to a symbol period. In the case of two

transmitting and two receiving antennas, the signal at the receiver side is derived as follows

$$\begin{bmatrix} y_1(1) & y_1(2) \\ y_2(1) & y_2(2) \end{bmatrix} = \underbrace{\begin{bmatrix} h_{11} & h_{12} \\ h_{21} & h_{22} \end{bmatrix}}_{\mathbf{H}_{MIMO}} \cdot \begin{bmatrix} x_1 & -x_2^* \\ x_2 & x_1^* \end{bmatrix} + \underbrace{\begin{bmatrix} w_1 & w_2 \\ w_3 & w_4 \end{bmatrix}}_{\mathbf{W}}, \tag{2.11}$$

where $\mathbf{H}_{MIMO}$ is the channel matrix, and $\mathbf{W}$ the matrix representing the AWGN noise samples. If the channel is multiplied by the first period symbol and then by the second, the received signals are obtained for both antennas y_1 and y_2, in each of the instants

$$y_1(1) = h_{11}(1) \cdot x_1 + h_{12}(1) \cdot x_2 + w_1, \tag{2.12}$$

$$y_1(2) = h_{11}(2) \cdot -x_2^* + h_{12}(2) \cdot x_1^* + w_2, \tag{2.13}$$

$$y_2(1) = h_{21}(1) \cdot x_1 + h_{22}(1) \cdot x_2 + w_3, \tag{2.14}$$

$$y_2(2) = h_{21}(2) \cdot -x_2^* + h_{22}(2) \cdot x_1^* + w_4. \tag{2.15}$$

The estimates at both antenna 1 and antenna 2 are obtained as follows using a maximum ratio combining (MRC) receiver

$$\hat{x_1} = h_{11}^*(1) \cdot y_1(1) + h_{12}(2) \cdot y_1^*(2) + h_{21}^*(1) \cdot y_2(1) + h_{22}(2) \cdot y_2^*(2), \tag{2.16}$$

$$\hat{x_2} = h_{12}^*(1) \cdot y_1(1) - h_{11}(2) \cdot y_1^*(2) + h_{22}^*(1) \cdot y_2(1) - h_{21}(2) \cdot y_2^*(2). \tag{2.17}$$

Thus, taking into account that each of the components of the channel has an amplitude and a phase

$$h_{11} = \alpha_{11} \cdot e^{j\theta_{11}}, \tag{2.18}$$

$$h_{12} = \alpha_{12} \cdot e^{j\theta_{12}}, \tag{2.19}$$

$$h_{21} = \alpha_{21} \cdot e^{j\theta_{21}}, \tag{2.20}$$

$$h_{22} = \alpha_{22} \cdot e^{j\theta_{22}}. \tag{2.21}$$

Replacing each of the components in the equation we get

$$\hat{x_1} = (\alpha_{11}^2 + \alpha_{12}^2 + \alpha_{21}^2 + \alpha_{22}^2) \cdot \hat{x_1} + h_{11}^* \cdot w_1 + h_{12} \cdot w_2^* + h_{21}^* \cdot w_3 + h_{22} \cdot w_4^*, \tag{2.22}$$

$$\hat{x_2} = (\alpha_{11}^2 + \alpha_{12}^2 + \alpha_{21}^2 + \alpha_{22}^2) \cdot \hat{x_2} - h_{11} \cdot w_2^* + h_{12}^* \cdot w_1 - h_{21} \cdot w_4^* + h_{22}^* \cdot w_3. \tag{2.23}$$

That is, the decoding is equivalent to performing two SISO detections. At the receiver side, MRC combines the received signals by each receiving antenna by weighting the different branches depending on the quality of its received signal.

2.7 Chapter Summary

This chapter has explained the main features of DVB-T2 standard and it has also highlighted the most significant differences introduced with respect to the previous DVB-T standard. All these improvements concentrate on physical and transport layer, providing a capacity improvement of 30%, greater efficiency in the use of the spectrum, improved robustness against interference and greater flexibility over the former specification. All this has been given to meet the needs of new services that require greater capacity as HDTV. These improvements are the result of a set of key techniques that have been included in the new standard, such as LDPC codes, higher order modulation schemes, lower code rates, longer modes and 8 different pilot patterns.

Regarding the channel model, this chapter gives an overview of channel models with special emphasis on multi-path and time-varying channel models. It also has described MIMO systems in DVB, focusing on the performance of the Alamouti space-time coding approach, which has been included in DVB-T2 as an optional technique.

Chapter 3

Channel estimation in OFDM systems

3.1 Introduction

Most communications systems require accurate channel state information (CSI) at the receiver side in order to detect the transmitted information properly. This information is obtained by channel estimations that minimize some criterion, e.g. mean squared error (MSE), while using the minimum resources as possible to achieve a simple computational implementation.

In this chapter, the main techniques for blind, supervised and semi-blind channel estimation will be reviewed, with special emphasis on the last two. Firstly, pilot-based techniques will be addressed, and for this purpose the set of pilots used in DVB-T and DVB-T2 will be explained in detail. In addition, taking the pilot scheme used in the DVB-T2 standard as reference, different channel estimation and interpolation techniques are analyzed for SISO and MISO systems, with and without mobility. Furthermore, the effect of time interleaving in this schemes is also studied.

Secondly, regarding semi-blind techniques and based on the coded decision directed demodulation (CD3) algorithm, originally proposed for DVB-T, a proposal for improved channel estimation will be made and applied to DVB-T2. This scheme does not require the transmission of so many pilots and thus the spectral efficiency is higher. This technique can also be applied to both static and mobile scenarios, taking into account that when the channel variations are slower (fixed receivers), the channel estimation loop can accept higher delays than in the reverse case.

The chapter is organized as follows. Section 3.2 briefly highlights the most relevant literature on channel estimation for slow and moderate time-varying fading channels. Section 3.2.2 explains the pilot patterns in DVB-T and DVB-T2 and presents the least squares (LS) and minimum mean squared error (MMSE) estimators. Section 3.2.3 proposes and improved channel estimation technique under a DVB-T2 framework, based on the CD3 algorithm originally proposed for DVB-T by [Mignone96]. Finally, numerical results are provided in section 3.3 to show the performance of several interpolation algorithms which have been

previously analyzed, showing that the best performance is achieved with the two-dimensional channel estimator. In addition, these algorithms are also tested for MISO with one and two receive antennas applying the above techniques to DVB-T2. Performance results are also provided for the proposed modified CD3 algorithm, which shows only a small performance loss compared to the ideal channel knowledge and outperforms the original CD3 algorithm, for which the PP8 pilot scheme of DVB-T2 was originally designed.

3.2 Channel estimation techniques

In order to achieve a successful reception and decoding of the transmitted data, accurate channel estimation is necessary. Three main kinds of channel estimators can be considered: blind, supervised or training based (TB) and semi-blind, e.g. decision-directed (DD) schemes. The former do not require training sequences, being specially suitable for applications where the bandwidth is a scarce resource. However, they are computationally intensive and hence not appropriate for real-time: implementation in complex systems or for low-cost receivers. The second, in contrast, may impose an unacceptable overhead that limits the effective data throughput, so it is necessary to minimize the number of pilot symbols in a data packet. However, a longer amount of pilot symbols implies a better channel estimation. These two premises are contrary to each other, so it is essential a trade-off between both. Semi-blind, such as DD techniques, which are based on a reduced number of pilots, can bridge the gap between blind an supervised techniques.

3.2.1 Blind channel estimation

The increased need for higher data rates has prompted blind identification methods because their more efficient bandwidth use. Therefore, much research has targeted on blind channel estimation in recent years and many works can be found in the literature on this topic. The most widely used methods are based on second and higher order statistics [Muquet99, Zheng93, Tong94, Cai00]. Other blind channel estimation techniques take advantage of the redundancy introduced in OFDM systems by the CP to identify the channel [Muquet02, Tureli98], and some others [Roy02] perform a subspace blind channel estimation method.

However, statistical blind channel estimation approaches are not suitable for mobile radio channels due to their slow convergence rate. [Chotikakamthorn99] tackle this problem applying a deterministic approach by means of amaximum likelihood (ML) channel estimator producing a channel estimate obtained over one OFDM symbol, being the main disadvantage the high computational complexity involved in it. In the case of channel estimation in DVB-T, this method is modified in [Necker04] and applied to a modified DVB-T system, maximizing the spectral efficiency removing the pilot symbols and maintaining a low com-

plexity. In order to avoid the need for reference symbols, they applied a combination of modulation schemes to resolve the absolute phase of the channel transfer function.

3.2.2 Pilot assisted channel estimation

Supervised (pilot-based) techniques simplify the receiver design, reduce the computational load and can be quite easily applied in wireless communications. In addition, these techniques outperform the aforementioned blind techniques in highly time-varying channels. There are two main issues in the analysis of pilot assisted channel estimators in wireless OFDM systems: The first one is the placement of the pilot carriers [Tong04], whereas the second one is the design of efficient estimators. Pilot assisted channel estimation can be performed in three different ways: Firstly, preamble based training, in which a training sequence is included at the beginning of a data burst; secondly, by means of pilot-symbol aided modulation (PSAM) [Cavers91], where training symbols are inserted periodically during transmission (also known as block-type scheme); and finally, through pilot tones inserted in different frequencies of each OFDM symbol (also known as comb-type scheme). The former two are more appropriate for slow fading channels, since they assume that the channel does not change over the transmission of a few OFDM symbols. On the other hand, the latter can withstand better the channel variations [Slock04].

Depending on whether the channel is invariant in time or not, different channel estimation techniques and pilot arrangements are applied in order to obtain a suitable performance. Therefore, a study on the optimal placement of the pilot carriers is necessary. In time-invariant channels, or when the channel transfer function changes slowly, some studies have shown that pilot tones should be equi-spaced [Negi98]. In such cases, the estimation of the channel parameters for the block-type scheme is generally based on LS or MMSE techniques, from which the latter has been shown to clearly outperform the former at the expense of greater complexity [vandeBeek95]. The MMSE estimator requires a real-time $N \times N$ matrix inversion, which implies a high complexity when N grows. To overcome this problem, plenty of works have been presented. In [vandeBeek95] the MMSE estimator is modified, given a certain knowledge about the channel statistics. In [Li98] the channel correlations in both the time and frequency-domain are exploited, so the performance improves compared to the estimator in [vandeBeek95]. In [Edfors98], a low-rank approximation is proposed, which makes use only of the frequency correlation of the channel, thus, reducing the complexity.

On the other hand, a comb-type scheme is more appropriate when it comes to a time varying frequency-selective fading channel, since the channel transfer function changes across subcarriers and OFDM symbols. The best pilot placement is accomplished by uniformly distributing them in both time and frequency [Nilsson97] and channel estimation can be again based on LS and MMSE, the best performance being achieved with the MMSE as in the previous case. The channel estimation is performed at pilot frequencies and thereafter

interpolation techniques are applied. In [Hsieh98] a low-rank approximation using singular value decomposition is derived to reduce complexity. Two one-dimensional Wiener filtering estimation is performed in [Hoeher97] and [Flament02, Sanzi03] have enhanced this method using decision-directed information. In [Ozbek05], instead of using hard-detected symbols, their reliability is used by means of the *a posteriori* probability (APP) provided by the channel decoder, in order to improve the channel estimates.

The interpolation can be linear, second-order, low-pass, spline cubic and time-domain interpolation. In [Hsieh98], second-order interpolation has been shown to perform better than linear interpolation. Low-pass interpolation is the one with the best performance among all, as is stated in [Coleri02], where all the mentioned techniques are compared with each other. Block-type and comb-type pilot-based channel estimators are also compared in [Coleri02], showing that the former scheme with decision feedback performs better than the comb-type scheme for low Doppler frequencies as pointed out in [Li00], except for the low-pass and spline interpolation.

When dealing with multiple antennas, different systems have been discussed. In [Li99] a channel estimator for MIMO has been developed, which requires a large matrix inversion. In order to simplify this, two reduced-complexity channel estimation techniques are presented in [Li02]. In [Barhumi03], the optimal pilot placement sequence with respect to the MSE is proposed, showing that it must be equipowered, equispaced, and phase shift orthogonal.

3.2.2.1 Pilot patterns in DVB-T and DVB-T2

An OFDM symbol consists of N elements, each corresponding to a carrier. In DVB-T, there are two possible FFT modes, 2K and 8K, with 1705 and 6817 used carriers respectively, of which only 1512 in the first case and 6048 in the second are active data carriers. The remainder are pilot carriers used for synchronization and channel estimation. These pilots are divided into three groups: continual (which are present in all symbols in the same positions), scattered (their positions vary in different symbols) and transmission parameter signaling (TPS) carriers, which are used to signal the parameters for the employed transmission scheme, i.e., to report information on channel coding and modulation used in transmission.

DVB-T2 introduces several differences, as it incorporates new reference signals. In this case, several groups of pilot carriers have been defined: Continual, scattered, edge, P2 and end of frame pilots. The placement and amplitude of the pilot carriers differs from the previous standard. Furthermore, DVB-T2 offers higher-order modulation schemes, lower code rates, more FFT sizes (1K, 2K, 4K, 8K, 16K and 32K) and 8 different pilot patterns (form PP1 to PP8) to adapt channel estimation to system requirements. Thus, depending on the FFT size, guard interval (GI) length, pilot pattern and mode being used (SISO or MISO), the number of pilots and data carriers vary. As in DVB-T, continual carriers, unlike

the scattered, always occupy the same positions. In addition, the positions of the continual carriers are chosen from one or more groups depending on the FFT size, belonging to each of the groups depending on the pilot pattern. For example, the following figure shows the positions of different pilot carriers for pilot pattern PP1 and SISO mode.

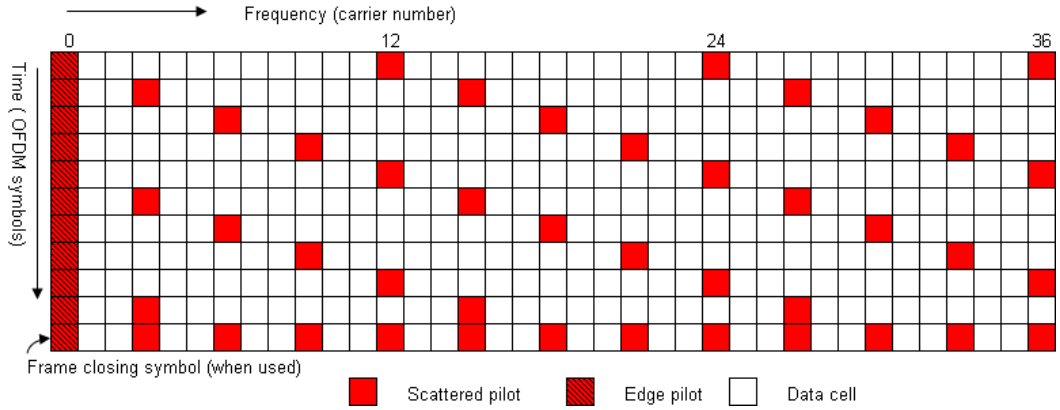

Figure 3.1: Scattered pilot pattern PP1 defined in DVB-T2 standard for SISO transmission.

3.2.2.2 One-dimensional estimation

The most common channel estimators for comb-type schemes are based on LS and MMSE algorithms, the best performance being achieved with the latter. These techniques are briefly explained next.

1. Least Squares:

   The symbols vectors can be divided into two sets, corresponding to the data and the pilot symbol positions. In the following, all the algorithms are described based on a single OFDM symbol and, consequently, the symbol index m is dropped out. The subscript p indicates symbols at the pilot positions, so the channel estimate at pilot carriers can then be estimated as shown in the following equation

   $$\hat{\mathbf{h}}_p^{\mathrm{LS}} = \mathbf{x}_p^{-1} \cdot \mathbf{y}_p, \tag{3.1}$$

   where $\mathbf{y}_p$, $\mathbf{x}_p$ and $\hat{\mathbf{h}}_p$ stand for the received signal vector, transmitted signal vector and the estimated channel frequency response for the pilot positions, respectively.

2. Minimum Mean Squared Error:

   Once a first LS estimate is obtained, a filter matrix $\mathbf{W}_{coeff}$ can be applied, leading to Wiener estimation [Hoeher97]. Thus, the filter coefficients are used to interpolate the channel response in data subcarriers as follows

$$\hat{\mathbf{h}} = \mathbf{W}_{coeff} \cdot \hat{\mathbf{h}}_p^{\mathrm{LS}}. \tag{3.2}$$

Given the design criteria presented in [Hoeher97], the filter coefficients are derived from the cross-correlation of the channel $\mathbf{R}_{\mathbf{h},\mathbf{h}_p} = E\left\{\mathbf{h}\mathbf{h}_p^H\right\}$ and the autocorrelation at the pilot symbol positions $\mathbf{R}_{\mathbf{h}_p,\mathbf{h}_p} = E\left\{\mathbf{h}_p\mathbf{h}_p^H\right\}$. Once both autocorrelation matrices are obtained, filter coefficients $\mathbf{W}_{coeff}$ are calculated as follows

$$\mathbf{W}_{coeff} = \mathbf{R}_{\mathbf{h},\mathbf{h}_p}(\mathbf{R}_{\mathbf{h}_p,\mathbf{h}_p} + \sigma_z^2\mathbf{I})^{-1}, \tag{3.3}$$

where $\mathbf{I}$ denotes the identity matrix.

3.2.2.3 Two-dimensional channel estimation

More accurate channel estimates can be obtained if the channel estimator operates in both time and frequency, thus following a two-dimensional channel estimation approach. Although this estimator, based on a two-dimensional Wiener filter interpolation, is the optimal in MSE terms, one-dimensional channel estimators are typically used to achieve a better trade-off between complexity and accuracy. However, even though this structure of a two-dimensional estimation is too complex for practical implementation, it is possible to replace the two-dimensional filters with two cascaded one-dimensional filters, i.e. one in time (OFDM symbols) and another one in frequency (carriers), so that it can mitigate more effectively the effect of Doppler spread in channel estimation [Hoeher97].

Focusing on the DVB-T2 specification, one can see that only the transmission parameters are defined, so the receiver side is open for any possible improvement. As DVB-T2 is designed for fixed and mobile scenarios, the reception needs can be very diverse. In the case of multi-antena transmissions, the estimation is performed every two OFDM symbols, as two symbols are required to estimate the channel, being the pilot carriers defined in this way in the standard. Hence, the channel estimation has to be somehow adapted. In the case of adopting the pilot pattern PP1, an adaptive estimation is performed so that every four OFDM symbols a window is taken as shown in Fig. 3.2. This way the value of each carrier is updated and therefore the changes in the channel are taken into account. In the following figure one can observe the transmitted and received OFDM symbols for MISO when 3FEC or 8 OFDM symbols are transmitted. As it can be seen the first filtering is performed in time, and thereafter when more values are availvable, a frequency filtering is performed in order to estimate the values of the unknown data carriers. This process is performed every 4 OFDM symbols in order to update the channel estimate of the time-varying channel.

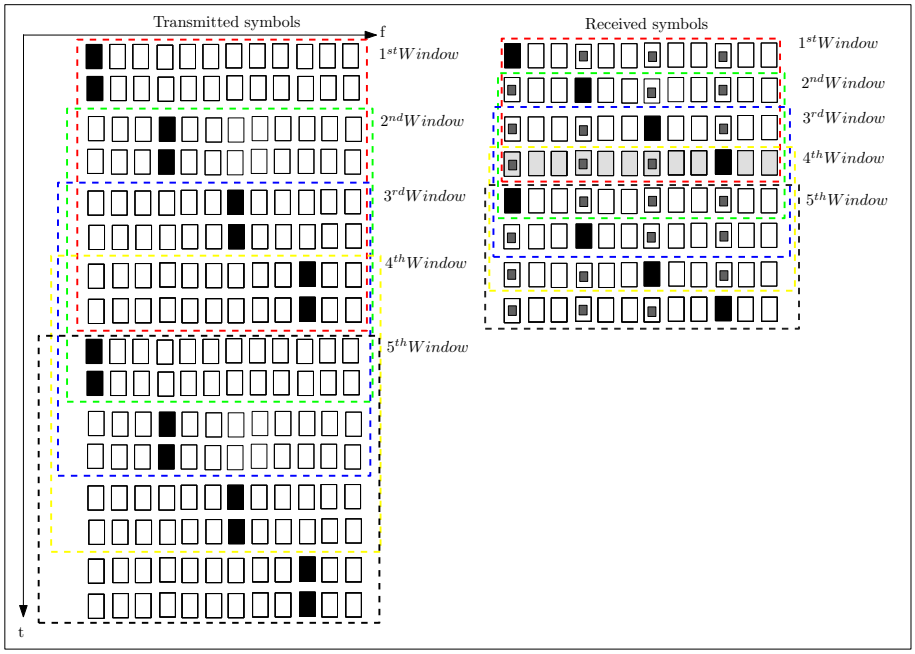

Figure 3.2: Transmitted and received symbols.

3.2.3 Semi-blind channel estimation

Blind methods can also be used together with training symbols in order to improve performance [Muquet02, De Carvalho97], being them referred as semi-blind methods. One of these approaches are the DD channel tracking schemes, which have been successfully tested in slow fading environments [Wilson94, Mignone96]. These methods transmit known pilot symbols at the beginning of each frame for synchronization and initial channel estimation, and then feed the decoded symbols back to the channel estimator updating the earlier estimate. However, the performance is not comparable to that of pilot assisted channel estimation as the Doppler frequency, and thereby, the speed of the receiver increases.

As already been pointed out, both DVB-T and DVB-T2 use OFDM modulation and comb-type pilot patterns. However, DVB-T2, unlike its predecessor DVB-T, allows a choice between different pilot patterns, of which one of them (PP8) is designed to carry very few pilots. In this case, channel estimation is based on a minimum number of pilots, thus getting increased spectral efficiency and a gain of 8%. If this pilot pattern is used, the channel can not be properly estimated from training sequences only, so it is necessary to estimate the channel using other techniques. This specific pilot pattern will be used to analyze and propose DD channel estimation methods for DVB-T2 in the following section.

3.2.3.1 Channel estimation for DVB-T2's PP8 pilot mode

The effects of multi-path propagation on OFDM (if the maximum excess delay is shorter than the GI length and the channel is slowly varying) can be modeled as

$$y_{m,k} = x_{m,k} \cdot h_{m,k} + w_{m,k}, \tag{3.4}$$

where $x_{m,k}$ is the transmitted signal in frequency-domain in OFDM symbol m at subcarrier position k, with the channel transfer function $h_{m,k}$ and the additional noise term $w_{m,k}$. The task of the channel estimator within the receiver is the estimation of the channel transfer function $\hat{h}_{m,k}$, which is normally achieved first by means of frequency-domain pilots that are transmitted at specific OFDM subcarrier positions. The receiver then interpolates the channel transfer function, for which a large number of algorithms exist [Hanzo03]. Hence, the receiver gets the equalized QAM symbols $\gamma_{m,k}$

$$\gamma_{m,k} = \frac{y_{m,k}}{\hat{h}_{m,k}} = \frac{h_{m,k}}{\hat{h}_{m,k}} \cdot x_{m,k} + \frac{w_{m,k}}{\hat{h}_{m,k}}. \tag{3.5}$$

If the channel is estimated correctly, the receiver is able to correct the channel distortions completely, whereby the noise may be amplified, depending on the absolute value of $\hat{h}_{m,k}$. Once the symbol $\hat{x}_{m,k}$ has been detected, it is possible to re-estimate the channel assuming it has been correctly detected, which is the basis of the CD3 algorithm introduced in [Mignone96] for DVB-T.

$$\hat{h}_{m,k} = \frac{y_{m,k}}{x_{m,k}} = \frac{h_{m,k} \cdot x_{m,k}}{x_{m,k}} + \frac{w_{m,k}}{x_{m,k}}. \tag{3.6}$$

Naturally, the value of $\hat{x}_{m,k}$ is unknown to the receiver before the decoding process. However, it is known after the decoding process with a latency of one FEC block, and can then be used for the estimation process. The block diagram of the CD3 algorithm using this principle is given in Fig. 3.3. The first step is to compute $\hat{h}_{m,k}$ by means of frequency-domain pilots or a reference sequence. Then, the OFDM symbols are equalized and this sequence is re-encoded and re-modulated in order to obtain the estimated transmitted data $\hat{x}_{m,k}$.

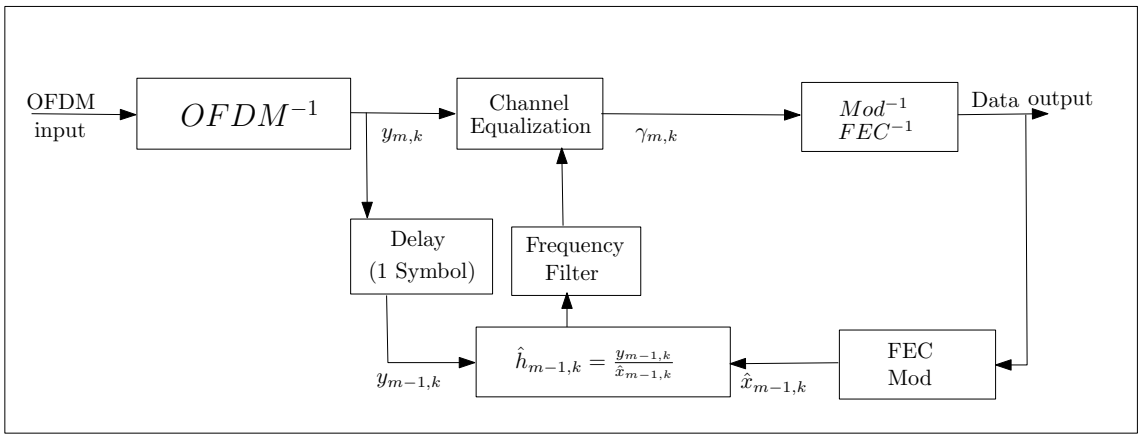

Figure 3.3: Principle of the CD3 equalization process.

The receiver regenerates the complete data of each OFDM symbol after the decoding

process, and hence, is able to use this information for channel estimation. If the channel is assumed to be time-invariant or changes slowly, the effect of the delay can be neglected and one is able to estimate the channel using the approximation

$$\hat{h}_{m,k} \approx \hat{h}_{m-1,k}. \tag{3.7}$$

In order to start this process, the receiver has to obtain the channel transfer function by other means, i.e., a reduced number of pilot subcarriers or a short preamble sequence. In case of DVB-T2, the P2 symbol within the preamble of each DVB-T2 frame can be used for this purpose. Afterwards, the decision-directed mode can be applied. However, a problem of this algorithm is the error probability when inner QAM constellation points are used. Fig. 3.4 depicts this problem for 16QAM. If a mean power of 1 is assumed for the symbols, the energy of the inner constellations points are $|x_1|^2 = 0.2$, while the values for the outer constellation points are $|x_2|^2 = 1.8$, which correspond to a difference of 9.54dB.

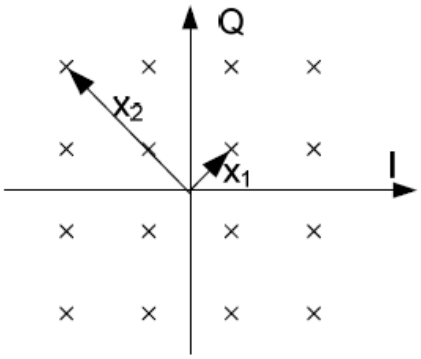

Figure 3.4: 16QAM constellation diagram and absolute values for inner and outer constellation points.

Hence, the inner constellation points increase the noise-induced errors in (3.6) due to their small amplitude, while the noise term is reduced if the constellation points in the edges of the diagram are used. This estimation noise can be reduced by filtering the estimated signal as depicted in Fig. 3.3. However, only the filtering within one OFDM symbol is practically possible, because the use of future OFDM symbols would further increase latency.

3.2.3.2 Proposal for improved channel estimation

As already mentioned, the amplification of the noise term in the estimation of the channel of an individual OFDM subcarrier depends on the absolute value of x, i.e. the transmitted QAM constellation symbol. That is why, transmission systems as DVB-T or DVB-T2 use boosted pilots, which are transmitted at higher amplitude compared to normal data. Therefore, a promising approach is just the use of the outer constellation points for channel estimation, establishing a threshold on the power of a detected symbol in order to include it in the

CD3 decision-directed estimation. This principle is depicted in Fig. 3.5, where a value of $\hat{x}$ is used for channel estimation only if the absolute value of the constellation point exceeds a threshold value, i.e. $|\hat{x}|>x_{min}$. Otherwise, it is linearly interpolated between two valid neighboring positions that exceed the threshold. As only a few OFDM subcarriers have to be typically interpolated, the loss in estimation accuracy is quite limited compared to the performance gain it provides. After the interpolation process, the normal CD3 algorithm can be applied. Additionally, it is also possible to filter the signal on the OFDM symbol to reduce the remaining estimation noise as for the CD3 algorithm.

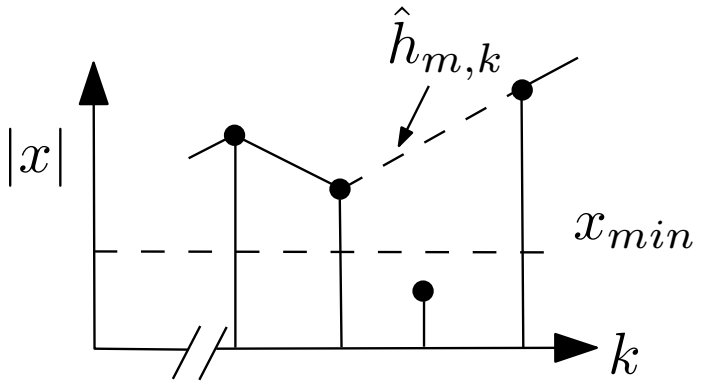

Figure 3.5: The channel is linearly interpolated over inner constellation points

Furthermore, the same principle can be applied if the LDPC decoder is not able to decode all subcarriers of an OFDM symbol. This effect occurs if an LDPC codeword is split over two OFDM symbols, which makes it practically impossible to correct the codeword before demodulating the following OFDM symbol.

3.3 Simulation results

Based on the DVB-T2 simulator developed by the Signal Theory and Communications research group, the channel estimation and interpolation techniques explained in the previous sections have been implemented for fixed and mobile reception, including LS channel estimation with linear interpolation, one-dimensional and two-dimensional Wiener estimation. In addition, this section also presents the simulations results that show the performance of the original CD3 algorithm and the improved threshold enabled decision-directed algorithm proposed in this chapter.

3.3.1 Effects of interpolation

The simulation parameters shown in Table 3.1 have been used for the results provided in this section. Before analyzing the performance of the channel estimation approach, the performance of the interpolation techniques will be shown.

Table 3.1: Simulation parameters

Parameter	**Value**
Carrier frequency	760 MHz
Bandwidth	8 MHz
Length of LDPC block	16200 bits
Code rate	2/3
Number of LDPC blocks per realisation (N)	$N_{FEC} = 3$
Constellation size	16QAM
FFT size	2048 carriers (2K)
Length of one OFDM block (T_u)	$224\mu s$
Length of the GI ($T_u/4$)	$56\mu s$
Pilot pattern	PP1 or PP2

Fig. 3.6 depicts the real part of the frequency-domain channel response at the pilot subcarriers. As expected, two-dimensional channel estimation is the one that offers the closest performance compared to the ideal CSI, being also the one that involves more computational complexity. However, one can see that one-dimensional Wiener estimation obtains good results with a straightforward implementation and less computational complexity than in the previous case, while linear estimation shows the worst performance, being the simplest of all.

Therefore, once it has been shown in Fig. 3.6 that one-dimensional Wiener estimation is the one that achieves the best trade-off between computational complexity and performance, and that two-dimensional Wiener filtering is the most precise of all, the following sections present the performance assessment of the aforementioned channel estimation techniques for DVB-T2, in both fixed and mobile scenarios. In addition, as MISO transmission can be beneficial in certain environments, and has been included in DVB-T2 the channel estimation techniques mentioned above have also been simulated for MISO (Alamouti with a single receiver) and MISO (Alamouti with two receive antennas) in the referred scenarios in order to verify the suitability of these techniques in different situations. The DVB-T2 implementation guidelines document [DVB09] proposes several channel models, from which the COST 207 TU6 has been chosen to analyze the performance of these techniques in fixed and mobile reception [COST207]. The results are compared to the perfect CSI case and the gain between BER curves is evaluated at BER=10^{-6}.

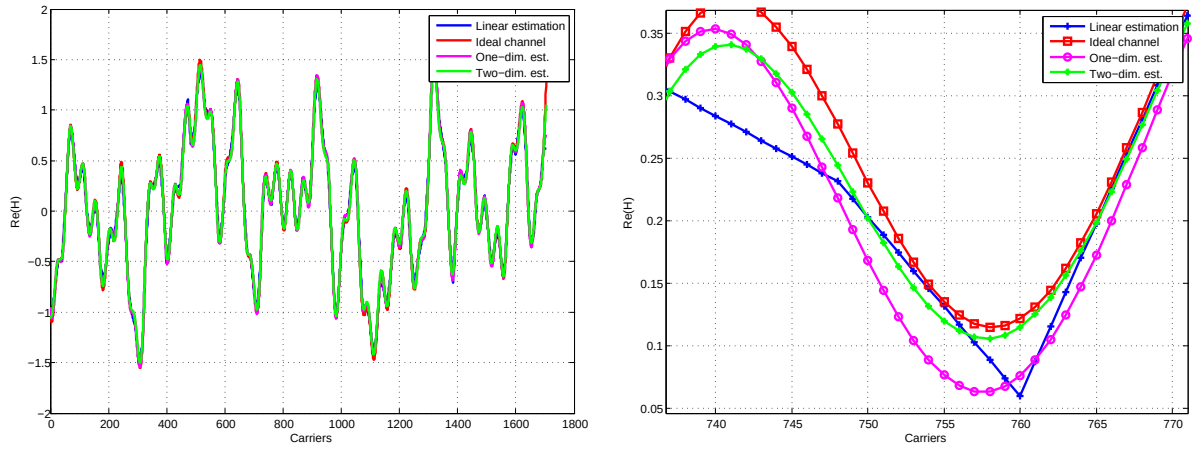

(a) (b)

Figure 3.6: Performance of the considered interpolation schemes showing all (a) and a subset (b) of the subcarriers.

3.3.2 Fixed reception

Fig. 3.7 depicts the results corresponding to the parameters described in Table 3.1. When it comes to fixed reception, the most widely used channel estimation techniques have been compared (LS and MMSE). In order to measure the degradation suffered by these systems in different environments when applying the aforementioned channel estimation techniques, the ideal channel estimation with perfect CSI has also been depicted and taken as a reference. The following cases have been considered; perfectly known channel, LS channel estimation with linear interpolation and one-dimensional Wiener channel estimation.

It can be seen in Fig. 3.7 that, for each of the configurations, either SISO, MISO with a single receiver or MISO with two receivers, Wiener estimation is the one that obtains the best performance, with 1 dB difference approximately in comparison to linear channel estimation. For a BER of 10^{-5} it can also be observed that the use of Alamouti for MISO provides 1 dB SNR gain over the SISO case, while when compared to MISO with two receive antennas, not specified in the standard, the gain grows up to 5 dB. As mentioned before, the latter case is more complex in the receiver side but may be convenient due to its good performance and the increase in channel capacity. Linear interpolation algorithm suffers a degradation of approximately 1.5 dB compared to the ideal estimation, whereas Wiener channel estimation outperforms the former, moving up to 1 dB closer to the ideal channel case.

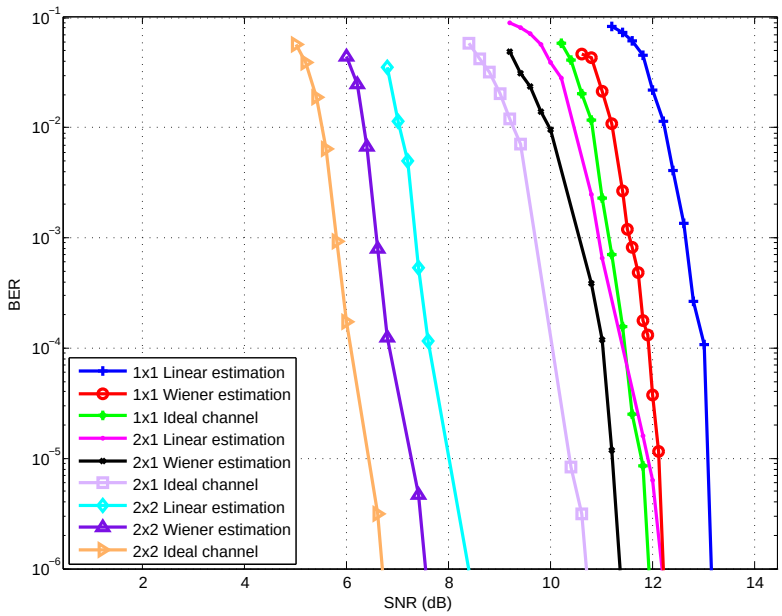

Figure 3.7: BER performance comparison of different channel estimation and interpolation schemes for SISO, MISO with a single receiver and MISO with two receivers in the TU6 channel. DVB-T2 parameters 2K mode, $GI = 1/4$, 16QAM, $CR = 2/3$, 16K LDPC, pilot pattern PP1, 48 FECs

3.3.3 Mobile reception

This section presents the simulation results of DVB-T2 including the proposed channel estimation algorithms in mobile reception. This time, the time variation of the channel must also be tracked and, consequently, two-dimensional Wiener estimation has to be applied. Therefore, in order to see the performance of the algorithm under consideration for a $f_d = 0.022$ of normalized Doppler frequency, this scheme is also assessed assuming perfect CSI with and without Doppler. In the following figures a comparison of BER vs. SNR is shown for SISO, MISO with a single receiver and MISO with two receivers, and the following cases are included; perfectly known time-invariant channel, perfectly known channel with $f_d = 0.022$ and two-dimensional channel estimation with $f_d = 0.022$.

Moreover, each case has been simulated using two FEC (18 and 48 FEC) block sizes, so the effect of temporal interleaving depth can be evaluated in the simulations. Under such conditions, $f_d = 0.022$ corresponds to about 142 km/h of vehicular speed. Fig. 3.8, 3.9 and 3.10 show the results for SISO, MISO with a single receiver and MISO with two receivers, respectively. In all three cases the Doppler frequency in conjunction with time-interleaving added diversity. Note that, in the simulation results provided in this chapter, the ICI term has not been either estimated nor taken into account for detection, as it will be the case in the following chapters.

3.3.3.1 SISO case

Fig. 3.8 depicts the comparison of the BER performance results for different time interleaving depths for ideal CSI and two-dimensional Wiener channel estimation. Focusing on the ideal channel case with no Doppler, 0.5 dB difference can be seen between the 18 and 48 FEC cases. It is also interesting to note that the ideal CSI with $f_d = 0.022$ outperforms the time-invariant case. It may seem contradictory at first glance as time-variations introduce ICI, and consequently, the greater the ICI, the greater the distortion. OFDM systems become more susceptible to time-variations as symbol length increases, which means densely spaced subcarriers, and for the very reason, the 2K mode provides increased robustness against ICI. Although there will come a point at which the Doppler frequency will be detrimental to the system and the performance will get worse, this does not happen here because the Doppler frequency is not high enough and a benefit is obtained due to the diversity introduced by the combination of the Doppler frequency and the time interleaver [Sklar01].

The higher the Doppler frequency, the higher is the obtained gain when introducing time interleaving, and this can be observed in Fig. 3.8, where a gain of 1 dB is obtained between the 18 FEC and 48 FEC cases. Furthermore, the time-variant case outperforms the time-invariant case in 1 dB. When Wiener channel estimation is performed, an error floor comes out both for 18 and 48 FECs.

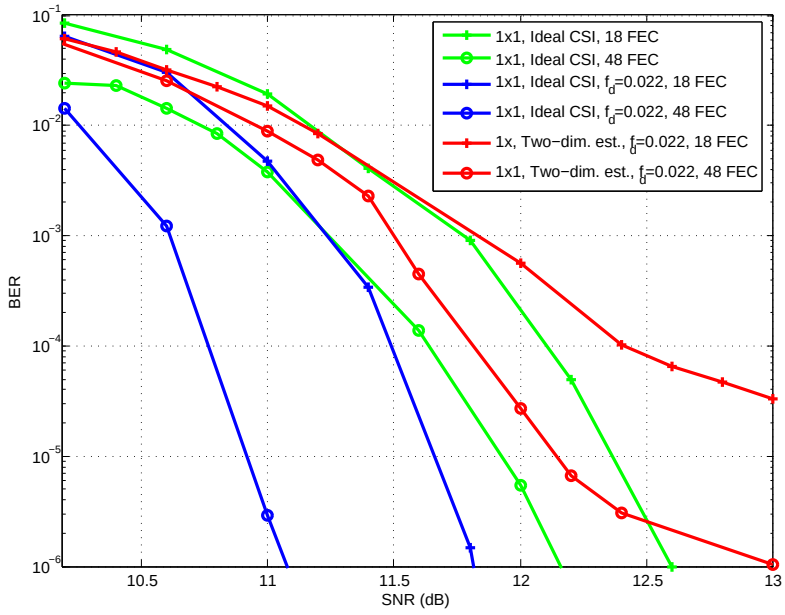

Figure 3.8: BER performance versus SNR for SISO scheme in different scenarios in the time variant TU6 channel with $f_d = 0.022$. DVB-T2 parameters 2K mode, $GI = 1/4$, 16QAM, $CR = 2/3$, 16K LDPC, pilot pattern PP2, 18 and 48 FECs

3.3.3.2 MISO transmission with a single receiver

When another transmission antenna is added, similar results are obtained as shown in Fig. 3.9. In the same way as in the SISO case, the best performance is achieved when perfect CSI is assumed and the channel variation is introduced in the system. The use of multiple antennas introduces diversity in the spatial-domain and its exploitation makes possible to remove the error floor suffered in the case shown in Fig. 3.8 for SISO.

When two-dimensional channel estimation is performed, a degradation of approximately 1.5 dB in SNR is observed between the perfectly known channel with $f_d = 0.022$ and the two-dimensional channel estimation by Wiener filtering for 48 FECs, as can be seen in Fig. 3.9.

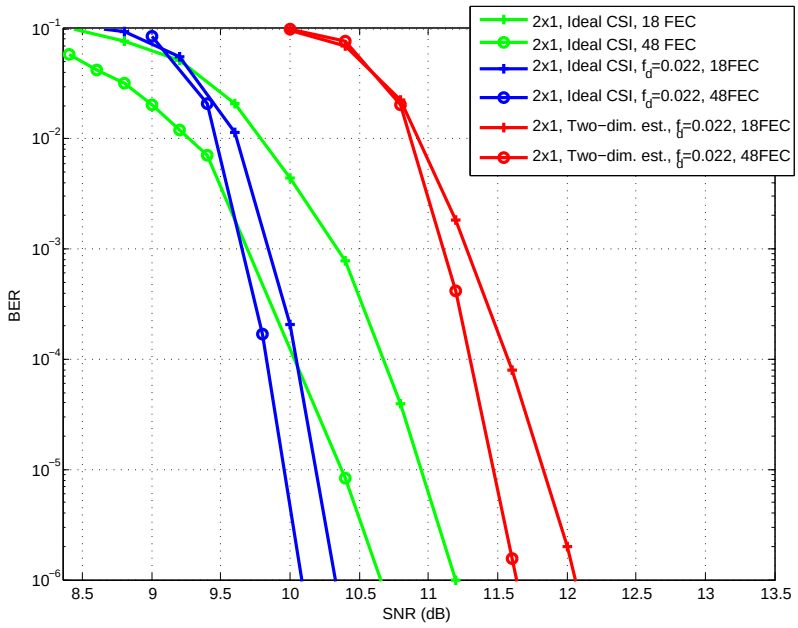

Figure 3.9: BER performance versus SNR for MISO scheme with a single receiver in different scenarios in the time variant TU6 channel with $f_d = 0.022$. DVB-T2 parameters 2K mode, $GI = 1/4$, 16QAM, $CR = 2/3$, 16K LDPC, pilot pattern PP1, 18 and 48 FECs

3.3.3.3 MISO transmission with two receivers

When another receive antenna is added to the system, more diversity gain is obtained as shown in Fig. 3.10, where the performance outperforms the MISO case with a single receiver. The inclusion of two-dimensional channel estimation leads to a degradation of 1 dB compared to the ideal estimation with $f_d = 0.022$, which still remains acceptable since the error floor disappears completely.

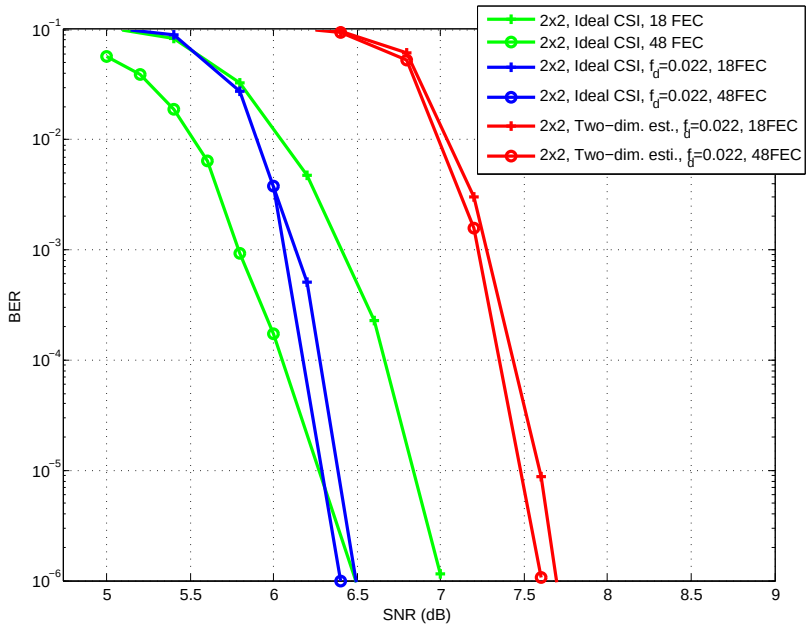

Figure 3.10: BER performance versus SNR for MISO scheme with two receivers in different scenarios in the time variant TU6 channel with $f_d = 0.022$. DVB-T2 parameters 2K mode, $GI = 1/4$, 16QAM, $CR = 2/3$, 16K LDPC, pilot pattern PP1, 18 and 48 FECs

3.3.4 Analysis on the effect of time interleaving

To test the effect of the use of time interleaving, different simulations have been carried out in MISO with one and two receive antennas with 3, 9, 18 and 48 FEC blocks. Note that for the considered time interleaving configuration and transmission parameters, the maximum number of FEC blocks in the TI-block is limited to 137, as set by the standard. However, it has only been simulated up to 48 FECs in order to limit the latency of the system. In addition, it can be seen in Fig. 3.11, that no significant performance improvement is obtained from 18 to 48 FEC blocks. More specifically, an improvement of 0.5 dB and 2.5 dB is observed at BER=10^{-4} between the first and the latter cases for two receive and one receive antennas, respectively.

3.3.5 Simulation results for the proposed improved decision-directed algorithm

This section presents the results obtained through simulations of the DVB-T2 system including the proposed CD3 algorithm for channel estimation. Different channel models have been evaluated: the AWGN channel and the time variant TU6 channel [COST207]. The DVB-T2 parameters employed for the simulations focus on stationary reception and high effective bit rates, as these are the intended modes for DVB-T2's PP8 scheme.

Realistic assumptions have been made for the different simulation blocks. For example

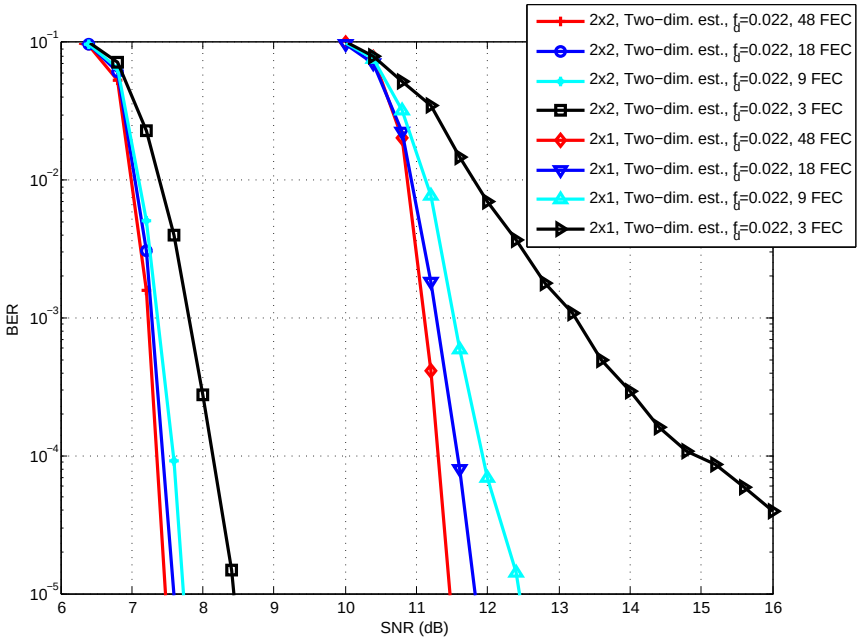

Figure 3.11: Time interleaving performance for MISO with a single receiver and MISO with two receivers in the time variant TU6 channel, 16QAM, $CR = 2/3$, 16K LDPC, 2K FFT, $GI = 1/4$, PP1 for 3, 9, 18 and 48 FECs

the genie-aided demapper defined in the DVB-T2 Implementation Guidelines has not been used. Therefore, simulation results may also vary for the ideal channel estimation from the values given in the DVB-T2 Implementation Guidelines. Additionally, only the non-rotated QAM constellations of DVB-T2 were used. However, the proposed algorithm is also applicable to rotated constellations. On the other hand, in order to limit the simulation time, the results were compared at a BER=10^{-4}. The simulation parameters described in Table 3.2 have been considered for the simulation results shown in this section.

3.3.5.1 AWGN channel

In order to set a proper threshold value of x_{min} for the improved decision-directed algorithm provided in this chapter, simulations have been first carried out for the AWGN channel. Fig. 3.12 depicts the required SNR to achieve a BER<10^{-4} for the DVB-T2 parameter set listed in Table 3.2.

Fig. 3.12 shows clearly the gain of the proposed algorithm compared to the original CD3 algorithm ($x_{min} = 0$). The avoidance of the inner constellation points reduces the required SNR by more than 1 dB, while the optimum threshold is located at $x_{min} = 0.7$. If the value of x_{min} is chosen too large, the required SNR increases again, as only few constellation points are used for the estimation of the channel.

A direct comparison of the analyzed channel estimation techniques (CD3 and the pro-

Table 3.2: Simulation parameters for the proposed modified CD3 algorithm

Parameter	**Value**
Carrier frequency	760 MHz
Bandwidth	8 MHz
Length of LDPC block	64800 bits
Code rate	3/5
Constellation size	256QAM
FFT size	16K
Length of one OFDM block (T_u)	$1792\mu s$
Length of the GI ($T_u/4$)	$448\mu s$
Pilot pattern	PP8

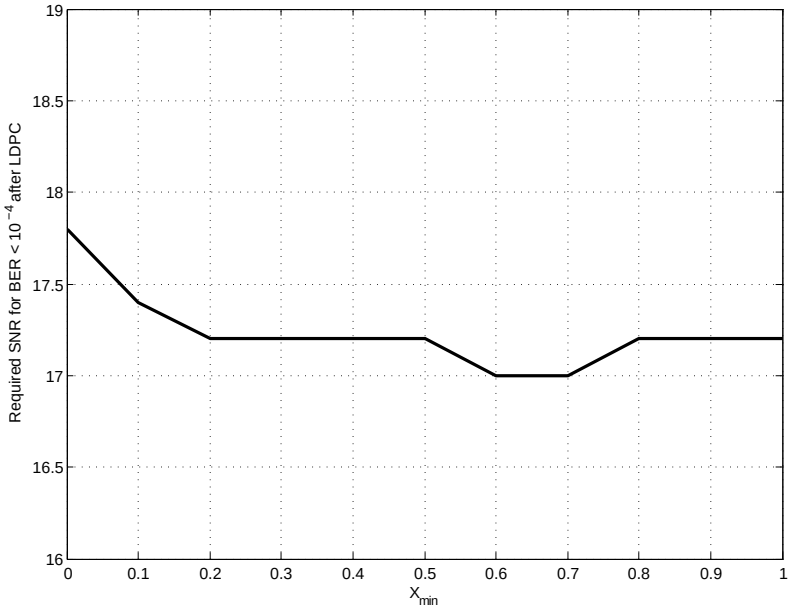

Figure 3.12: Required SNR for BER$<10^{-4}$ in the AWGN channel for different values of x_{min}, where x_{min}=0 corresponds to the original CD3 algorithm with no threshold.

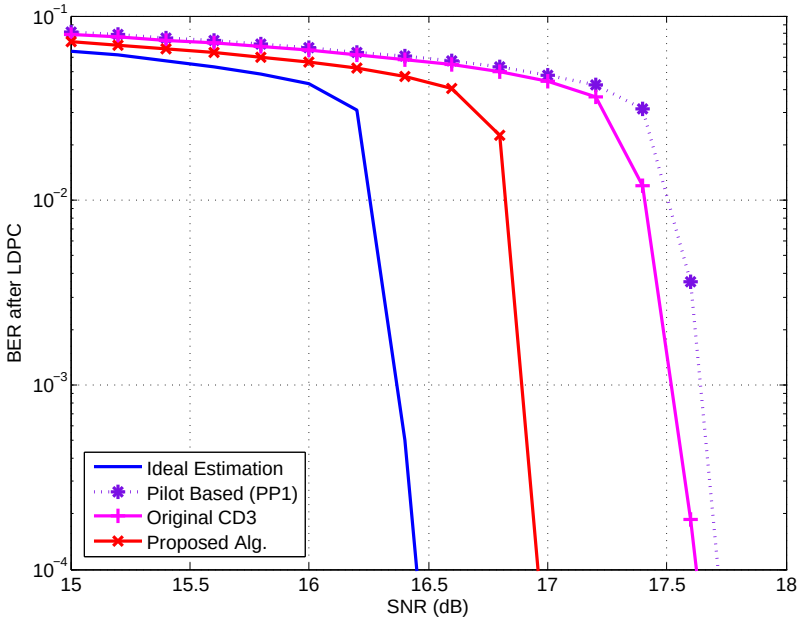

Figure 3.13: Comparison of BER vs. SNR for different channel estimation methods in the AWGN channel, $x_{min} = 0.7$ for the proposed algorithm.

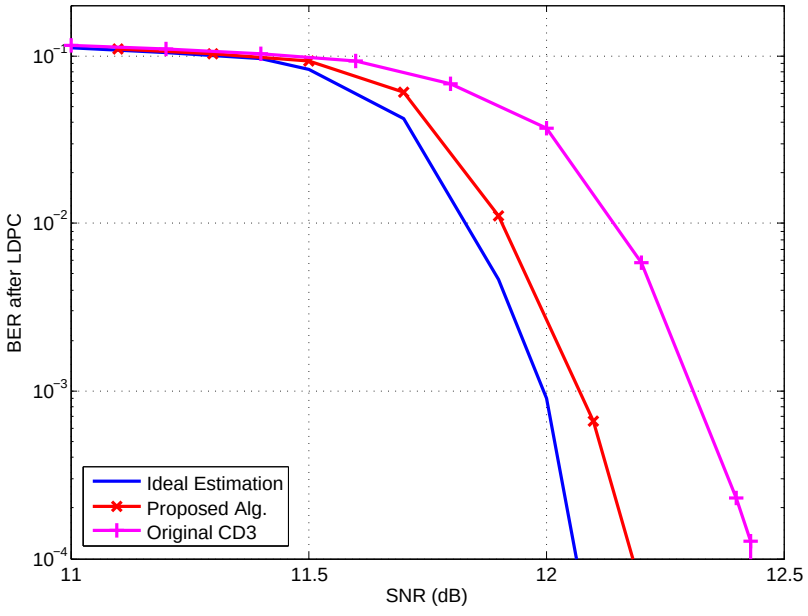

Figure 3.14: Comparison of BER vs. SNR for different channel estimation methods in the AWGN channel, $x_{min} = 1.0$ for the proposed algorithm.

posed algorithm) is shown in Fig. 3.13 for the parameters listed in Table 3.2. Naturally, the ideal channel estimation shows the highest performance, as it knows the channel perfectly. The pilot based channel estimation using the DVB-T2 pilot pattern PP1, which is also the pilot pattern used in DVB-T, shows a degradation of more than 1 dB, while the original CD3 algorithm only provides a slightly better performance. In contrast, the improved algorithm proposed in this chapter suffers a degradation of only 0.5 dB compared to the ideal estimation, and hence outperforms the rest under consideration.

Similar results can also be obtained for 64QAM constellations, as Fig. 3.14 shows for the following DVB-T2 parameter set: 8K FFT, 64QAM and LDPC short code. However, as the ratio of the amplitudes between the inner and outer constellation points is smaller, the gain of the proposed algorithm is reduced to 0.4 dB.

3.3.5.2 TU6 channel

Fig. 3.15 shows simulation results for different channel estimation methods at normalized Doppler frequency of $f_d = 0.0089$, which corresponds to approximately 14 km/h receiver velocity at 760 MHz signal frequency. This simulation has been carried out for the following DVB-T2 parameter set: 8K FFT, GI 1/8, 64QAM (normal) and LDPC long code.

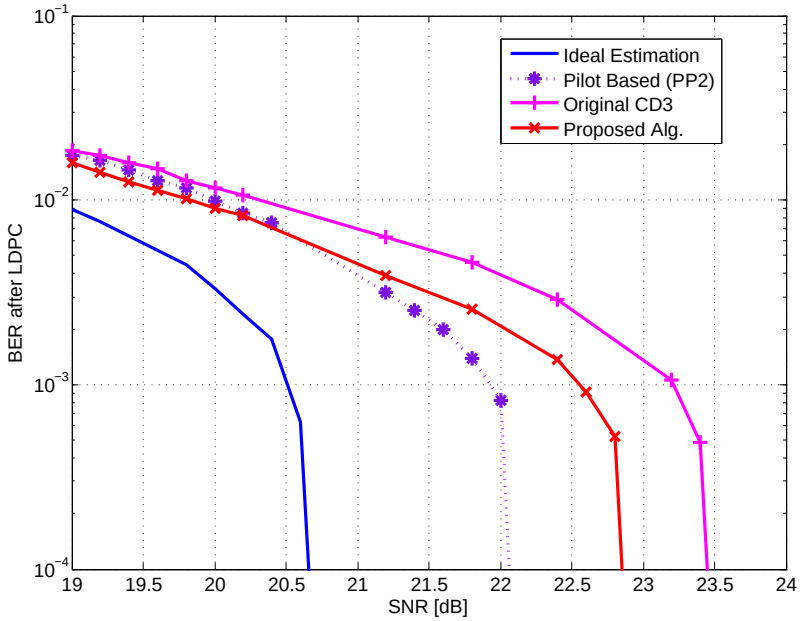

Figure 3.15: Comparison of BER vs. SNR for different channel estimation methods in the time variant TU6 channel with $f_d = 0.0089$, $x_{min} = 0.7$ for the proposed algorithm.

A time-variant channel has increased demands with respect to channel estimation. This specially holds for CD3 and the proposed algorithm, as the channel equalization uses the channel transfer function of the previous OFDM symbol. While the degradation is negligible for lower Doppler frequencies (i.e. low receiver speeds), this degradation gets very important

for high-mobility scenarios. As expected, the ideal channel estimation offers the highest performance. The degradation of the pilot-based estimation is approximately 1 dB, while the pilot pattern PP2 has been used, which is especially optimized for higher receiver speeds. The CD3 and the proposed algorithm show an additional degradation, while the proposed algorithm still outperforms the original CD3 algorithm. However, the degradation compared to the pilot-based channel estimation still remains in an acceptable range.

3.4 Chapter Summary

This chapter has reviewed the main channel estimation techniques for wireless OFDM channels, with particular emphasis on pilot assisted estimation in DVB-T and DVB-T2. Several channel estimation and interpolation techniques and their effects on DVB-T2 systems have been assessed. Accordingly, two-dimensional Wiener interpolation has been proven to be the optimal. Numerical results have been presented under different scenarios and with different interleaving depths for SISO and MISO transmission. It is worth noting that short OFDM blocks are less susceptible to ICI and combined with a suitable Doppler frequency, provide a remarkable performance improvement. Simulation results show that the additional diversity exploited by means of the inclusion of higher Doppler frequency and the combination with the time interleaving can enhance the performance of the system with the proposed parameters. In addition to considering perfect channel estimates, the two-dimensional Wiener filtering has been applied to DVB-T2, studying the behavior of the system making a more realistic assumption and analyzing the effect of channel estimation errors on the BER performance.

The last part of the chapter has focused on decision-directed techniques. A novel scheme has been proposed under the assumption of a slow fading channel in a DVB-T2 framework. The proposed algorithm is designed for channel estimation with a reduced number of pilots in DVB-T2 or similar OFDM-based transmission systems. The proposed algorithm outperforms the original CD3 algorithm [Mignone96] and the pilot-based channel estimation in stationary channels, while the loss in the time-variant channel remains acceptable. Note that the PP8 pilot pattern, in addition to the proposed algorithm, offers an increased spectral efficiency of approximately 8%, as the number of pilots is reduced significantly in comparison to pilot patterns PP1 and PP2. This increased spectral efficiency could also be converted to a lower code rate (CR) of the LDPC code, which will furthermore increase the robustness at similar payload bitrates.

Chapter 4

Basis Expansion Model channel estimation for ICI cancellation in OFDM systems

4.1 Introduction

The first purpose of this chapter is to briefly review the most relevant works that have been published in recent years on channel estimation and equalization in mobile environments, and then analyze the improvements that can be done in these two fields. Regarding channel estimation in DVB-T2, much work has been done in fixed environments, but when it comes to mobile scenarios with rapid time variations, there are only few studies addressing the performance of mobile receivers. In fact, although DVB-T2 was originally designed to support fixed reception, it must also have a positive trend in mobile scenarios. In such case, as it has previously been pointed out in Chapter 2, the channel suffers from ICI, and the channel estimation techniques that were used for time invariant channels are no longer appropriate. Therefore, with the aim of having an efficient performance in mobile environments, the first thing to do is to estimate the complete channel, including ICI, in order to be able to cancel it. Different techniques have been proposed in the literature but basis expansion model (BEM) channel estimation has prevailed in high-mobility scenarios because of its effectiveness and computational affordability.

This chapter makes two proposals to combine ICI detection and channel estimation algorithms. The first one focuses on the use of BEM channel estimation in combination with a maximum a-posteriori (MAP) ICI mitigation algorithm in order to remove the error floor experienced with mid-range normalized Doppler frequencies (from $f_d = 0.045$ to $f_d = 0.18$), with both TU6 and RA6 channels. The second proposed scheme goes further, being able to remove the error floor for much higher normalized Doppler frequencies such as $f_d = 0.5$. This approach is based on the belief propagation (BP) algorithm that has recently been presented in [Ochandiano11b]. Based on the latter and including clustered pilot structures,

which have not ever been proposed for DVB-T and DVB-T2, a joint channel estimation and equalization scheme is proposed, which effectively cancels the ICI with very good results for high-mobility and large FFT modes.

To the author's knowledge, no ICI compensation algorithm has been considered with channel estimation for high-mobility DVB-T2 receivers. Nor has the mentioned BP ICI cancellation algorithm been applied with any technique to track the channel. Therefore, this chapter shows two novel schemes for channel estimation and ICI compensation for high-mobility DVB-T2 receivers. Furthermore, simulation results are provided that show the performance of the system over TU6 and RA6 channels.

4.2 ICI and channel estimation in mobile OFDM

Channel estimation in mobile OFDM systems is a challenging problem. The most useful techniques to combat the ICI and obtain an accurate estimate of the channel in time-varying scenarios, rely on TB or DD methods.

When no a priori knowledge of the channel is available and robust channel estimation has to be achieved, parametric models with a priori knowledge on time-varying multipath channel model parameters can be used. In order to reduce the dimensionality of the problem, these channel estimation schemes assume that the variation of the channel can be described using a finite number of parameters. This issue has been addressed in [vandeBeek95, Hoeher97, Edfors96]. These methods use pilot symbols in order to perform channel estimation with one and two-dimensional filtering imposing a parametric structure on the channel. Other algorithms, require knowledge of some channel parameters that are unknown in general, i.e. in [Yang01], a channel estimation scheme based on the parametric channel modeling which require knowledge of the channel is proposed. High-accurate channel estimation can be achieved if the time-varying channel parameters are known or at the expense of introducing many pilot symbols in the transmitted signal. These assumptions are rarely enforced, because the parameters are unknown and because a trade-off between complexity and performance has to be reached. In [Rom07, Rom08], a study of how the estimation errors in the channel model influences the performance of the system is assessed.

Another parametric models rely on Kalman filter [Banelli07], LS [Cannizzaro06] and MMSE [Barhumi05] channel estimators based on BEM and Slepian basis [Zemen05]. Taylor series are used in [Tomasin05] to counteract the effect of ICI using derivatives of the channel amplitudes. Other channel estimation algorithms are based on second-order statistics [Schniter06] and adaptive channel estimation [Rousseaux04]. The latter exploits all the received symbols that contain contributions from the training sequences and filters out the contribution of the unknown surrounding data symbols.

Many of the above techniques are based on BEM because of its accuracy in doubly-

selective channels. In addition, this model maintains a trade-off between complexity and performance, since the channel can be estimated with a limited number of parameters. Consequently, this model has been chosen and applied to the scenario considered in this thesis to obtain the results provided in this chapter.

4.3 BEM channel estimation

In order to reduce the number of parameters required for channel estimation in time-varying channels, the BEM channel estimation was originally introduced in [Giannakis98]. The latter and [Tsatsanis96a, Tsatsanis96b, Ma03, Kannu05] represent the doubly selective channel by means of a complex exponential BEM (CE-BEM). Thenceforth, several authors have used BEM to successfully model the time-varying channel [Ma03, Gorokhov04]. For block transmissions, [Ma03] has modeled the channel using BEM and has shown the optimality of time-domain training pilots in terms of MSE for PSAM. In [Kannu05] the same criterion was considered in the frequency-domain, that is to say, instead of using zero-guarded time-domain pilot symbols, pilot carriers surrounded by zeros were used in a pilot scheme referred to as frequency-domain Kronecker delta (FDKD). These frequency guard bands surrounding the pilots are necessary to keep the orthogonality between data and pilots. Nevertheless, non orthogonal designs can also be used [He08].

Apart from CE-BEM, several BEM methods are proposed in the literature: Polynomial BEM (P-BEM) [Borah99], Legendre polynomials [Hrycak11], (DPS-BEM) [Zemen05] and complex exponentials oversampled in the frequency-domain [Leus04], also called General Complex Exponential BEM (GCE-BEM). In [Tang07a], the modeling error of several BEM bases is evaluated, analyzing the criterion to select the interference to be taken into account for different channel estimators. Among all BEM bases, the best performance is obtained via DPS sequences as is explained and tested in [Zemen03a, Zemen03b].

As it has been described in Section 2.5.3.1, as the ICI becomes more important, the ICI power is spread out throughout the matrix with most of its power concentrated around the main diagonal. For that reason, in order to obtain a perfect estimate, the full frequency matrix should be taken into account [Gorokhov04, Cui05]. The simplest approach is to view the frequency-domain channel matrix as approximately banded instead, that is to say, to consider a channel matrix where most of its power is located around the main diagonal [Tang07a]. This approach is not followed by the CE-BEM technique since it views the matrix as strictly banded, selecting $Q/2$ subdiagonals at each side of the main diagonal. Although taking the matrix as strictly banded may induce a larger error than in the approximately banded case, CE-BEM is considered in this thesis due to its algebraic ease and its performances at high-Doppler frequencies.

On the other hand, in [Giannakis98] blind techniques are reviewed and applied to esti-

mate the BEM parameters and the model orders. Blind techniques using a basis expansion approach are also studied in [Tsatsanis96a, Cirpan99, Leus03, Tugnait02]. These methods provide high spectral efficiency, since they do not require known reference signals to be inserted at the transmitter for subsequent channel estimation and therefore do not have overhead loss. Besides, these techniques rely on statistical information and hence, long data records are required.

Considering that DVB-T2 always carries a minimum amount of pilots, pilot-aided BEM channel estimation has been chosen in this thesis for mobile DVB receivers due to its lower computational complexity and better performance in time-varying environments.

4.3.1 BEM model

A very efficient way to approximate the banded channel response is using a BEM model, where the relation between BEM channel coefficients and the full channel response can be defined as

$$\overline{\mathbf{h}}_l = \mathbf{B} \cdot \mathbf{h}_{u,l}, \tag{4.1}$$

where $\overline{\mathbf{h}}_l$, is an $N \times 1$ vector that contains the channel coefficients for the l-th channel tap over the N samples of an OFDM symbol. This way, instead of estimating the N channel coefficients for each tap, we only need to estimate the $(Q+1)$ BEM coefficients $\mathbf{h}_{u,l} = [h_{0,l}, \cdots, h_{Q,l}]^T$, resulting in a significant reduction of the number of parameters to be estimated, namely $(Q+1) \times L$ for each OFDM symbol. $\mathbf{B} = [\mathbf{b}_0, \cdots, \mathbf{b}_Q]$ is an $N \times (Q+1)$ matrix that contains $Q+1$ basis functions $\mathbf{b}_q$ as columns, where $\mathbf{b}_q = [b_{q,0}, \cdots, b_{q,N-1}]^T$. Stacking all the channel taps, i.e. $\mathbf{h}_u = [h_{0,0}, \cdots, h_{0,L-1}, \cdots, h_{Q,0}, \cdots, h_{Q,L-1}]$, yields

$$\overline{\mathbf{H}} = (\mathbf{B} \otimes \mathbf{I}_L)\mathbf{h}_u, \tag{4.2}$$

For the case of the CE-BEM algorithm analyzed in this chapter, the elements of the matrix $\mathbf{B}$ at indexes α and β, i.e. $b_{\alpha,\beta}$, are defined as

$$b_{\alpha,\beta} = exp(j2\pi\alpha/N)(\beta - \beta/2). \tag{4.3}$$

Substituting (4.2) in (2.4), yields

$$\mathbf{y} = \mathbf{F}\overline{\mathbf{H}}\mathbf{F}^H\mathbf{x} + \mathbf{F}\mathbf{z} = \sum_{q=0}^{Q} \mathbf{D}_q \cdot \mathbf{\Delta}_q \cdot \mathbf{x} + \mathbf{w}, \tag{4.4}$$

where $\mathbf{D}_q$ is a circulant matrix containing the frequency response of the qth basis function as its first column. This matrix is graphically shown in Fig. 4.1 and can be expressed as

$$\mathbf{D}_q = \mathbf{F}\text{diag}\left\{\mathbf{b}_q\right\}\mathbf{F}^H. \tag{4.5}$$

On the other hand, $\mathbf{\Delta}_q$ is the frequency response of the q-th BEM component and is calculated as

$$\mathbf{\Delta}_q = \text{diag}\left\{\mathbf{F}_L[h_{q,0}, \cdots, h_{q,L-1}]^T\right\}, \tag{4.6}$$

where $\mathbf{F}_L$ consists of the first L columns of the matrix $\sqrt{N}\mathbf{F}$. The columns of $\mathbf{D}_q$ correspond to the positions of the data and pilot symbols, whereas the rows contain the observation samples.

In order to estimate ICI and isolate data symbols from pilots, the latter are grouped into C clusters, each containing L_p pilots, as it will be explained in the next section. Stacking together all the transmitted and receive samples for each cluster c yields

$$\mathbf{y}_c = \underbrace{\sum_{q=0}^{Q} \mathbf{D}_{q,c}^{(p)} \cdot \mathbf{\Delta}_q^{(p)} \cdot \mathbf{x}^{(p)}}_{\mathbf{p}_c} + \underbrace{\sum_{q=0}^{Q} \mathbf{D}_{q,c}^{(d)} \cdot \mathbf{\Delta}_q^{(d)} \cdot \mathbf{x}^{(d)}}_{\mathbf{d}_c} + \mathbf{w}_c. \tag{4.7}$$

The term $\mathbf{p}_c$ reflects the effects of known pilot carriers on the received samples of a cluster, while $\mathbf{d}_c$ reflects the effect of unknown data, which is neglected and regarded as interference. More specifically, $\mathbf{D}_{q,c}^{(p)}$ is a $(L_p + 2B_c) \times CL_p$ submatrix of $\mathbf{D}_q$ that contains information concerning the relationship between the positions of the pilot carriers and the received samples for cluster c, and is represented by the striped areas in Fig. 4.1. In contrast, $\mathbf{D}_{q,c}^{(d)}$ is a $(L_p + 2B_c) \times (N - CL_p)$ is a submatrix related to the data carriers represented by the light shaded areas, where the vertical axis represents the contribution of the q-th component to the received sample and the horizontal axis is $\mathbf{\Delta}_q \cdot \mathbf{x}$.

A pilot cluster of length L_p is defined as $\mathbf{x}_c^{(p)} = \left[x_{b_c}, \cdots, x_{b_c+L_p-1}\right]^T$, where b_c is the first position in the cluster. The observation samples considered for channel estimation can then be expressed as

$$\mathbf{y}_c = \left[y_{b_c-B_c}, \cdots, y_{b_c+L_p+B_c-1}\right]. \tag{4.8}$$

The B_c parameter controls the amount of receive subcarriers that are going to be taken into account. A negative B_c means that fewer observation samples than transmitted pilots are going to be considered for estimation purposes, so the interference of data symbols is reduced. An example of this can be seen in Fig. 4.4, where $L_p = 5$ and $B_c = -1$. On the other hand, a positive B_c means that samples affected wholly or partially by unknown information are also used for channel estimation, resulting in severe performance degradation.

In order to obtain the BEM coefficients, (4.7) can be rewritten as a function of $\mathbf{h}_u$, (see [Tang07a] for further details), yielding

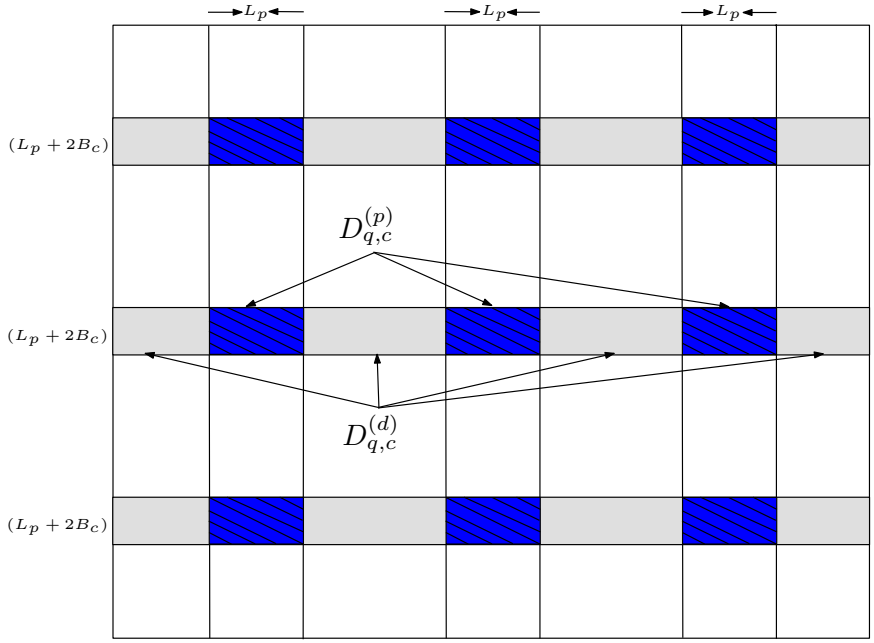

Figure 4.1: Relationship between transmitted pilots and received symbols for the q-th basis.

$$\mathbf{y}_c = \mathbf{D}_c^{(p)} \mathtt{X}^{(p)} \mathbf{h}_u + \mathbf{d}_c + \mathbf{w}_c, \tag{4.9}$$

with,

$$\mathbf{D}_c^{(p)} = \left[\mathbf{D}_{0,c}^{(p)}, \cdots, \mathbf{D}_{Q,c}^{(p)} \right], \tag{4.10}$$

and

$$\mathtt{X}^{(p)} = \mathbf{I}_{Q+1} \otimes \left(\text{diag} \left\{ \mathbf{x}^{(p)} \right\} \mathbf{F}_L^{(p)} \right), \tag{4.11}$$

where $\mathbf{F}_L^{(p)}$ are the rows of the matrix $\mathbf{F}_L$ corresponding to the position of the pilots. Similarly, applying the same process to all the observation vectors leads to the following expression

$$\mathbf{y}^{(p)} = \mathbf{D}^{(p)} \mathtt{X}^{(p)} \mathbf{h}_u + \mathbf{d} + \mathbf{w}^{(p)} = \mathtt{P} \mathbf{h}_u + \mathbf{d} + \mathbf{w}^{(p)}, \tag{4.12}$$

where all the pilots have been stuck together, i.e., $\mathbf{y}^{(p)} = \left[\mathbf{y}_0^T, \cdots, \mathbf{y}_{C-1}^T \right]^T$, $\mathbf{d} = \left[\mathbf{d}_0^T, \cdots, \mathbf{d}_{C-1}^T \right]^T$, $\mathbf{w}^{(p)} = \left[\mathbf{w}_0^T, \cdots, \mathbf{w}_{C-1}^T \right]^T$ and $\mathtt{P} = \mathbf{D}^{(p)} \mathtt{X}^{(p)}$ have been defined, with

$$\mathbf{D}^{(p)} = \left[\mathbf{D}_0^{(p)T}, \cdots, \mathbf{D}_{C-1}^{(p)T} \right]^T = \begin{bmatrix} \mathbf{D}_{0,0}^{(p)} & \cdots & \mathbf{D}_{Q,0}^{(p)} \\ \vdots & \ddots & \vdots \\ \mathbf{D}_{0,C-1}^{(p)} & \cdots & \mathbf{D}_{Q,C-1}^{(p)} \end{bmatrix}. \tag{4.13}$$

The same analysis can be done for the interference term $\mathbf{d}$ in 4.12 as follows

$$\mathbf{d} = \mathbf{D}^{(d)} \mathbb{X}^{(d)} \mathbf{h}_u, \tag{4.14}$$

where

$$\mathbf{D}^{(d)} = \left[\mathbf{D}_0^{(d)T}, \cdots, \mathbf{D}_{C-1}^{(d)T} \right]^T = \begin{bmatrix} \mathbf{D}_{0,0}^{(d)} & \cdots & \mathbf{D}_{Q,0}^{(d)} \\ \vdots & \ddots & \vdots \\ \mathbf{D}_{0,C-1}^{(d)} & \cdots & \mathbf{D}_{Q,C-1}^{(d)} \end{bmatrix}. \tag{4.15}$$

However, for CE-BEM the matrix is assumed strictly banded, and hence, this term $\mathbf{d}$ is neglected. Consequently, this approach will induce an error since the channel matrix is not actually strictly banded. Now, the goal is to estimate $\mathbf{h}_u$ from (4.12) through a MMSE estimator. Note that, although this technique requires a matrix inversion, it does not involve so much computational complexity, as the channel has been modeled with BEM and, therefore, has less parameters. Hence the estimation of the channel coefficients in the BEM basis can be obtained as

$$\hat{\mathbf{h}_u} = \mathbf{W}_{\text{MMSE}} \mathbf{y}^{(p)}, \tag{4.16}$$

where

$$\mathbf{W}_{\text{MMSE}} = \mathtt{P}^H (\mathtt{P}\mathtt{P}^H + \mathbf{R}_w^{(p)})^{-1}. \tag{4.17}$$

The covariance matrix of the noise is $\mathbf{R}_w^{(p)} = E\left\{ \mathbf{w}^{(p)} \mathbf{w}^{(p)H} \right\}$. By substituting $\hat{\mathbf{h}_u}$ in (4.2), the full channel matrix $\overline{\mathbf{H}}$ in time-domain is obtained. This way, taking the FFT of $\overline{\mathbf{H}}$ leads to the CFR. Note that there is no need to calculate the entire $\mathbf{H}$ matrix, which would add a prohibitive complexity, as the power is mostly concentrated around the main diagonal. Therefore, only the main and two neighboring diagonals are estimated for $Q = 2$.

4.3.1.1 Complexity considerations

The complexity of the considered CE-BEM channel estimation technique is briefly analyzed here, where it is important to distinguish between offline and online complexity. Offline complexity accounts for the computation that is not performed in real-time. In this case, some matrices, such as $\mathbf{B}$, $\mathbf{D}$ and $\mathbf{F}_L$, can be precomputed and stored. That is why the online complexity of the estimator is mainly related to the matrix inversion involved in (4.17). Consequently, it is conditioned by the total pilot carriers in an OFDM symbol and implies a cubic complexity order with $\mathcal{O}\left(((L_p + 2B_c)C)^3\right)$. Once $\mathbf{W}_{\text{MMSE}}$ has been obtained through a matrix product, the BEM coefficients for all the channel taps $\hat{\mathbf{h}_u}$ are calculated, for which the number of channel taps L and the number of basis function $Q + 1$ are the key parameters. Finally, in order to obtain the time-domain channel matrix $\overline{\mathbf{H}}$, the number of

adjacent diagonals used to estimate the ICI, i.e. Q, are decisive in the final calculation.

4.3.2 Proposed pilot clustering for high-mobility DVB-T2

The problem of combating the ICI that arises in time-varying channels has been addressed in [Stamoulis02, Dai07], where they addressed the problem of different pilot placement schemes for a given number of pilot carriers, showing that it is beneficial and therefore necessary to group the pilots together into different clusters in order to obtain a good estimate of the channel. Recently in [Tang07b] a comparative study of different clustered pilot schemes with GCE-BEM was carried out. Three different pilot schemes were presented (block-type, comb-type and mixed-type), the latter being a combination of the previous two, in order to assess the effects of the pilot schemes on the estimation performance for different channel conditions and Doppler frequencies. In a less frequency selective channel, the comb-type pilot scheme outperforms the other two. However, when the channel varies faster, the mixed-type works better. This has been tested for a very small normalized Doppler frequency ($f_d = 0.004$) and, as long as the Doppler frequency gets higher, this no longer holds true due to the stronger variation between different OFDM symbols, being the comb-type scheme the one that works best as it carries pilot clusters in each OFDM symbol [Nilsson97].

In order to estimate the channel correctly, we adapt the pilot structure of DVB-T2 so that pilots have to be clustered in C groups of L_p pilots as illustrated in Fig. 4.2.

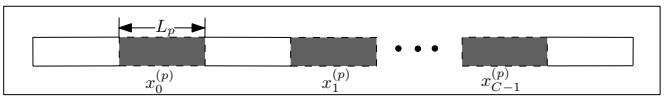

Figure 4.2: Proposed pilot placement for BEM-based ICI and channel estimation.

Inside each cluster $\mathbf{x}_c^{(p)}$, where $c = 0, 1, \cdots, C-1$, the scheme that has been adopted is the FDKD structure mentioned in the previous section, where a nonzero pilot is placed in the middle of the cluster with zero guard bands on both sides [Kannu05]. Stacking all the pilot clusters together into a pilot vector yields $\mathbf{x}^{(p)} = \left[\mathbf{x}_0^{(p)T}, \cdots, \mathbf{x}_{C-1}^{(p)T}\right]^T$. By keeping constant the number of pilots carriers, these pilots can be grouped in different ways to address intercarrier interference caused by the Doppler effect. Put in other words, for a given amount of pilot subcarriers, the performance changes depending on the size of the clusters being used.

Fig. 4.3 shows the evolution of channel estimation accuracy for different cluster lengths for high Doppler frequencies. However, when this Doppler frequency remains small (up to f_d = 0.1), the common pilot pattern scheme with L_p=1, that is to say, with only one pilot per cluster, outperforms the L_p=3 case. That makes sense, because when there is no ICI or this is very low, it is more advantageous to have equally spaced pilots in order to estimate the channel better in the frequency-domain. In contrast, when the channel varies faster due to

the motion of the receiver, the orthogonality between the subcarriers is broken and the pilot carriers receive interference from neighboring data carriers. For that reason, it is necessary to use larger clusters when estimating the channel in mobile environments.

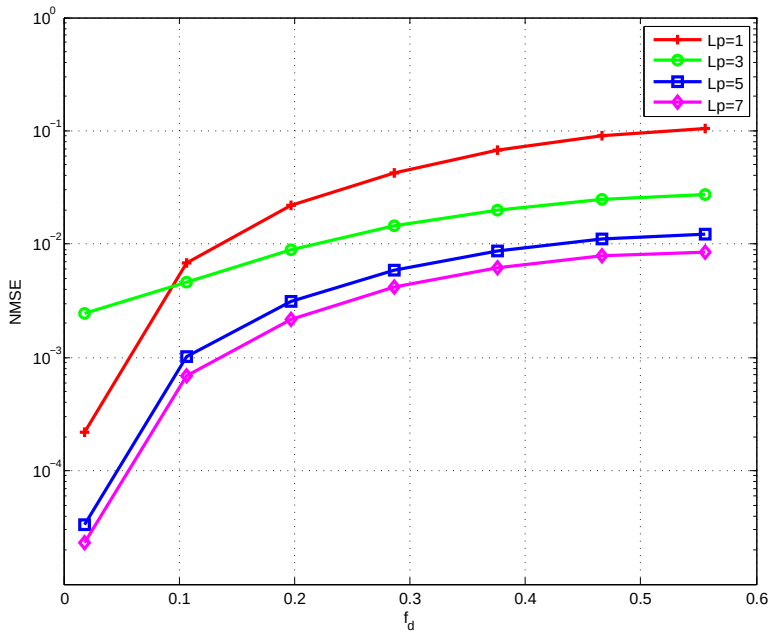

Figure 4.3: NMSE performance versus normalized Doppler frequency for TU6 channel in 32K mode for high SNR (60 dB).

Although the best performance is obtained with L_p=7 and 5 observation samples, in order to achieve a trade-off between complexity and performance and to follow the same criterion for all the simulations, the parameters that have been chosen are L_p=5 and 3 observation samples, i.e. $B_c = -1$. The transmitted signal is formed by pilot (PC) and data carriers (DC), as can be seen in Fig. 4.4. Some observation samples are affected by unknown information (data carriers), some others are affected by known pilot carriers and the rest are affected by both (pilot and data carriers). In order to have an accurate estimation, it is simpler to take into account only the samples affected by pilot carriers, so the effect in each observation is known and can be easily removed. In the case of 5 pilot carriers in each cluster, this condition is fulfilled with 3 observations, as are those that are free from interference as is depicted in Fig. 4.4. Note that, if the FDKD pilot structure is used, only $P3$ would have a non-zero value in Fig. 4.4.

As can be seen in the Fig. 4.3, the results with L_p=5 are satisfactory and a great saving in computational effort is achieved when adding the improvements that will be explained later on, in Chapter 5.

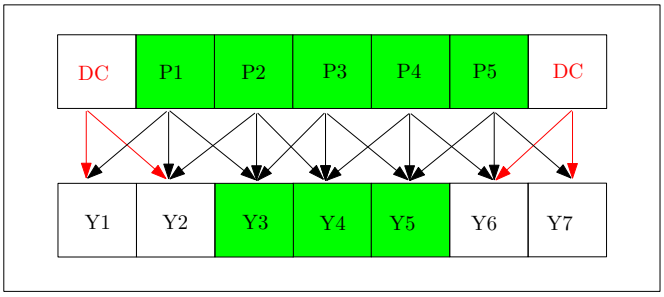

Figure 4.4: Transmitted and received samples.

4.4 ICI cancellation techniques

Many research works have addressed ICI cancellation in the literature. In general, ICI suppressing techniques can be classified into two different groups. The first ones estimate the interference produced by the ICI and subtract it from the signal [Peng06, Hwang09], and the other ones use ICI as an advantage to exploit the frequency diversity it introduces [Liu09, Ochandiano11a].

On one hand, linear equalizers have been widely used, specially zero forcing (ZF) [Hsu09] and MMSE algorithms [Rugini05b, Fang08, Rugini06, Jeon99]. These equalization techniques require a large matrix inversion, so they are prohibitively complex. Hence, these problem has been solved by taking into account only some off-diagonal elements of the channel matrix, which is pretty accurate since most of the power is concentrated around the main diagonal.

If joint detection and decoding are done at the receiver, the soft information coming from the decoder can help ICI cancellation and the BER performance can be significantly improved. This scheme, called turbo ICI equalization [Douillard95, Tuchler02], is explained in more detail in Section 4.4.3.2. In [Schniter04] this approach is applied through an iterative MMSE serial linear equalizer (SLE) in time-domain and in [Fang08] this approach is outperformed by a block linear equalizer (BLE).

On the other hand, non-linear equalizers are more complex but have a better performance. Following these approaches, the ICI is removed by serial interference cancellation (SIC) in [Hwang09], and parallel interference cancellation (PIC) in [Molisch07]. The sphere decoder (SD) has also been applied to suppress inter-carrier interference in [Kou05].

This chapter presents two novel schemes that have been proposed to deal with ICI cancellation with BEM channel estimation. The first one uses a MAP ICI canceler whereas the second one addresses a belief-propagation or factor-graph based ICI detection. The former is directly addressed over a DVB-T2 framework whereas the latter is evaluated over a BICM-OFDM system model, although its results will extended to DVB-T2 in the following chapter, where a fully iterative receiver is proposed for very high mobility.

4.4.1 ICI cancellation in DVB-T and DVB-T2

If we focus more specifically on DVB systems, many research works have addressed the issue of ICI cancellation for DVB-T [Tomasin05, Wilhelmsson07, Poggioni09], but not much attention has been put on DVB-T2 [Ochandiano10, Baracca11]. In [Baracca11] they focus on systems with very long OFDM blocks and propose a pre-equalizer to combat time variations of the channel for the DVB-T2 standard. The main disadvantage of the latter is that pilot carriers can not be used for channel estimation purposes. In [Ochandiano10], the impact of using a MAP ICI compensating scheme [Peng06], and an iterative turbo version of it is analyzed for DVB-T2, showing its good performance in realistic scenarios and assuming perfect knowledge of the channel. Nevertheless, their efficiency in realistic DVB-T2 reception including channel estimation remains an open issue.

The following sections describe the two ICI canceling algorithms that have been considered as candidate for their combination with BEM estimation.

4.4.2 Iterative MAP ICI canceler

Once the ICI parameters are estimated, a low-complexity MAP detector [Peng06] can suppress it profiting from the frequency diversity it provides. The detection process consists of two stages: the first one estimates the transmitted signal X_n in frequency-domain through a pseudo-Viterbi algorithm. The second one improves the detection process by suppressing the effects of ICI based on the estimated signal.

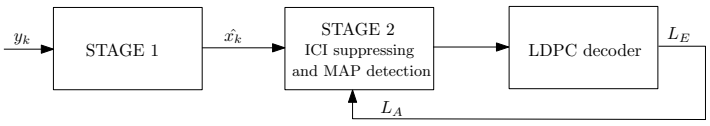

Figure 4.5: Structure of the iterative ICI suppressing soft MAP detector.

This iterative soft demapper, shown in Fig. 4.5 and introduced in [Ochandiano10] for a DVB scenario, uses the extrinsic likelihood values provided by the LDPC decoder as a priori information (L_A) for the demapping process. Thus, it is no longer assumed that all states of the constellation are equiprobable. In the implementation guidelines of [DVB09], an iterative receiver scheme based on feeding the extrinsic information generated by the LDPC decoder back to the demapping process as a priori information is suggested. This can be achieved with the proposed ICI detector, where 3 external (information exchange between the LDPC decoder and the MAP suppressing demapper) and 50 internal (iterations within the LDPC decoder) iterations are carried out.

4.4.3 Belief Propagation ICI detection algorithm

Although the previous scheme, presented in [Martínez11] for DVB-T2 reception with channel estimation, provides good results for a normalized Doppler frequencies of up to $f_d = 0.045$ at urban (TU6) scenario for a 16QAM constellation, more suitable techniques are needed to counteract this effect as the Doppler frequency increases. Hence, new ICI detection techniques are required to provide good reception in high-mobility DVB receivers.

Recently, a novel ICI mitigating approach based on the so-called BP algorithm has been presented in [Ochandiano11b]. When the ICI power is high or large FFT sizes are being used, very good performance is achieved with the proposed iterative equalizer. The proposed receiver has the following architecture:

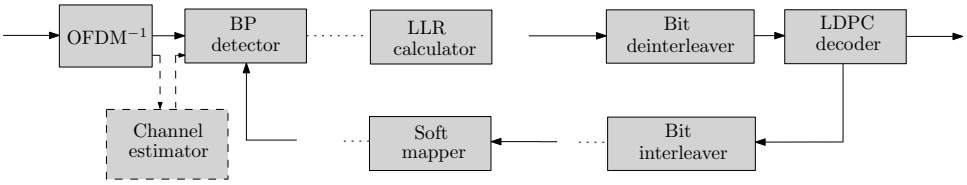

Figure 4.6: Simplified block diagram of the proposed iterative BP-based receiver.

As it can be seen in the figure, this receiver comprises a BP detector, a LDPC decoder and a BEM channel estimator. In addition a turbo approach is applied exchanging soft information between the decoder and the detector. For this scheme, 2 iterations are performed in the BP detector and 20 iterations in the LDPC decoder. 5 turbo iterations (extrinsic information exchange between the LDPC decoder and the BP detector) are performed.

This proposal encompasses a new iterative receiver, combining BEM channel estimation and a BP algorithm for ICI cancellation in DVB systems with very high mobility. The high ICI power can provide diversity if it is correctly processed by the detector, which requires a good knowledge of the complete channel, including ICI. Simulation results show the very good performance of the proposed novel joint algorithm that not only cancels the ICI, but also greatly benefits from the diversity it introduces, providing specially good results under high mobility scenarios. In the approach of Fig. 4.6, channel estimation is only calculated once, and then introduced in the BP detector. This architecture will be extended to a fully iterative scheme in the last chapter of this PhD dissertation.

4.4.3.1 Belief propagation algorithm

This algorithm is based on the application of the sum-product algorithm (SPA) algorithm to a factor graph (FG), representing the joint APP of the transmitted symbols. Following the Bayesian theory, the transmission of a random signal over an AWGN-affected channel can be modeled as

$$P(\mathbf{x},\mathbf{y}) = P(\mathbf{x}|\mathbf{y})\,P(\mathbf{y}) = P(\mathbf{y}|\mathbf{x})\,P(\mathbf{x}), \tag{4.18}$$

where $P(\cdot)$ refers to the probability density function, and $\mathbf{x}$ and $\mathbf{y}$ are the transmitted and received vectors in frequency-domain, respectively. In order to minimize the BER, a MAP symbol detection strategy can be performed, which is formulated as

$$\hat{x}_k = \arg\max_{x_k} P(x_k|\mathbf{y}). \tag{4.19}$$

The calculation of the marginal APP $P(x_k|\mathbf{y})$ is a quite challenging task and it is here where FGs offer an elegant solution. The factorization of $P(\mathbf{y}|\mathbf{x})$ is given by

$$P(\mathbf{y}|\mathbf{x}) \propto \prod_{k=1}^{N} f_k(x_{k-1}, x_k, x_{k+1}), \tag{4.20}$$

where N is the number of subcarriers in the model and hence, $x_k = 0$ for $k \leq 0$ and $k > N$ and

$$f_k(x_{k-1}, x_k, x_{k+1}) \propto \exp\left(-\frac{\left|y_k - \sum_{n=k-1}^{k+1} H_{kn}x_n\right|^2}{\sigma_k^2}\right), \tag{4.21}$$

where H_{kn} is the (k-th, n-th) value of the frequency-domain channel matrix $\mathbf{H}$. Fig. 4.7 depicts the equalizer's factor graph considering two neighboring subcarriers involved in ICI, one at each side of a subcarrier, where variable nodes x_k are associated with factor nodes f_k. Applying the SPA algorithm (the same as the one used in LDPC decoding) to this graph allows us to compute marginal APPs after iterating between function and variable nodes. As it is pointed out in [Ochandiano11b], this iterative process not only corrects the ICI, but also exploits the frequency diversity introduced by it.

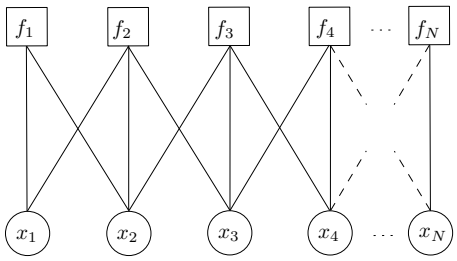

Figure 4.7: Structure of the ICI detector factor graph corresponding to factor $f_k(x_{k-1}, x_k, x_{k+1})$.

Simulation results show that this new iterative detection strategy achieves good performance when ICI power is high, which can be due to high mobility or the use of large FFT sizes. Its application to the new DVB-T2 broadcasting standard has been tested for different

realistic mobile scenarios, allowing good reception even in receivers with very high mobility, up to $f_d = 0.5$ of normalized Doppler frequency. These results will be discussed at the end of this chapter, in Section 4.5.3.

4.4.3.2 Turbo receiver

An iterative turbo receiver exchanges soft information between the detector and the decoder, in order to reduce the BER, as shown in Fig. 4.8. More specifically, a LDPC decoder and the BP detector described in Section 4.4.3.1 have been considered in this research work.

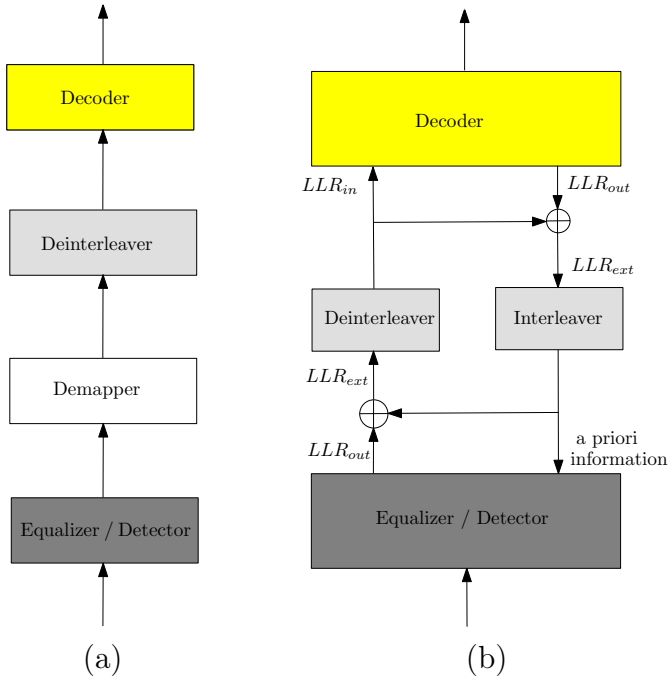

Figure 4.8: Block diagram of Single-tap equalization (a). Turbo-equalization (b).

As can be seen in Fig. 4.8, the LDPC decoder requires soft estimates of the transmitted information bits, which are provided by the soft output detector. This information is calculated through the APP of the received symbols as:

$$P(b_k = b|\mathbf{y}) = \sum_{\forall \mathbf{b}:b_k=b} P(\mathbf{b}|\mathbf{y}) = \sum_{\forall \mathbf{b}:b_k=b} \frac{p(\mathbf{y}|\mathbf{b})P(\mathbf{b}))}{p(\mathbf{y})}, \tag{4.22}$$

where $\mathbf{b} = (b_1, b_2, \cdots, b_k)^T$ is a sequence of independent data bits b_k and $P(b)$ is the *a priori* probability that enters the detector depicted in Fig. 4.8. The *a priori* information is provided by the decoder and hence, in the initial equalization step, no *a priori* information is available.

This APP is expressed with the log-likelihood ratio (LLR)'s or L-values [Hagenauer96], which can be defined as:

$$L(b_k) = ln\frac{P_r\left[b_k = +1\right]}{P_r\left[b_k = -1\right]}, \tag{4.23}$$

where positive and negative LLR mean logical 1 and 0, respectively. Hence, the absolute value of each LLR corresponds to the reliability of that particular bit. Given the received symbol y, the *a posteriori* information $L(b_k|y)$ can be expressed as follows:

$$L(b_k|y) = ln\frac{P_r\left[b_k = +1|\, y\right]}{P_r\left[b_k = -1|\, y\right]} = L_{ext}(b_k|\mathbf{y}) + L(b_k), \tag{4.24}$$

The a priori information $L(b_k)$ is substracted from the *a posteriori* information to obtain the extrinsic information, that is to say, the information about b_k contained in $\mathbf{y}$.

4.5 Simulation Results

In this section, the performance of the systems previously described has been analyzed in terms of BER. Firstly, simulations results for the MAP detector are shown with BEM channel estimation. This novel receiver, provides good results at high Doppler frequencies in both TU6 and RA6 channels. The performance of the algorithm is tested through computer simulations showing a BER improvement with respect to single-tap equalization in several commonly used channels. Moreover, the combination of ICI cancellation and BEM channel estimation algorithms outperforms the perfect channel knowledge case with low and moderate Doppler frequencies (ideal channel with no ICI cancellation), and the error floor experienced with the latter is removed.

However, although this results are good enough, e.g. for a normalized Doppler frequency of $f_d = 0.045$ at urban TU6 scenario and 16QAM constellation, more suitable techniques are needed to counteract this effect as the Doppler frequency increases. This limitations can be overcome if the second proposed scheme is used. Provided results show that the proposed BP ICI detector with BEM channel estimation receiver outperforms the former scheme, having an excellent performance in very demanding high-mobility environments, e.g. for $f_d = 0.5$. Given results prove that the proposed receiver could also be used to boost the performance of the forthcoming DVB-NGH standard in very demanding high-mobility environments.

4.5.1 Accuracy of BEM channel estimation

The normalized mean square error (NMSE) and the BER performance results will be examined in this section with respect to Doppler spread and the SNR, respectively. The NMSE, defined as shown in the following equation, has been used as mismatch measure between the perfect channel and the BEM estimation

$$NMSE = \frac{\sum_{n=0}^{N-1} \left| \mathbf{h}_m(n) - \hat{\mathbf{h}}_m(n) \right|^2}{\sum_{n=0}^{N-1} |\mathbf{h}_m(n)|^2}. \tag{4.25}$$

Fig. 4.9 depicts the evolution of the NMSE as the Doppler frequency grows for the considered CE-BEM estimation. The solid line represents the main diagonal while the dashed one represents a secondary diagonal. It is observed that with low Doppler frequencies, the error is negligible in the main diagonal, and therefore the estimate is better. Likewise, as the Doppler frequency increases, the error is greater. Nonetheless, the BEM estimate works very well and the NMSE remains within an acceptable range. The second diagonal does not get as accurate results as the main one but it helps the detector to obtain very important information for ICI cancellation.

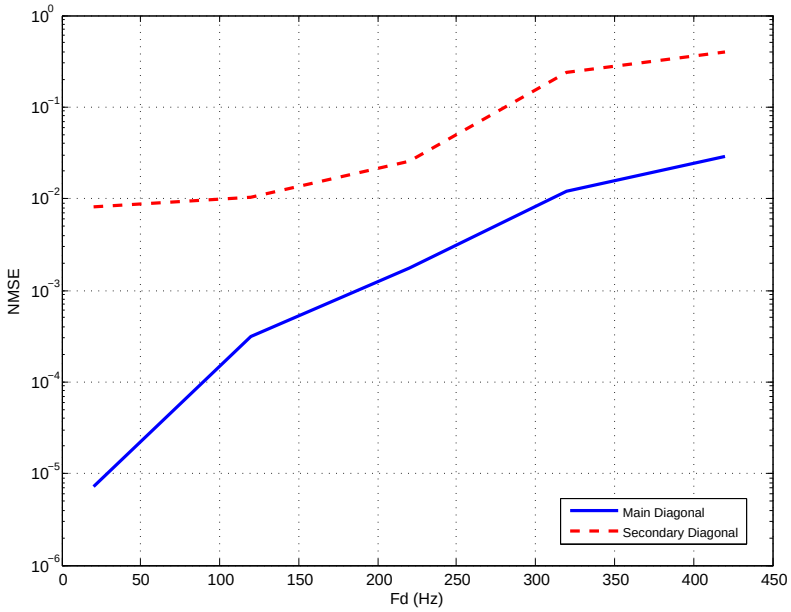

Figure 4.9: NMSE performance versus Doppler frequency for the main and secondary diagonals in the time variant TU6 channel. DVB-T2 parameters: 8K mode, $GI = 1/4$, 16QAM, $CR = 2/3$, 16K LDPC.

4.5.2 MAP ICI canceler with BEM channel estimation

In order to see the behavior of the first proposed scheme, simulations under different scenarios have been carried out. For this purpose, commonly used channels models in digital video broadcasting standards, such as TU6 and RA6 have been chosen in order to test its performance.

4.5.2.1 TU6 channel analysis

In order to evaluate the performance of the proposed DVB-T2 receiver, commonly used channel models are considered. In the first place, a 6-taps Typical Urban TU6 channel is considered in 8K mode, thus having $N = 8192$ subcarriers, with a CR of 2/3 and a constellation of 16QAM.

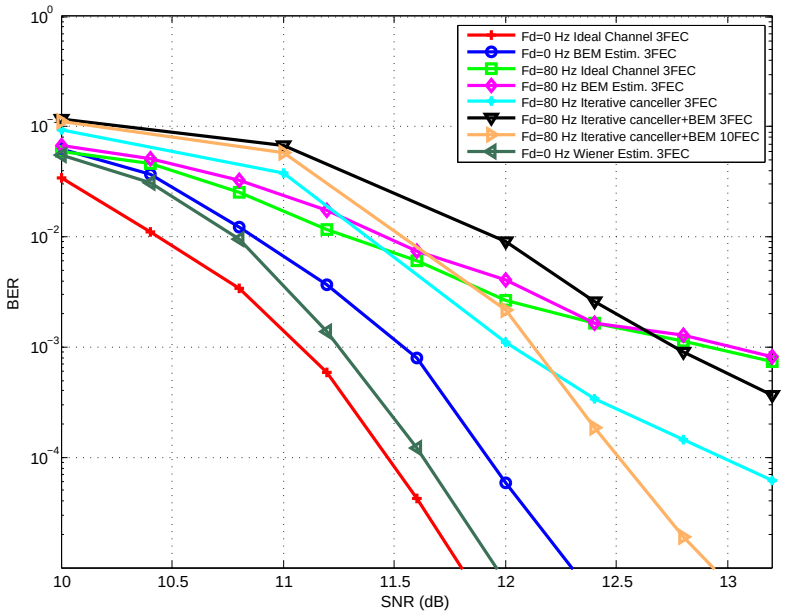

Figure 4.10: BER performance versus SNR for different channel estimation methods in the time variant TU6 channel with 80 Hz Doppler. DVB-T2 parameters 8K mode, $GI = 1/4$, 16QAM, $CR = 2/3$, 16K LDPC.

Fig. 4.10 shows the performance of the proposed receiver and the ones described in Chapter 3, specially the ones based on Wiener filtering. In the case of BEM, a CE-BEM with $Q = 2$ was used to model the time-varying channel up to two interfering adjacent subcarriers. The number of pilots is the same as those used in DVB-T2 for pilot pattern PP1. However, in this case they are clustered in $C = 122$ groups, each containing $L_p = 5$ pilots. The Doppler frequency (F_d) values that have been taken as references for mobile environments are 80 Hz and 50 Hz, equivalent to speeds of 114 Km/h and 71 Km/h, respectively, with 760 MHz carrier frequency. It can be seen that channel estimation by Wiener filtering performs better than BEM estimation when there is no Doppler. However, when Doppler is added to the system, BEM channel estimation and the proposed ICI canceler obtain better performance, behaving close to the ideal channel knowledge case. We can also observe that the combination of the proposed algorithms, the ICI canceler and the BEM estimator, is the best solution and outperforms the perfect channel knowledge case with Doppler. This is so because the MAP detector profits from the frequency diversity ICI provides.

When testing with less severe Doppler frequencies, the system performance is even better

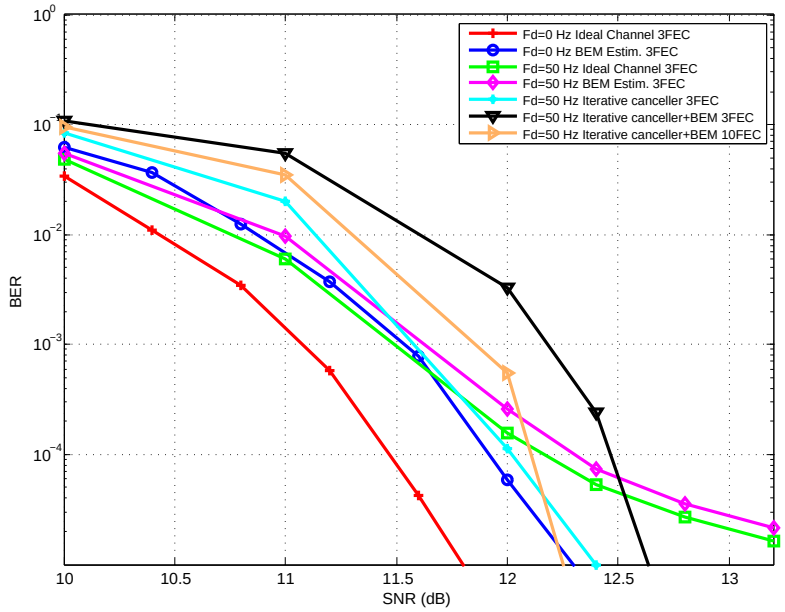

Figure 4.11: BER performance versus SNR for different channel estimation methods in the time variant TU6 channel with 50 Hz Doppler. DVB-T2 parameters: 8K mode, $GI = 1/4$, 16QAM, $CR = 2/3$, 16K LDPC.

through the combination of the proposed ICI canceler and BEM estimator. Consequently there is more diversity gain due to the ICI cancellation, and the error floor experienced with the ideal channel knowledge disappears, as is depicted in Fig. 4.11. 3 FECs have been considered for all the cases except for the iterative canceler and BEM estimator, which has also been simulated for 10 FECs, obtaining a significant performance increase.

4.5.2.2 RA6 channel analysis

Simulations have also been carried out for less frequency-selective propagation environments, such as the RA6 channel, in order to assess the behavior of the proposed scheme when the effects of pilot clustering are less severe. The tested parameters are the same as in the previous cases, but with a more robust code-rate of $CR = 1/2$ and a $F_d = 200$ Hz, equivalent to a speed of 284 Km/h with 760 MHz carrier frequency.

Fig. 4.12 depicts the BER performance of DVB-T2 for the combination of the proposed algorithms. For a time interleaving depth of 3 FEC blocks, the BEM channel estimation is very close to the ideal channel knowledge case. Nevertheless, although the proposed algorithm does not remove the existing error floor for F_d=200 Hz, it remains very close to the ideal channel case, which suffers from error floor too. In order to solve this problem, more complex receivers, as the one based on BP detection, are needed to remove the error floor with high Doppler frequencies.

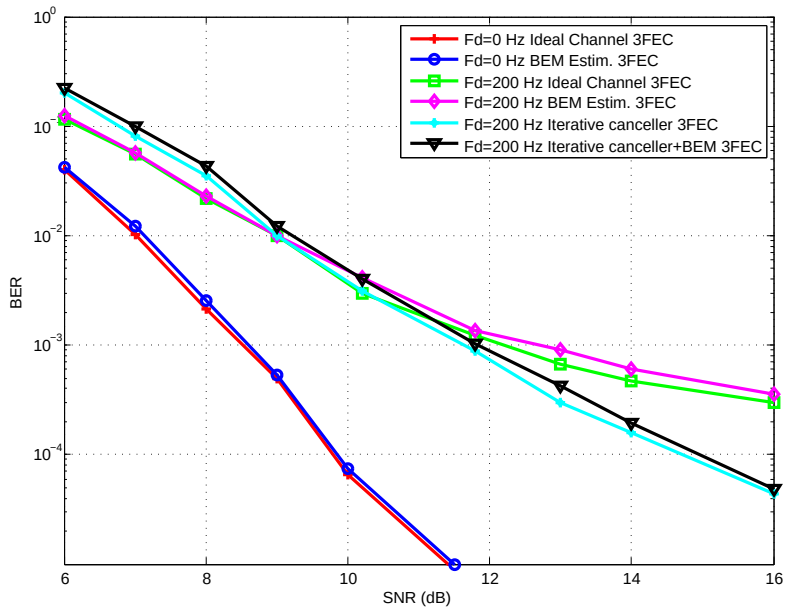

Figure 4.12: BER performance versus SNR for different channel estimation methods in the time variant RA6 channel with 200 Hz Doppler. DVB-T2 parameters: 8K mode, $GI = 1/4$, 16QAM, $CR = 1/2$, 16K LDPC.

4.5.3 BP ICI detector with BEM channel estimation

As in the case of the first proposed scheme, in order to see the performance improvement provided by the second proposed scheme, simulations under different scenarios have been carried out.

4.5.3.1 TU6 channel analysis

The performance of the proposed joint scheme has been analyzed over a TU6 channel model using 32K-subcarrier transmission mode with $CR = 2/3$ and QPSK modulation. Different normalized Doppler frequencies have been simulated to show the good performance of the proposed receiver with very high mobility and large FFT sizes. Regarding the CE-BEM algorithm used for channel estimation, Q=2 has been selected to model the time-varying channel up to two interfering adjacent subcarriers. As for the previously proposed scheme, the pilot structure has been modified to include C=122 pilot clusters, each containing L_p=5 pilots.

Fig. 4.13 depicts the evolution of the BER for various SNR values, showing the performance of the proposed joint channel estimation and BP detector scheme. Naturally, except for the case of no ICI, the ideal channel estimation shows the highest performance. The higher the Doppler frequency, the greater the difference becomes with respect to the ICI-free case, since only two neighboring subcarriers are taken into account and the power of

the residual ICI increases. However, although considering more adjacent subcarriers would improve the performance, it would also increase significantly the complexity of the proposed scheme.

The results in Fig. 4.13 clearly show that a huge profit is obtained with this scheme. The error floor disappears completely even with channel estimation. Furthermore, in the case of f_d=0.13, the performance of the BP detector with ideal channel knowledge, outperforms the ICI-free case, since it is able to exploit the frequency diversity introduced by ICI. If instead of considering the ideal channel, a more realistic approach is considered, and hence the channel estimate is taken into account, the degradation is negligible with respect to the ICI-free case, being of only 0.3 dB.

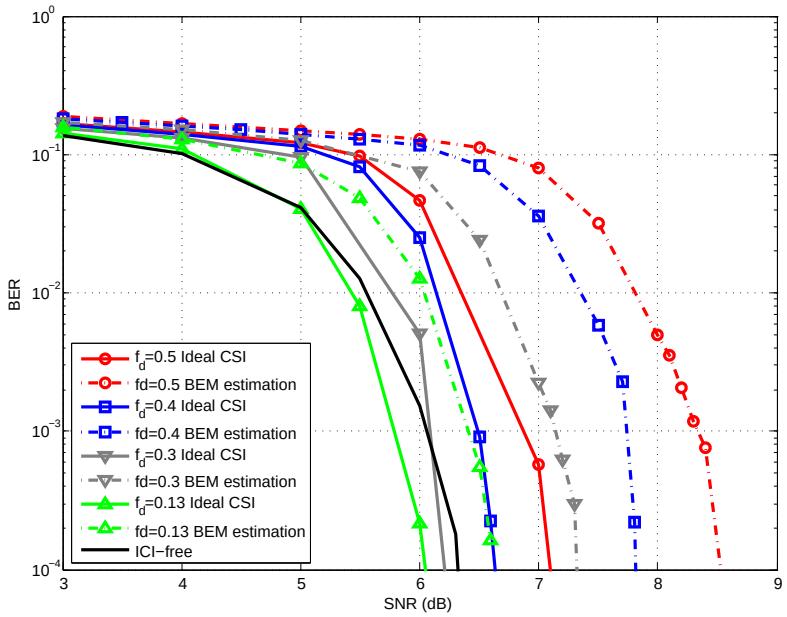

Figure 4.13: BER performance versus SNR for the joint turbo BEM channel estimation and BP detection in the time variant TU6 channel for different values of f_d. System parameters 32K mode, $GI = 1/4$, QPSK, $CR = 2/3$, 64K LDPC.

It can be observed that the gaps between the BP detector with the ideal channel and the joint scheme with channel estimation become larger as the Doppler frequency increases. Thereby, the degradation compared to the ideal channel case is of 0.6, 0.9, 1.3 and 1.4 dB for f_d=0.13, f_d=0.3, f_d=0.4 and f_d=0.5, respectively. Nevertheless, the results in Fig. 4.13 clearly show an excellent performance for all cases, since the error floor disappears completely even with channel estimation. In addition, even for the most severe case ($f_d = 0.5$), the joint scheme performs well, with only 2 dB degradation with respect to the free ICI case. On the other hand, a huge profit is obtained when compared with the MAP canceler considered in the previous section.

4.5.3.2 RA6 channel analysis

The proposed scheme has also been analyzed for a RA6 channel, as it is shown in Fig. 4.14. In contrast to the previous case, the proposed joint scheme with BEM channel estimation and BP detection has a significantly better performance than the ICI-free case, depending on the normalized Doppler frequency, removing the error floor completely except for f_d=0.13 and f_d=0.5. This happens because the proposed novel joint algorithm, not only cancels the ICI, but also can benefit from the diversity it introduces. Therefore, the higher the Doppler frequency is, better results are obtained in the case of ideal channel knowledge up to a certain limit, thus providing specially good results under high mobility scenarios. In this case, $f_d = 0.3$ obtains the best performance of all, and thereafter is degraded. However, Fig. 4.14 shows that up to $f_d = 0.5$, very good results are obtained, significantly improving the ICI-free case. When channel estimation is added to the system, the introduced errors are detrimental to the detector and there is a lower performance as long as the errors become more important.

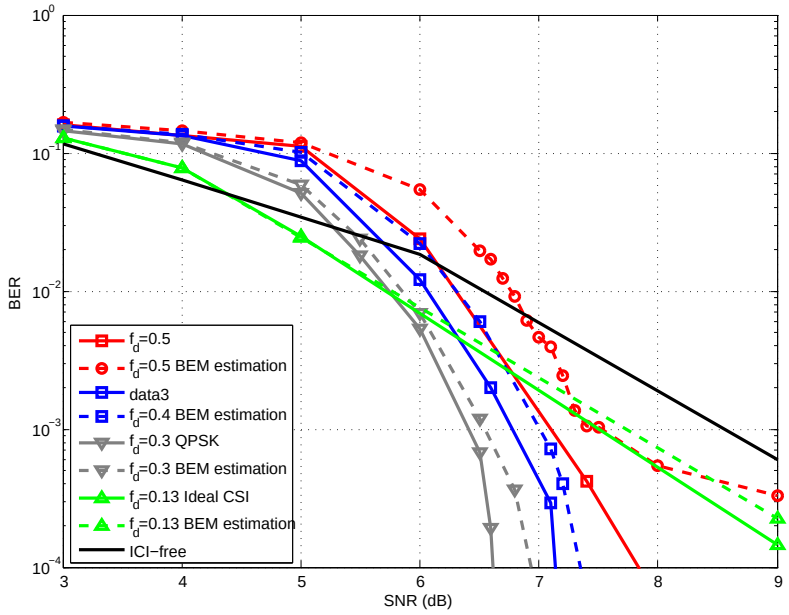

Figure 4.14: BER performance versus SNR for the joint turbo BEM channel estimation and BP detection in the time variant RA6 channel for different values or f_d. System parameters 32K mode, $GI = 1/4$, QPSK, $CR = 2/3$, 64K LDPC.

The diversity introduced by the whole system is given by the channel frequency diversity, the frequency-domain diversity introduced by ICI and the time-domain diversity introduced by time-interleaving. The first of them is determined by $\min(d_{free};L)$, where d_{free} is the Hamming distance of the channel code and L is the number of channel taps. The Hamming distance of the LDPC code is very high, and therefore the diversity order of the system is limited by the total number of channel taps, i.e. 6 for RA6 and 47 for TU6. Consequently,

the frequency diversity that can be achieved with a TU6 channel is much greater than that provided by a RA6 channel.

The diversity introduced by the time-varying channel is the same regardless of the channel model being used. Therefore, in a RA6 channel, the frequency diversity introduced by the Doppler is most noticeable than in a TU6 channel. For this reason, the BP detector has a better performance in a RA6 channel and with $f_d = 0.3$, where the diversity benefit it introduces is larger.

4.6 Chapter Summary

This chapter deals with the problem of combating ICI and emphasizes the importance of its proper characterization, for the subsequent task of channel estimation in a time-varying scenario. The most important works that have addressed this issue have been reviewed and analyzed, concluding that it is necessary to group the pilots together into different clusters in order to obtain a good estimate of the channel in mobile environments. Therefore, the design of optimized pilot clusters is analyzed for high-mobility scenarios, comparing the results with the distributed pilot patterns proposed in the standards, showing a remarkable improvement when 5 or 7 pilots are clustered together. In order to obtain a trade-off between complexity and accuracy, $L_p = 5$ has been chosen for the simulation results proposed in this dissertation.

In order to reduce the number of parameters required for channel estimation, the most promising method in the literature, named basis expansion model (BEM), has been selected, which represents the doubly selective channel by means of CE-BEM, which has been parametrized to model the time-varying channel up to two interfering adjacent subcarriers.

Moreover, this chapter has proposed two different schemes to combine ICI suppression and BEM channel estimation. The first one combines BEM and a MAP ICI equalizer, removing effectively the error floor experienced with mid-mobility systems, such a $f_d = 0,045$ over a TU6 channel. However, as long as the Doppler frequency increases, more suitable methods are needed to counteract the effect of channel estimation and residual ICI.

No ICI-aware channel estimation and detection algorithm has been proposed so far for very high mobility systems in the literature. Even for other standards, the use of a turbo receiver combining channel estimation and ICI detection has not been addressed for high-mobility systems with large FFT orders. Therefore, an iterative (turbo) receiver architecture has been proposed as the second scheme in this chapter, which consists of a BEM channel estimator and a BP detector.

The last part of the chapter has provided novel simulations results for high-mobility DVB-T2 receivers, showing the suitability of the proposed schemes. Within this context, the behavior of the proposed algorithms has been shown for different normalized Doppler frequencies and for different channel models (i.e. TU6 and RA6). The results clearly show

that the second scheme outperforms the first one and the ones in the literature significantly, since it removes the error floor even for a normalized Doppler frequency of $f_d = 0.5$ in TU6 channels and for $f_d = 0.4$ in RA6 channels.

Chapter 5

Iterative BEM channel estimation and ICI cancellation in very high mobility DVB

5.1 Introduction

This chapter proposes a novel receiver combining BEM channel estimation and a BP-based algorithm for signal detection in an iterative (turbo) architecture for high-mobility DVB systems. As it has been previously stated, OFDM transmission suffers from ICI in time-varying channels, due to the loss of orthogonality among subcarriers. At high mobility, i.e. high Doppler frequencies, the distortion caused by ICI is so strong that a classical receiver is not able to provide quasi-error free (QEF) reception. To deal with this problem, two different reception schemes are here proposed in order to achieve the best solution in terms of performance, complexity and latency.

The first proposed scheme, named PS1, substitutes the frequency-domain one-tap equalizer in conventional DVB-T2 receivers by the BP detector and maintains the time interleaver. In the second proposed scheme, named PS2, the time interleaver is subtracted out and the turbo approach is applied exchanging soft information between the decoder, the detector and the channel estimator. Therefore, in addition to the BEM channel estimation considered in the previous chapter, soft data estimates are taken into account and the system performance can be further improved moving closer to the ideal channel case.

Throughout this chapter, the behavior of the proposed channel estimators and receivers will be shown for several Doppler frequencies and for the classical channel models, (i.e. TU6 or RA6), in order to see how the exploitation of soft information affects the performance of the system. Simulation results show the very good performance of the proposed novel receivers, that not only cancel ICI, but can also benefit from the diversity it introduces, providing specially good results under very high mobility scenarios, even up to 0.5 of normalized Doppler frequency.

5.2 Soft-input Channel Estimation

Soft-input BEM channel estimation involves that, not only the pilot carriers are used to estimate the channel, but also soft data estimates are considered in order to obtain a more accurate estimate of the channel. Unlike the case of only taking into account the pilots for channel estimation purposes, in which having a positive B_c was detrimental due to the interference introduced by unknown data, the B_c parameter must now have a positive value, in order to exploit the greater amount of reliable samples as possible. However, this B_c parameter must be carefully chosen in order to achieve a trade-off between complexity and performance. Although it may seem at first glance that the larger B_c, the greater benefit is obtained, this does not happen in practice, because in the case where the reliability of the samples is not good enough, increasing B_c means a growing number of unreliable terms, leading to interference in the estimation. Therefore, taking into account a positive B_c, the matrix D_q previously depicted in Fig. 4.1, is transformed into the matrix shown in Fig. 5.1

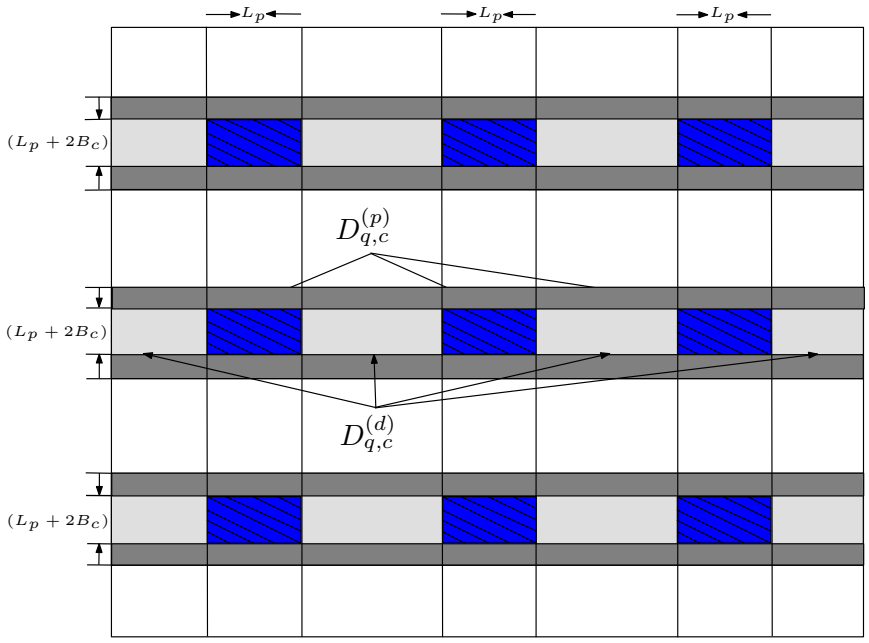

Figure 5.1: Diagram with the elements of matrix D_q for a positive B_c.

The dark shaded areas refer to the widening that occurred when considering a positive B_c, that is, a larger amount of observation samples considered for channel estimation. The received signal can then be expressed as a function of the vector of soft data estimates $\mathbf{m}$ [Fang10] as

$$\mathbf{y}_c = \sum_{q=0}^{Q} \mathbf{D}_{q,c} \cdot \mathbf{\Delta}_q \cdot \mathbf{m} + \underbrace{\sum_{q=0}^{Q} \mathbf{D}_{q,c} \cdot \mathbf{\Delta}_q \cdot (\mathbf{x} - \mathbf{m})}_{\mathbf{d}_c^{soft}} + \mathbf{w}_c, \tag{5.1}$$

where $\mathbf{D}_{q,c}$ is a $(L_p + 2B_c) \times N$ matrix represented by the colored areas in Fig. 5.1 and the second term can be regarded as interference. Assuming QPSK modulation, the ith soft symbol value of $\mathbf{m}$ can be computed as

$$m_i = \frac{\tanh(L_e(x_{i,1})/2) + \sqrt{-1}\,\tanh(L_e(x_{i,2})/2)}{\sqrt{2}}, \tag{5.2}$$

where $L_e(x_{i,1})$ and $L_e(x_{i,2})$ are the extrinsic LLRs of the two bits that compose the symbol obtained from the LDPC decoder. After some algebraic operations, (5.1) can be rewritten as

$$\mathbf{y}_c = \mathbf{D}_c \mathtt{X}_{soft} \mathbf{h}_u + \mathbf{d}_c^{soft} + \mathbf{w}_c, \tag{5.3}$$

with,

$$\mathbf{d}_c^{soft} = \mathbf{D}_c \left[\mathbf{I}_{Q+1} \otimes (\operatorname{diag}\{\mathbf{x} - \mathbf{m}\}\, \mathbf{F}_L)\right] \mathbf{h}_u, \tag{5.4}$$

and,

$$\mathtt{X}_{soft} = \mathbf{I}_{Q+1} \otimes (\operatorname{diag}\{\mathbf{m}\}\, \mathbf{F}_L). \tag{5.5}$$

Substituting (5.5) and (5.4) in (5.3), and stacking all the clusters together, the received signal can be expressed as follows:

$$\begin{aligned} \mathbf{y} &= \mathbf{D}\left[\mathbf{I}_{Q+1} \otimes (\operatorname{diag}\{\mathbf{m}\}\, \mathbf{F}_L)\right] \mathbf{h}_u + \mathbf{D}\left[\mathbf{I}_{Q+1} \otimes (\operatorname{diag}\{\mathbf{x} - \mathbf{m}\}\, \mathbf{F}_L)\right] \mathbf{h}_u + \mathbf{w} \\ &= \mathtt{P}_{soft} \mathbf{h}_u + \mathbf{d}_{soft} + \mathbf{w}, \end{aligned} \tag{5.6}$$

where $\mathtt{P}_{soft} = \mathbf{D}\mathtt{X}_{soft}$ and $\mathbf{D} = \left[\mathbf{D}_0^T, \cdots, \mathbf{D}_{C-1}^T\right]^T$, and $\mathbf{D}_c$ has been previously defined in (4.10) for pilot positions. In addition, $\mathbf{y} = \left[\mathbf{y}_0^T, \cdots, \mathbf{y}_{C-1}^T\right]^T$, $\mathbf{d}_{soft} = \left[\mathbf{d}_{soft,0}^T, \cdots, \mathbf{d}_{soft,C-1}^T\right]^T$ and $\mathbf{z}_f = \left[\mathbf{z}_{f,0}^T, \cdots, \mathbf{z}_{f,C-1}^T\right]^T$ are column vectors of length $C(L_p + 2B_c)$.

In order to update the soft symbol value, the soft data at the output of the LDPC decoder L_e are taken into account. This can be done in each iteration of the equalizer, provided that a trade-off between complexity and performance is accomplished. The generated soft symbol estimates can now be used as pilots, and (4.17) is transformed into

$$\mathbf{W}_{\text{MMSE}} = \mathbf{R}_{\mathbf{h}_u} \mathtt{P}_{soft}^H (\mathtt{P}_{soft} \mathbf{R}_{\mathbf{h}_u} \mathtt{P}_{soft}^H + \mathbf{R}_{\mathbf{d}_{soft}} + \mathbf{R}_w)^{-1}, \tag{5.7}$$

where $\mathbf{R}_{\mathbf{d}_{soft}} = E\left\{\mathbf{d}^{soft} \mathbf{d}_{soft}^H\right\}$ and can be obtained as stated in [Fang10], and $\mathbf{R}_w =$

$E\left\{\mathbf{w}\mathbf{w}^H\right\}$. Since a first channel estimate has already been obtained by means of BEM using (4.16) and (4.17), the channel autocorrelation function $\mathbf{R}_{\hat{\mathbf{h}}_l}$ can be used to obtain the covariance matrix of BEM coefficients as

$$\mathbf{R}_{\mathbf{h}_u} = E(\mathbf{h}_u \mathbf{h}_u^H) = \mathbf{R}_{\mathbf{h}_{u,l}} \otimes diag(\sigma_0^2, \cdots, \sigma_{L-1}^2), \tag{5.8}$$

where,

$$\mathbf{R}_{\mathbf{h}_{u,l}} = E(\mathbf{h}_{u,l} \mathbf{h}_{u,l}^H) = \mathbf{B}^\dagger \mathbf{R}_{\hat{\mathbf{h}}_l} \mathbf{B}^{\dagger H}. \tag{5.9}$$

5.2.1 Complexity considerations

When soft data estimates are taken into account to perform channel estimation, the B_c parameter must be carefully chosen, in order to achieve a trade-off between complexity and performance. Compared to the case of only taking into account pilot carriers to perform channel estimation, a greater B_c means that the observation vector is enlarged and hence the complexity increases.

This time, not only the CE-BEM channel estimation has to be carried out, but also the soft channel estimation has to be taken into account. In order to compute the complexity of the whole channel estimation process, as in the previous chapter, it is important to distinguish between offline and online operations. In the first case, some matrices, such as $\mathbf{B}$, $\mathbf{D}$ and $\mathbf{F}_L$, can be precomputed and stored. That is why the online complexity of the estimator is given mainly by the matrix inversion involved in (5.7), which involves cubic complexity order with $\mathcal{O}\left(((L_p + 2B_c)C)^3\right)$. In addition, the calculation of the autocorrelation function $\mathbf{R}_{\hat{\mathbf{h}}_l}$, needed to obtain the covariance matrix $\mathbf{R}_{\mathbf{h}_u}$, also involves a complexity of order $\mathcal{O}(N^2)$ [Golub96].

5.3 Proposed receivers for very high mobility reception

In this section, numerical results are provided to show the performance of the proposed algorithms for several mobile broadcasting scenarios. Fig. 5.3 depicts the simplified block diagram of the three reception schemes analyzed in this chapter; from top to down: CONV stands for the conventional DVB-T2 receiver, PS1 for the first proposed scheme and PS2 for the second proposed scheme. PS1 substitutes the frequency-domain one-tap equalizer in the conventional DVB-T2 receiver by the BP detector and maintains the time interleaver. In PS2, the time interleaver is subtracted out and the turbo approach is applied exchanging soft information between the decoder, the detector and the channel estimator. The aim of both proposed schemes is to achieve a reasonable trade-off among performance, complexity and latency. The combination of the turbo approach and the inclusion of the time interleaver

would cause excessive delays in signal reception, having been therefore dismissed.

The mechanism behind the proposed ICI combating schemes is the exploitation of the frequency and time-diversity caused by the time-varying channel. PS1 makes use of both frequency-domain diversity (frequency correlation in the received signal due to ICI) and time-domain diversity (due to the use of a time interleaver along with error correction coding in a time-varying channel) to provide error-free reception. In PS2, the lack of the time interleaver is replaced by the performance gain offered by the turbo approach. Optional signal processing stages included in the standard (e.g., constellation rotation) are not considered in this chapter.

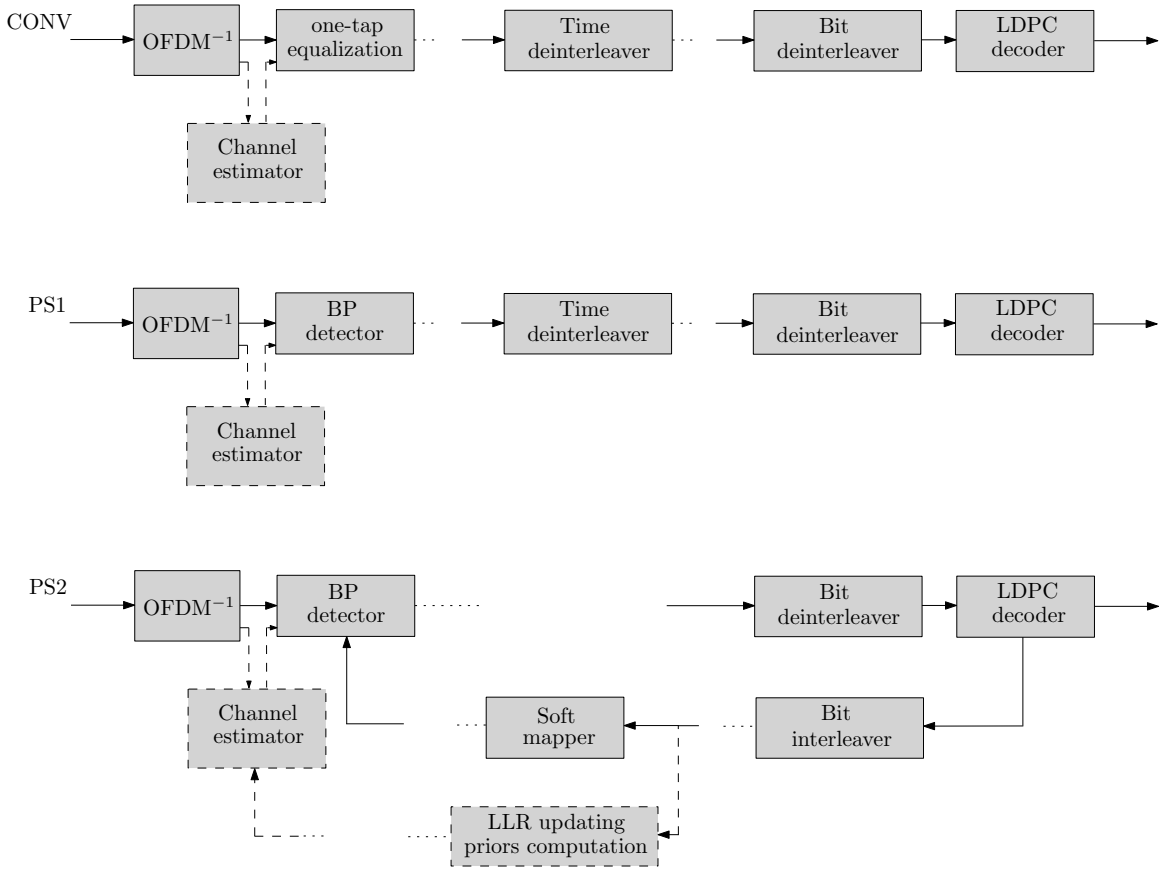

Figure 5.2: From top to down: simplified block diagrams of the conventional DVB-T2 receiver (CONV), the first proposed receiver scheme (PS1), and the second proposed receiver scheme (PS2).

5.4 Simulation results

The DVB-T2 implementation guidelines document [DVB09] proposes several channel models, from which two have been chosen to analyze the performance of the proposed detection techniques in mobile environments: COST 207 TU6 and RA6 channels [COST207]. We consider two very high values for normalized Doppler frequency: $f_d = 0.5$ and $f_d = 0.4$.

Table 5.1: Simulation parameters

Parameter	**Value**
Carrier frequency	760MHz
Bandwidth	8MHz
Number of subcarriers (N)	32784
Subcarrier spacing	280Hz
Length of one OFDM block (T_u)	$3584\mu s$
Length of the guard interval ($T_u/4$)	$896\mu s$
Modulation	QPSK
FEC length	64800
Code rate	2/3

Table 5.1 describes the simulation parameters adopted for the results depicted in this chapter. Under such conditions, $f_d = 0.5$ and $f_d = 0.4$ correspond to about 200 and 160 km/h of vehicular speed, respectively. All the results are obtained running Monte Carlo simulations based on 232 trials of 1 FEC block each. Note that, 32K is the highest FFT size used in DVB-T2 and, hence, the most sensitive to ICI.

Simulation results are organized as follows: Section 5.4.1 analyzes the performance of conventional DVB-T2 reception (CONV) for different number of FEC blocks per TI-block. In Section 5.4.2 and 5.4.3 the performance of the proposed schemes, PS1 and PS2, is assessed and compared to their respective ideal CSI cases.

5.4.1 DVB-T2 performance at high-mobility scenarios

Mobile reception of DVB-T2 signals is assessed according to the number of FEC blocks considered in the TI-block in order to evaluate the robustness provided by the time interleaving at very high Doppler scenarios. Note that, for the time interleaving configuration and transmission parameters adopted in this chapter, the maximum number of FEC blocks in the TI-block is limited to 17, as set by the standard.

According to Fig. 5.3, error-free reception is possible for the RA6 channel up to $f_d = 0.3$ without the inclusion of any specific signal processing technique for ICI suppression. However, beyond this Doppler frequency, the performance crashes giving rise to a high error floor. The BER curves for TU6 channel follow similar trends. In this case, the maximum Doppler frequency for error-free communication is even lower. These results clearly show that the ICI canceling algorithms and the channel estimation architectures provided in this thesis are necessary if DVB-T2 reception is required in very high mobility scenarios.

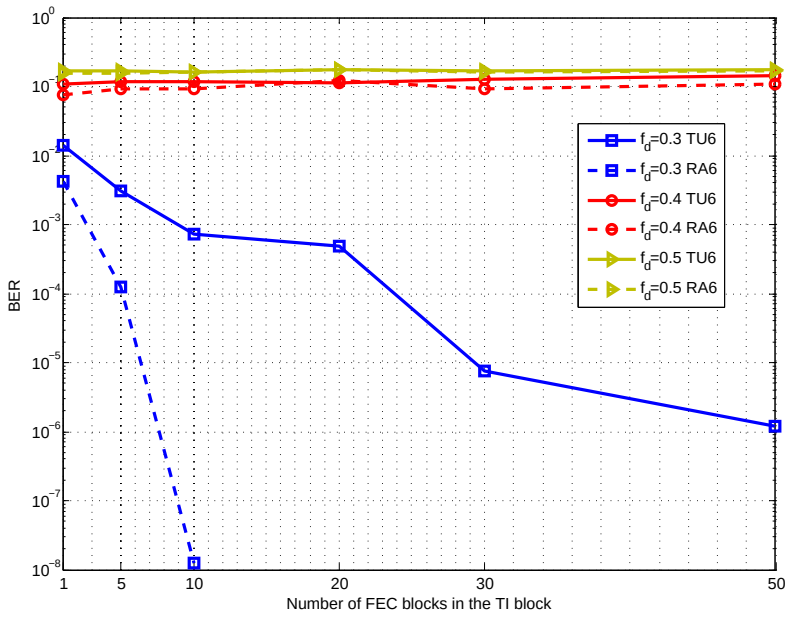

Figure 5.3: DVB-T2 performance for different number of FEC blocks in the TI-block (Time Interleaving depth) at high SNR regime (SNR=30 dB).

5.4.2 Performance with ideal channel estimation

Thorough simulation results not included in this chapter show that the best BER performance in broadcasting channel conditions is achieved by the next turbo strategies [Ochandiano11a]: for PS1 reception scheme, 3 iterations are carried out in the BP detector and 50 iterations in the LDPC decoder. For PS2 receiver, 2 iterations are performed in the BP detector and 20 iterations in the LDPC decoder for each of the 5 outer turbo iterations (extrinsic information exchange between the LDPC decoder and the BP detector).

5.4.2.1 Proposed scheme one (PS1)

Fig. 5.4 and Fig. 5.5 show the BER performance of PS1 for TU6 channel assuming ideal channel knowledge. As it was mentioned, this scheme makes use of both frequency-selectivity (BP detector) and time-selectivity (time interleaver). In Fig. 5.4 BER results are depicted for 1, 2, and 3 iterations in the detector considering 10 FEC blocks per TI block. As it can be seen, the second iteration is able to remove the error floor caused by the Doppler spread, and the third iteration gives a tight performance gain of about 0.3 dB at BER= 10^{-4}, approaching the ICI-free curve up to 1 dB. This corroborates the efficiency of the proposed BP detector in such channel conditions.

In turn, time interleaving performance is assessed in Fig. 5.5 by keeping the number of iterations fixed and varying time interleaving depths (1, 5 and 10 FEC blocks per TI block). As it is shown, the maximum performance gain that time interleaving can offer is around 0.5

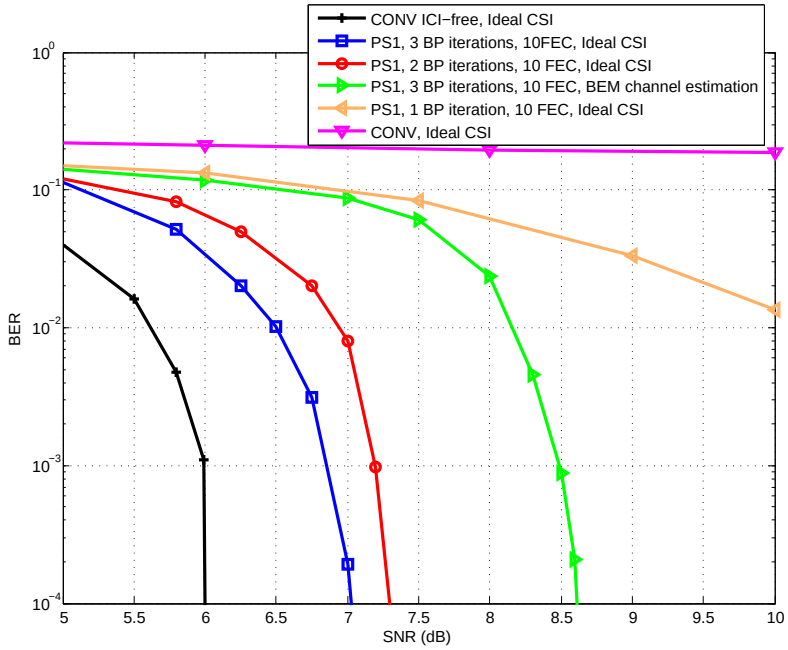

Figure 5.4: PS1 BER performance comparison for different BP iterations, with $f_d = 0.5$ over TU6 channel, considering ideal and partial CSI. 10 FEC blocks per TI-block are assumed.

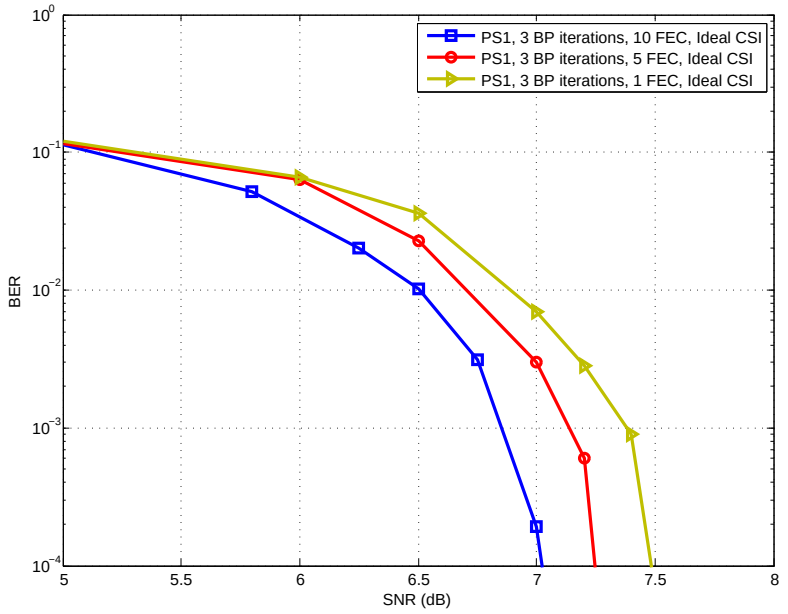

Figure 5.5: PS1 BER performance for different number of FEC blocks per TI block, with $f_d = 0.5$ over TU6 channel, considering 3 BP iterations.

dB. Consequently, for the TU6 channel model, the frequency-selectivity exploitation by the ICI-aware BP detector is much more efficient than the effects of the time-selectivity provided by the time interleaver.

Fig. 5.6 and 5.7 show an analogue analysis for the RA6 channel model. As it is well-known, the BER behavior of a BICM-OFDM scheme is substantially different in less selective channels. Therefore, it is interesting to extend the simulation results of Fig. 5.4 and 5.5 to the RA6 channel model. The high correlation in frequency-domain due to the short delay spread of the channel can largely degrade the BER performance, that is, the lower delay spread leads to frequency-diversity loss. Therefore, as it is shown in Fig. 5.6, PS1 scheme produces a remarkable impact on the BER, giving a performance gain of about 4 dB with respect to the ICI-free case at BER= 10^{-4}.

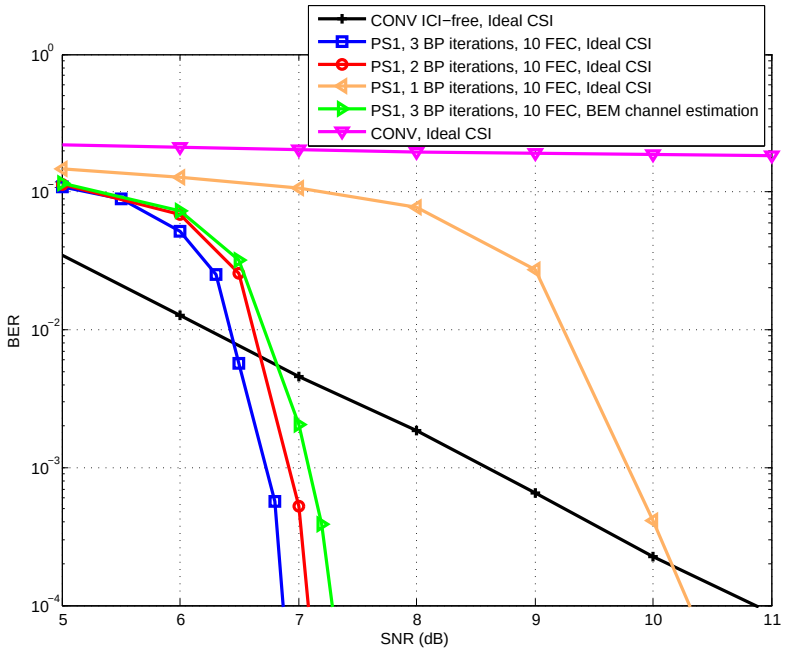

Figure 5.6: PS1 BER performance comparison for different BP iterations, with $f_d = 0.5$ over RA6 channel, considering ideal and partial CSI. 10 FEC blocks per TI-block are assumed.

On the other hand, comparing Fig. 5.5 and 5.7, we can observe that the contribution of the time interleaver is higher in RA6 than in TU6. The reason behind this behavior is that spreading out symbols by means of the time interleaver emulates an ergodic channel, offering a high diversity order gain with respect to the RA6 channel. Besides, it is worth noting that there is no performance gain beyond 5 FEC blocks per TI-block.

5.4.2.2 Proposed scheme two (PS2)

Fig. 5.8 and 5.10 show BER results for PS2 reception scheme and $f_d = 0.5$ over TU6 and RA6, respectively. Note that comparing Fig. 5.8 and 5.4, PS1 outperforms PS2 up to 0.5 dB

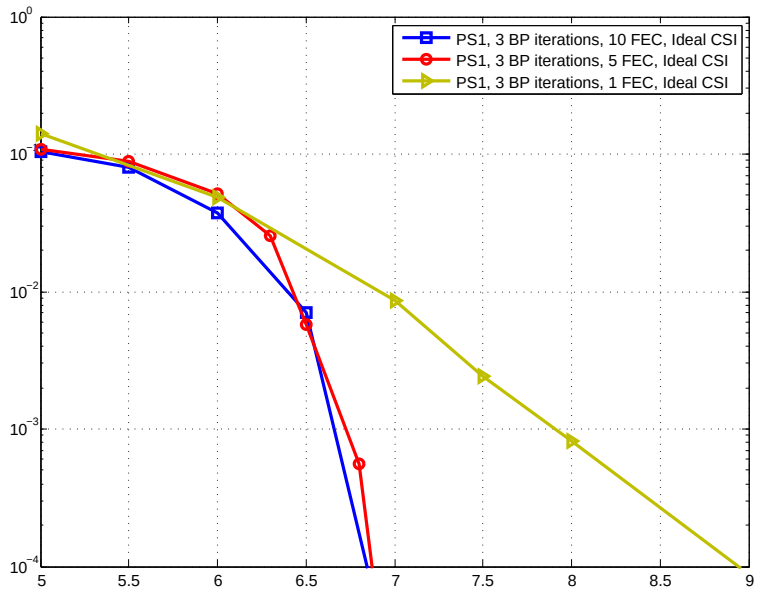

Figure 5.7: PS1 BER performance for different number of FEC blocks per TI block, with $f_d = 0.5$ over RA6 channel, considering 3 BP iterations.

over TU6 channel. In the same way, an analogue behavior can be seen over RA6 comparing Fig. 5.10 and 5.6, where PS1 presents a gain of 1.2 dB with respect to PS2. Therefore, PS1 turns out to be the best solution in terms of performance for both channel models when ideal CSI is assumed. It is worth noting that due to the higher contribution of the time interleaver, the conjunction of BP detector and time interleaver (PS1) provides higher gains with respect to PS2 in less selective channels.

5.4.3 Performance with channel estimation

Regarding the CE-BEM algorithm proposed for channel estimation, $Q = 2$ has been selected to model the time-varying channel up to two interfering adjacent subcarriers as it has been stated in the previous chapter. The pilot structure of DVB-T2 has been modified to include $C = 122$ pilot clusters, each containing $L_p = 5$ pilots. For the PS2 scheme, $B_c = 1$ has been set in order to estimate the channel correctly without increasing the complexity too much. Note that the total amount of pilots has been maintained identical to the PP1 pattern in DVB-T2 specification in order to provide a fair comparison.

5.4.3.1 Proposed scheme one (PS1)

The performance of PS1 scheme has also been tested including the BEM channel estimator for both TU6 and RA6 channels. As expected, PS1 offers the highest performance when 3 BP iterations are performed, and hence, this configuration has been chosen for simulating

PS1 with channel estimation. Regarding TU6 channel, Fig. 5.4 shows a performance loss of 1.5 dB compared to the ideal channel. Nevertheless, the degradation still remains acceptable since the error floor disappears completely.

On the other hand, regarding RA6 channel model (Fig. 5.6), the inclusion of channel estimation leads to a degradation of only 0.3 dB compared to the ideal CSI. This is because the channel is less selective in the frequency-domain and the estimate turns out to be more accurate.

5.4.3.2 Proposed scheme two (PS2)

This scheme has been tested for both TU6 and RA6 channel models and for different normalized Doppler frequencies, $f_d = 0.5$ and $f_d = 0.4$, in order to analyze the behavior of the proposed scheme under different scenarios. Although $f_d = 0.4$ can still be considered as high mobility, estimation errors are considerably reduced. Fig. 5.8 depicts the evolution of BER for various SNR values over TU6, showing the performance of PS2 scheme with two different approaches for channel estimation. The first one combines solely the BEM channel estimator and the BP detector, while the second reconstructs soft symbols using extrinsic information from the decoder to re-estimate the channel in the turbo process. The results in Fig. 5.8 clearly show that a huge profit is obtained when compared with the no ICI compensation case (CONV scheme).

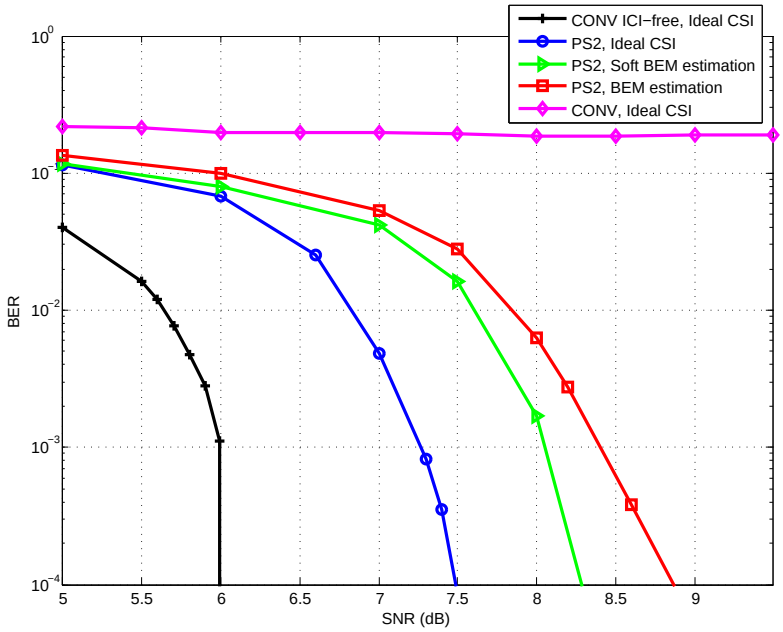

Figure 5.8: PS2 BER performance comparison for 3 BP iterations, with $f_d = 0.5$ over TU6 channel, considering ideal and partial CSI.

The degradation of PS2 considering BEM estimation is approximately 1.3 dB compared to the ideal CSI case. Moreover, when soft data estimates are taken into account, the system

performance can be even improved up to 0.5 dB, moving closer to the ideal channel case. Note that considering higher values of Q would improve the performance at the expense of increased complexity.

Similar results are depicted in Fig. 5.9, for $f_d = 0.4$ of normalized Doppler frequency. In this case, a degradation of 0.7 dB can be seen when comparing PS2 with BEM estimation and the ideal CSI case. This degradation is smaller than in the previous case because the Doppler frequency is lower, and hence the introduced estimation error is also lower. When soft data estimates are taken into account, the performance is again closer to the ideal channel case, showing an improvement of 0.4 dB.

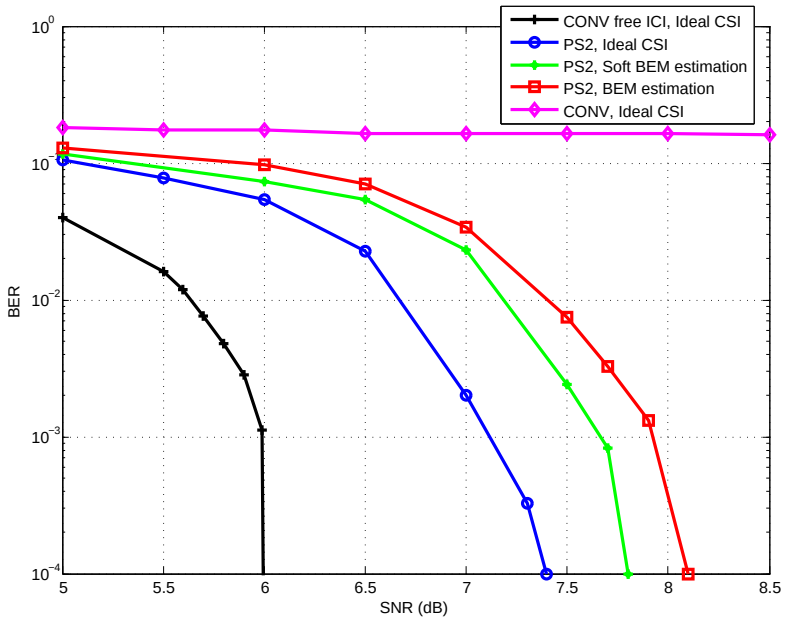

Figure 5.9: PS2 BER performance comparison for 3 BP iterations, with $f_d = 0.4$ over TU6 channel, considering ideal and partial CSI.

Fig. 5.10 and Fig. 5.11 show results for RA6 channel. In this case, the soft data estimates are not taken into consideration since the BEM channel estimation itself is good enough, and adding soft estimates would only increase complexity. PS2 including the BEM channel estimation algorithm suffers a degradation of 0.2 dB compared to the ideal channel knowledge case with $f_d = 0.5$. In the case of $f_d = 0.4$, the degradation is negligible, losing only 0.1 dB with respect to CSI.

To sum up, the overall system performance of both schemes is compared: regarding TU6 channel (Fig. 5.4 and 5.8), due to the performance gain introduced by the inclusion of soft data estimates in BEM channel estimation, PS2 shows a performance improvement of 0.3 dB over PS1. Therefore, although PS1 outperformed PS2 in the case of ideal CSI, when channel estimation is assumed, PS2 turns out to be the most effective solution. In contrast, since channel estimation is much more accurate in RA6 channel (Fig. 5.6 and 5.10), PS1

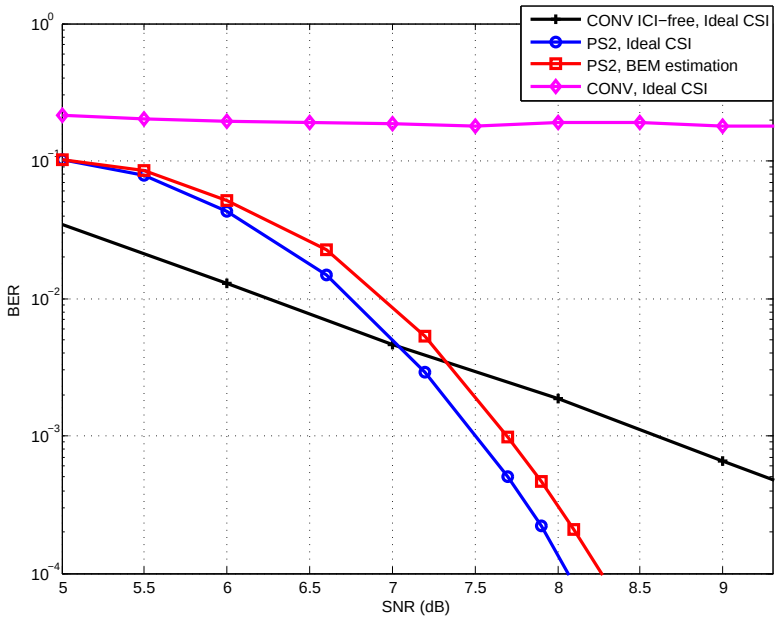

Figure 5.10: PS2 BER performance comparison for 3 BP iterations, with $f_d = 0.5$ over RA6 channel, considering ideal and partial CSI.

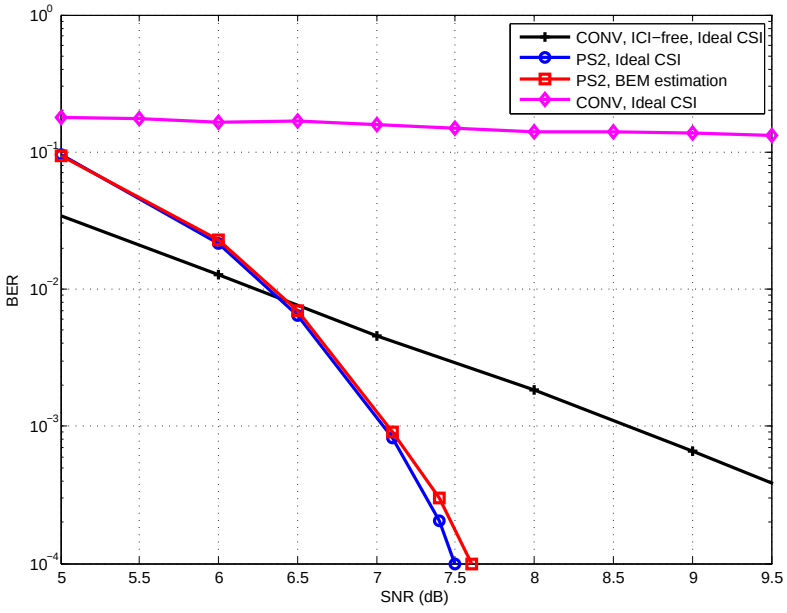

Figure 5.11: PS2 BER performance comparison for 3 BP iterations, with $f_d = 0.4$ over RA6 channel, considering ideal and partial CSI.

outperforms PS2, and hence we conclude that PS1 is better suited to less selective channels.

5.5 Chapter Summary

This chapter deals with the problem of joint channel estimation and signal detection for high mobility reception when long OFDM blocks are employed. First of all, the performance of a classical DVB-T2 receiver has been assessed in high-mobility channel conditions, concluding that it is not able to provide error-free reception at high Doppler frequencies when using long OFDM blocks. In order to solve this problem, a novel approach has been proposed which consists of the combination of a BP detector and a powerful channel estimation technique based on the well-known BEM algorithm. The proposed algorithms have been assessed over the DVB-T2 physical layer in realistic broadcasting channel conditions. For this purpose, two different reception schemes have been proposed which make use of both frequency and time selectivity available in time-varying OFDM systems. The first proposed scheme (PS1) substitutes the one-tap frequency-domain equalizer by the BP detector and maintains the time inteleaver, whereas the second proposed scheme (PS2) removes the time interleaver and incorporates the turbo principle instead. The performance has been tested over TU6 and RA6 channel models for a range of normalized Doppler frequencies.

No ICI-aware channel estimation and detection algorithm has been proposed so far for very high mobility DVB systems in the literature. Even for other standards, the use of a turbo receiver combining channel estimation and ICI detection has not been addressed for high-mobility with large FFT sizes. In this chapter, we have proposed an iterative (turbo) receiver architecture which consists of a BEM channel estimator and a BP detector, both of which exchange soft information with the LDPC decoder, exploiting soft data estimates to improve the performance of the BEM channel estimator, showing very good results. Furthermore, an information exchange and iteration strategy is proposed, as well as a more suitable pilot structure for identifying the ICI channel.

Provided simulation results show that the proposed receivers can be used to boost the performance of DVB-T2 and the forthcoming DVB-NGH standards in very demanding high-mobility environments. We conclude that, from the two proposed schemes, the second one is better suited to highly-selective channels, while the first one performs better in less-selective channel environments with $f_d = 0.5$. In addition, the soft BEM channel estimator applied to the second proposed scheme achieves a gain of 0.5 dB in average over the classical BEM estimator in TU6 channels, while it is not worthwhile to use it in RA6 channels due to the good behavior of the non-iterative BEM estimator.

Chapter 6

Summary and Conclusions

This PhD dissertation deals with channel estimation architectures for mobile reception in emerging DVB standards. As a first step, a Matlab based DVB-T2 transmission-reception chain was developed in order to test the performance of the new digital terrestrial television standard under different conditions. Chapter 2 explains the main features of DVB-T2 and also highlights the most significant differences introduced in comparison to DVB-T. All these improvements concentrate on physical and transport layer, providing a capacity improvement of 30%, greater efficiency in the use of the spectrum, improved robustness against interference and greater flexibility over the former DVB-T specification. These improvements are the result of a set of key techniques that have been included in the new standard, such as LDPC codes, higher order modulation schemes, lower code rates, longer modes and 8 different pilot patterns.

Chapter 3 reviews the main channel estimation techniques for wireless OFDM channels, with particular emphasis on pilot assisted estimators. Regarding comb-type channel estimation, different algorithms for multi-antenna transmissions and mobile reception have been tested based on the DVB-T2 specification. Numerical results have been presented under different scenarios and with different interleaving depths. It is worth noting that short OFDM blocks are less susceptible to ICI and combined with a moderate Doppler frequency, provide a remarkable performance improvement. Simulation results show that the additional diversity exploited through the combination of higher Doppler frequencies and the time interleaver can enhance the performance of the system with the proposed parameters. In addition to considering perfect channel estimates and the classical one-dimensional estimation techniques, two-dimensional Wiener filtering has been applied to DVB-T2, analyzing the behavior of the system under channel estimation errors. Furthermore, a decision-directed scheme has been developed under the assumption of a slow fading channel in a DVB-T2 framework. The proposed algorithm is designed for channel estimation with few pilots for DVB-T2 and other OFDM-based transmission systems. It shows only a small performance loss compared to the ideal channel knowledge and outperforms the reference CD3 algorithm, for which the PP8 pilot scheme of DVB-T2 was originally designed. Furthermore, the proposed algorithm outperforms the pilot-based channel estimation in stationary channels, while the loss in the

time variant channel remains acceptable.

Chapter 4 proposes the use of BEM channel estimation with two different schemes to combat ICI and clustered pilot patterns are proposed for DVB-T2. The first scheme, where BEM is combined with a MAP equalizer, effectively removes the error floor experienced with mid-mobility systems, such a $f_d = 0,045$ and TU6 channel. As long as the Doppler frequency increases, more suitable methods are needed to counteract the effect of channel estimation and residual ICI. Therefore, the second scheme consists of a BEM channel estimator and a BP detector, assessed under a BICM-OFDM framework, and the results clearly show that this scheme outperforms the first one and the ones in the literature significantly, since it removes the error floor completely even for a normalized Doppler frequency of $f_d = 0.5$ in TU6 channels and for $f_d = 0.4$ in RA6 channels. Within this context, the behavior of the proposed algorithms has been shown for different normalized Doppler frequencies and for different channel models (i.e. TU6 and RA6).

Chapter 5 deals with the assessment of the performance of the classical DVB-T2 receiver with one-tap frequency-domain equalization in high-mobility channel conditions, concluding that is not able to provide error-free reception at high Doppler frequencies when using long OFDM blocks. In order to solve this problem, a novel approach has been proposed which consists of the combination of a BP detector and a powerful channel estimation technique based on the well-known BEM algorithm. The proposed algorithms have been assessed over the DVB-T2 physical layer in realistic broadcasting channel conditions. For this purpose, two different reception schemes have been proposed which make use of both frequency and time selectivity available in time-varying OFDM systems. The first proposed scheme (PS1) substitutes the one-tap frequency-domain equalizer by the BP detector and maintains the time inteleaver, whereas the second proposed scheme (PS2) removes the time interleaver and incorporates the turbo principle instead. The performance has been tested over TU6 and RA6 channel models and for different normalized Doppler frequencies. It is concluded that PS2 is better suited to highly-selective channels, while PS1 performs better in less-selective channel environments.

6.1 Thesis Contributions

The main contributions of this research work are the following:

- Performance analysis of different channel estimation and interpolation schemes under a DVB-T2 framework for SISO, in both fixed and mobile scenarios. The effect of extending the time interleaving has also been assessed for different number of FEC blocks. This work was published in [Martínez10b].

- Analysis of the behavior of two-dimensional channel estimation techniques based on

Wiener filtering for the new DVB-T2 standard. Simulations results with MISO transmission are provided for both fixed and mobile receivers. This work was published in [Martínez10b, Mendicute10].

- An optimized algorithm for decision-directed blind channel estimation in DVB-T2 has been presented. This algorithm shows a small performance loss compared to the ideal channel knowledge case and outperforms the original CD3 algorithm, for which the PP8 pilot scheme of DVB-T2 was originally designed. Furthermore, the proposed algorithm outperforms the pilot-based channel estimation in stationary channels, while the loss in the time variant channel remains acceptable. This work was published in [Martínez10a].

- The design of optimized pilot clusters is analyzed for high-mobility DVB-T2 scenarios, comparing the results with the distributed pilot patterns proposed in the standards.

- The performance of the physical layer of DVB-T2 has been assessed in high-mobility channel conditions, concluding that it is not able to provide error-free reception at high Doppler frequencies when using long OFDM blocks, e.g. 32K and $f_d = 0.5$.

- The combination of a BEM channel estimator and a MAP ICI detector has been proposed for mid-mobility DVB systems. The proposed receiver architecture is assessed with new pilot designs, showing the effectiveness of this technique by removing the error floor experienced with mid-mobility systems, such a $f_d = 0.045$ and TU6 channel. However, as long as the Doppler frequency increases, more suitable methods are needed to counteract the effect of channel estimation and residual ICI. This work was published in [Martínez11].

- A novel scheme has been proposed, which combines a BEM channel estimator with a BP detector. This scheme substitutes the one-tap MAP equalizer by the BP detector in the conventional DVB-T2 receiver, and maintains the time interleaver [Ochandiano12].

- An iterative receiver architecture has been proposed, which consists of a BEM channel estimator and a BP detector. The proposed scheme removes the time interleaver and incorporates the turbo principle instead. This scheme cancels the ICI with very good results for high-mobility and large FFT modes. The performance of the algorithm is tested through computer simulations showing a remarkable BER improvement in several commonly used channels, such as TU6 and RA6. This scheme is based on a BICM-OFDM system model.

- The previous scheme has been assessed over a DVB-T2 framework. In addition, an iterative receiver architecture has been proposed, in order to provide good results under high mobility scenarios over TU6 and RA6 channel models for very-high normalized

Doppler frequencies ($f_d = 0.4$ and $f_d = 0.5$). The proposed receiver can be used to boost the performance of mobile terrestrial standards, such as the forthcoming DVB-NGH, in very demanding high-mobility environments [Martínez12, Ochandiano12].

6.2 Suggestions for Further Research

Many issues described in this PhD dissertation can be addressed in the future as an improvement and extension of the current work. These are some of the suggestions for further research:

- The application of the CD3 algorithm for MISO transmission remains an open issue, as MISO requires the estimation of two separate channel transfer functions.
- Under a BICM-OFDM framework, the proposed receiver (BEM estimation and BP detection) suffers an error floor for $f_d = 0.5$ in RA6 channel. However, when the same conditions are applied to DVB-T2, this error floor disappears for both PS1 and PS2 schemes. Therefore, thorough analysis of how interleavers affect the channel estimation should be necessary.
- Although the complexity of the considered receiver architecture has been briefly analyzed, a real-time hardware implementation (in rapid prototyping environments) should be the next step in order to prove the validity and applicability of the proposed receivers.
- The forthcoming DVB-NGH specification, which will be probably based on the DVB-T2 specification considered in this research work, should be the scenario where these techniques should be applied.

Appendix A
Publications

The research work that has been carried out during the development of this thesis has been published in the following refereed conference contributions and journal articles:

Book Chapter:

- M. Mendicute, I. Sobrón, L. Martínez and P. Ochandiano, "Digital Video" chap. DVB-T2: New Signal Processing Algorithms for a Challenging Digital Video Broadcasting Standard, pp. 185-206, InTech, Feb. 2010.

Journal papers:

- I. Sobrón, M. Barrenechea, P. Ochandiano, L. Martínez, M. Mendicute and J. Altuna, "Low-Complexity Detection of Space-Frequency Block Codes in LDPC-Based OFDM Systems", *IEEE Transactions on Communications, vol. 60, n. 3, 626-631, March 2012. ISSN: 0090-6778.*

- P. Ochandiano, H. Wymeersch, M. Mendicute, L. Martínez and I. Sobrón "Factor graph based detection approach for high-mobility OFDM systems with large FFT sizes", submitted to *EURASIP Wireless Communications and Networking* (under review).

- P. Ochandiano, L. Martínez, I. Sobrón, M. Mendicute, "Iterative Detection and Channel Estimation for Mobile Terrestrial TV with Long OFDM Blocks", submitted to *IEEE Transactions on Broadcasting* (under review).

International conference papers:

- I. Sobrón, M. Mendicute, L. Martínez and P. Ochandiano, "Impact of self interference in DVB-T2 broadcasting single frequency networks", in *Proc. 9th International Workshop*

on Electronics, Control, Modeling, Measurement and Signals (ECMS '09), pp. 97-103, Mondragon, Spain, Jul. 2009.

- L. Martínez, J. Robert, H. Meuel, I. Sobrón and M. Mendicute, "Improved Robustness for Channel Estimation without Pilots for DVB-T2", in *Proc. IEEE International Symposium on Broadband Multimedia Systems and Broadcasting (BMSB '10)*, pp. 1-5, Shanghai, China, Mar. 2010.

- P. Ochandiano, I. Sobrón, L. Martínez, M. Mendicute and J. Altuna, "Analysis of ICI compensation for DVB-T2", in *Proc. 7th International Symposium on Wireless Communication Systems (ISWCS '10)*, pp. 427-430, York, United Kingdom, Sep. 2010.

- I. Sobrón, M. Barrenechea, P. Ochandiano, L. Martínez, M. Mendicute and J. Altuna, "Low-Complexity Detection of Golden Codes in LDPC-Coded OFDM Systems", submitted to *IEEE International Conference on Acoustics, Speech and Signal Processing (ICASSP '11)*, Prague, Czech Republic, May 2011.

- L. Martínez, I. Sobrón, P. Ochandiano and M. Mendicute, "Novel pilot structures for BEM channel estimation and ICI compensation in high-mobility DVB", *In Proc. IEEE International Symposium on Broadband Multimedia Systems and Broadcasting (BMSB 2011)*, Nürnberg, Germany, June 2011.

- P. Ochandiano, H. Weymeersh, I. Sobrón, L. Martínez, and M. Mendicute, "Novel ICI suppressing receiver for high-mobility DVB-T2 reception with large FFT modes", *In Proc. IEEE International Symposium on Broadband Multimedia Systems and Broadcasting (BMSB 2011)*, Nürnberg, Germany, June 2011.

- P. Ochandiano, H. Weymeersh, M. Mendicute, L. Martínez and I. Sobrón, "Iterative ICI cancellation based on factor graphs for large FFT sizes", *In Proc. EURASIP European Signal Processing Conference (EUSIPCO 2011)*, Barcelona, Spain, August 2011.

- L. Martínez, P. Ochandiano, I. Sobrón, and M. Mendicute, "Iterative BEM channel estimation and BP detection for ICI cancellation in DVB systems with very high mobility", (Accepted) *IEEE International Symposium on Broadband Multimedia Systems and Broadcasting (BMSB 2012)*, Seoul, South Korea, June 2012.

National conference papers:

- I. Sobrón, P. Ochandiano, L. Martínez, M. Mendicute and J. Altuna, "Análisis de robustez de DVB-T2 en redes SFN", in *Proc. XXII Simposium Nacional de la Unión Científica Internacional de Radio (URSI '09)*, Cantabria, Spain, Sep. 2009.

- L. Martínez, I. Sobrón, P. Ochandiano, M. Mendicute and J. Altuna, "Estimación de canal para transmisión multiantena y recepción móvil en DVB-T2", in *Proc. XXIII Simposium Nacional de la Unión Científica Internacional de Radio (URSI '10)*, Bilbao, Spain, Sep. 2010.

- P. Ochandiano, I. Sobrón, L. Martínez, M. Mendicute and J. Altuna, "Detección iterativa en receptores DVB-T2", in *Proc. XXIII Simposium Nacional de la Unión Científica Internacional de Radio (URSI '10)*, Bilbao, Spain, Sep. 2010.

- I. Sobrón, P. Ochandiano, L. Martínez, M. Mendicute and J. Altuna, "Transmisión SFBC distribuida en redes SFN de DVB-T2", in *Proc. XXIII Simposium Nacional de la Unión Científica Internacional de Radio (URSI '10)*, Bilbao, Spain, Sep. 2010.

References

[Alamouti98] S. Alamouti, "A simple transmit diversity technique for wireless communications", *IEEE Journal on Selected Areas in Communications*, vol. 16, no. 8, 1451–8, 1998.

[Baddour05] K. Baddour and N. Beaulieu, "Autoregressive modeling for fading channel simulation", *IEEE Transactions on Wireless Communications*, vol. 4, no. 4, 1650–62, 2005.

[Banelli07] P. Banelli, R. Cannizzaro, and L. Rugini, "Data-aided Kalman tracking for channel estimation in Doppler-affected OFDM systems", pp. 133–6, 2007.

[Baracca11] P. Baracca, S. Tomasin, L. Vangelista, N. Benvenuto, and A. Morello, "Per Sub-block Equalization of Very Long OFDM Blocks in Mobile Communications", *IEEE Transactions on Communications*, vol. 59, no. 2, 363–8, 2011.

[Barhumi03] I. Barhumi, G. Leus, and M. Moonen, "Optimal training design for MIMO OFDM systems in mobile wireless channels", *IEEE Transactions on Signal Processing*, vol. 51, no. 6, 1615–24, 2003.

[Barhumi05] I. Barhumi, G. Leus, and M. Moonen, "MMSE estimation of basis expansion model for rapidly time-varying channels", 2005.

[Bello63] P. A. Bello, "Characterization of randomly time-variant linear channels", *IEEE Transactions on Communications Systems*, vol. 11, 360–393, 1963.

[Berenguer03] I. Berenguer and X. Wang, "Space-time coding and signal processing for MIMO communications", *Journal of Computer Science and Technology (English Language Edition)*, vol. 18, no. 6, 689–702, 2003.

[Borah99] D. Borah and B. Hart, "Frequency-selective fading channel estimation with a polynomial time-varying channel model", *IEEE Transactions on Communications*, vol. 47, no. 6, 862–73, 1999.

[Cai00] X. Cai and A. Akansu, "A subspace method for blind channel identification in OFDM systems", in *IEEE International Conference on Communications (ICC)*, vol. 2, pp. 929–33, 2000.

[Cannizzaro06] R. C. Cannizzaro, P. Banelli, and G. Leus, "Adaptive channel estimation for OFDM systems with Doppler spread", pp. France Telecom Research and Development; Centre National de la Recherche Scientifique (CNRS); Institut Eurecom; Centre pour l'Energie Atomique (CEA) –, Cannes, France, 2006.

[Cavers91] J. Cavers, "An analysis of pilot symbol assisted modulation for Rayleigh fading channels [mobile radio]", *IEEE Transactions on Vehicular Technology*, vol. 40, no. 4, 686–93, 1991.

[Chotikakamthorn99] N. Chotikakamthorn and H. Suzuki, "On identifiability of OFDM blind channel estimation", in *IEEE Vehicular Technology Conference (VTC)*, vol. 4, pp. 2358–61, 1999.

[Cirpan99] H. Cirpan and M. Tsatsanis, "Maximum likelihood blind channel estimation in the presence of Doppler shifts", *IEEE Transactions on Signal Processing*, vol. 47, no. 6, 1559–69, 1999.

[Clarke68] R. H. Clarke, *A statistical theory of mobile-radio reception*, 1968.

[Coleri02] S. Coleri, M. Ergen, A. Puri, and A. Bahai, "Channel estimation techniques based on pilot arrangement in OFDM systems", *IEEE Transactions on Broadcasting*, vol. 48, no. 3, 223–9, 2002.

[COST207] COST207, "Digital land mobile radio communications (final report)", Tech. rep., Commision of the European Communities, Directorate General Telecommunications, Information Industries and Innovation.

[Cui05] T. Cui, C. Tellambura, and Y. Wu, "Low-complexity pilot-aided channel estimation for OFDM systems over doubly-selective channels", in *IEEE International Conference on Communications (ICC)*, vol. 3, pp. 1980–4, 2005.

[Dai07] X. Dai, "Optimal training design for linearly time-varying MIMO/OFDM channels modelled by a complex exponential basis expansion", *IET Communications*, vol. 1, no. 5, 945–53, 2007.

[De Carvalho97] E. De Carvalho and D. Slock, "Cramer-Rao bounds for semi-blind, blind and training sequence based channel estimation", in *IEEE Signal Processing Advances in Wireless Communications (SPAWC)*, pp. 129–32, 1997.

[Diggavi97] S. Diggavi, "Analysis of multicarrier transmission in time-varying channels", in *IEEE International Conference on Communications (ICC)*, vol. 3, pp. 1191–5, 1997.

[Douillard95] C. Douillard, M. Jezequel, C. Berrou, A. Picart, P. Didier, and A. Glavieux, "Iterative correction of intersymbol interference: turbo-equalization", *European Transactions on Telecommunications*, vol. 6, no. 5, 507–11, 1995.

[DVB09] DVB, "Implementation guidelines for a second generation digital terrestrial television broadcasting system (DVB-T2)", Document A133, February 2009.

[Edfors96] O. Edfors, M. Sandell, J.-J. van de Beek, S. Wilson, and P. O. Borjesson, "OFDM Channel Estimation By Singular Value Decomposition", in *IEEE Vehicular Technology Conference*, 1996.

[Edfors98] O. Edfors, M. Sandell, J.-J. van de Beek, S. Wilson, and P. Borjesson, "OFDM channel estimation by singular value decomposition", *IEEE Transactions on Communications*, vol. 46, no. 7, 931–9, 1998.

[ETSI94a] ETSI, "Digital Video Broadcasting (DVB); Framing structure, channel coding and modulation for 11/12 GHz satellite services. EN 300 421", December 1994.

[ETSI94b] ETSI, "Digital Video Broadcasting (DVB); Framing structure, channel coding and modulation for cable systems. EN 300 429", December 1994.

[ETSI97] ETSI, "Digital video Broadcasting (DVB); Framing structure, channel coding and modulation for digital terrestrial television (DVB-T) ETS EN 300 744", March 1997.

[ETSI04] ETSI, "Digital Video Broadcasting (DVB); Transmission System for Handheld Terminals (DVB-H). EN 302.304 V1.1.1", November 2004.

[ETSI05] ETSI, "Digital Video Broadcasting (DVB); Second generation framing structure, channel coding and modulation systems for Broadcasting,

Interactive Services, News Gathering and other broadband satellite applications (DVB-S2). EN 302 307", March 2005.

[ETSI07] ETSI, "Digital Video Broadcasting (DVB); System Specifications for Satellite services to Handheld devices (SH) below 3 GHz. TS 102 585", July 2007.

[ETSI09] ETSI, "Digital Video Broadcasting (DVB); Frame structure channel coding and modulation for a second generation digital terrestrial television broadcasting system (DVB-T2)ETS EN 302 755", Tech. rep., ETSI, 2009.

[ETSI10] ETSI, "Digital Video Broadcasting (DVB); Frame structure channel coding and modulation for a second generation digital transmission system for cable systems (DVB-C2). EN 302 769", April 2010.

[Fang08] K. Fang, L. Rugini, and G. Leus, "Low-complexity block turbo equalization for OFDM systems in time-varying channels", *IEEE Transactions on Signal Processing*, vol. 56, no. 11, 5555–5566, 2008.

[Fang10] K. Fang, L. Rugini, and G. Leus, "Block Transmissions over Doubly Selective Channels: Iterative Channel Estimation and Turbo Equalization", *EURASIP Journal on Advances in Signal Processing*, 2010.

[Flament02] M. Flament, B. Mielczarek, and A. Svensson, "Joint channel estimation and turbo decoding for OFDM-based systems", in *International Symposium on Wireless Personal Multimedia Communications (WPMC)*, vol. 3, pp. 1299–303, 2002.

[Foschini96] G. Foschini, "Layered space-time architecture for wireless communication in a fading environment when using multi-element antennas", *Bell Labs Technical Journal*, vol. 1, no. 2, 41–59, 1996.

[Giannakis98] G. Giannakis and C. Tepedelenlioglu, "Basis expansion models and diversity techniques for blind identification and equalization of time-varying channels", *Proceedings of the IEEE*, vol. 86, no. 10, 1969–86, 1998.

[Golub96] G. Golub and C. Van Loan, *Matrix computations (3rd ed.)*, Johns Hopkins University Press Baltimore, MD, USA, 1996.

[Gorokhov04] A. Gorokhov and J.-P. Linnartz, "Robust OFDM receivers for dispersive time-varying channels: equalization and channel acquisition", *IEEE Transactions on Communications*, vol. 52, no. 4, 572–83, 2004.

[Gross05] F. Gross, *Smart Antennas for Wireless Communications*, McGraw-Hill, 2005.

[Hagenauer96] J. Hagenauer, E. Offer, and L. Papke, "Iterative decoding of binary block and convolutional codes", *IEEE Transactions on Information Theory*, vol. 42, no. 2, 429–45, 1996.

[Hanzo03] L. Hanzo, M. Münster, B. Choi, and T. Keller, *OFDM and MC-CDMA for Broadband Multi-User Communications, WLANs and Broadcasting*, IEEE Press, 2003.

[He08] S. He and J. K. Tugnait, "On doubly selective channel estimation using superimposed training and discrete prolate spheroidal sequences", *IEEE Transactions on Signal Processing*, vol. 56, no. 7 II, 3214–3228, 2008.

[Hoeher97] P. Hoeher, S. Kaiser, and P. Robertson, "Two-dimensional pilot-symbol-aided channel estimation by Wiener filtering", in *IEEE International Conference on Acoustics, Speech, and Signal Processing (ICASSP)*, vol. 3, pp. 1845–8, 1997.

[Hrycak11] T. Hrycak, S. Das, G. Matz, and H. Feichtinger, "Practical Estimation of Rapidly Varying Channels for OFDM Systems", *IEEE Transactions on Communications*, vol. 59, no. 11, 3040–8, 2011.

[Hsieh98] M.-H. Hsieh and C.-H. Wei, "Channel estimation for OFDM systems based on comb-type pilot arrangement in frequency selective fading channels", *IEEE Transactions on Consumer Electronics*, vol. 44, no. 1, 217–25, 1998.

[Hsu09] C.-Y. Hsu and W.-R. Wu, "Low-complexity ICI mitigation methods for high-mobility SISO/MIMO-OFDM systems", *IEEE Transactions on Vehicular Technology*, vol. 58, no. 6, 2755–68, 2009.

[Hwang09] S. U. Hwang, J. H. Lee, and J. Seo, "Low complexity iterative ICI cancellation and equalization for OFDM systems over doubly selective channels", *IEEE Transactions on Broadcasting*, vol. 55, no. 1, 132–9, 2009.

[Jakes74] W. Jakes, *Microwave Mobile Communications*, 1974.

[Jeon99] W. G. Jeon, K. H. Chang, and Y. S. Cho, "An equalization technique for orthogonal frequency-division multiplexing systems in time-variant

multipath channels", *IEEE Transactions on Communications*, vol. 47, no. 1, 27–32, 1999.

[Kannu05] A. Kannu and P. Schniter, "MSE-optimal training for linear time-varying channels", in *IEEE International Conference on Acoustics, Speech, and Signal Processing (ICASSP)*, vol. 3, pp. 789–92, 2005.

[Kim02] B. Kim, *Smart Base Station Antenna Performance for Several Scenarios and Experimental and Modeling Investigation*, Ph.D. thesis, Faculty of the Virginia Polytechnic Institute and State University, May 2002.

[Kou05] Y. Kou, W.-S. Lu, and A. Antoniou, "Application of sphere decoding in intercarrier-interference reduction for OFDM systems", in *IEEE Pacific Rim Conference on Communications, Computers and Signal Processing (PACRIM)*, pp. 360–3, 2005.

[Leus03] G. Leus and M. Moonen, "Deterministic subspace based blind channel estimation for doubly-selective channels", in *IEEE Workshop on Signal Processing Advances in Wireless Communications (SPAWC)*, pp. 210–14, 2003.

[Leus04] G. Leus, "On the estimation of rapidly time-varying channels", in *Proc. of the European Signal Processing Conference (EUSIPCO)*, 2004.

[Li98] Y. Li, J. Cimini, L.J., and N. Sollenberger, "Robust channel estimation for OFDM systems with rapid dispersive fading channels", *IEEE Transactions on Communications*, vol. 46, no. 7, 902–15, 1998.

[Li99] Y. Li, N. Seshadri, and S. Ariyavisitakul, "Channel estimation for OFDM systems with transmitter diversity in mobile wireless channels", *IEEE Journal on Selected Areas in Communications*, vol. 17, no. 3, 461–71, 1999.

[Li00] Y. Li, "Pilot-symbol-aided channel estimation for OFDM in wireless systems", *IEEE Transactions on Vehicular Technology*, vol. 49, no. 4, 1207–15, 2000.

[Li02] Y. Li, "Simplified channel estimation for OFDM systems with multiple transmit antennas", *IEEE Transactions on Wireless Communications*, vol. 1, no. 1, 67–75, 2002.

[Liu01] Z. Liu, G. Giannakis, S. Zhou, and B. Muquet, "Space-time coding for broadband wireless communications", *Wireless Communications and Mobile Computing*, vol. 1, no. 1, 35–53, 2001.

[Liu09] D. N. Liu and M. P. Fitz, "Iterative MAP equalization and decoding in wireless mobile coded OFDM", *IEEE Transactions on Communications*, vol. 57, no. 7, 2042–2051, 2009.

[Ma03] X. Ma, G. Giannakis, and S. Ohno, "Optimal training for block transmissions over doubly selective wireless fading channels", *IEEE Transactions on Signal Processing*, vol. 51, no. 5, 1351–66, 2003.

[Martínez10a] L. Martínez, J. Robert, H. Meuel, I. Sobrón, and M. Mendicute, "Improved Robustness for Channel Estimation without Pilots for DVB-T2", in *IEEE International Symposium on Broadband Multimedia Systems and Broadcasting (BMSB)*, 2010.

[Martínez10b] L. Martínez, I. Sobrón, P. Ochandiano, , M. Mendicute, and J. Altuna, "Estimación de canal para transmisión multiantena y recepción móvil en DVB-T2", in *Simposium Nacional de la Unión Científica Internacional de Radio (URSI)*, 2010.

[Martínez11] L. Martínez, P. Ochandiano, I. Sobrón, and M. Mendicute, "Novel pilot structures for BEM channel estimation and ICI compensation in high-mobility DVB", in *IEEE International Symposium on Broadband Multimedia Systems and Broadcasting (BMSB)*, 2011.

[Martínez12] L. Martínez, P. Ochandiano, I. Sobrón, and M. Mendicute, "Iterative BEM channel estimation and BP detection for ICI cancellation in DVB systems with very high mobility", 2012.

[Matz06] G. Matz and F. Hlawatsch, "Time-varying communication channels: fundamentals, recent developments, and open problems", in *Proc. European Signal Processing Conference (EUSIPCO)*, 2006.

[Mendicute10] M. Mendicute, I. Sobrón, L. Martínez, and P. Ochandiano, *DVB-T2: New signal processing algorithms for a challenging digital video broadcasting standard*, 2010.

[Mignone96] V. Mignone and A. Morello, "CD3-OFDM: a novel demodulation scheme for fixed and mobile receivers", *IEEE Transactions on Communications*, vol. 44, no. 9, 1144–51, 1996.

[Molisch07] A. Molisch, M. Toeltsch, and S. Vermani, "Iterative methods for cancellation of intercarrier interference in OFDM systems", *IEEE Transactions on Vehicular Technology*, vol. 56, no. 4, 2158–67, 2007.

[Muquet99] B. Muquet and M. de Courville, "Blind and semi-blind channel identification methods using second order statistics for OFDM systems", in *IEEE International Conference on Acoustics, Speech, and Signal Processing (ICASSP)*, vol. 5, pp. 2745–8, 1999.

[Muquet02] B. Muquet, M. de Courville, and P. Duhamel, "Subspace-based blind and semi-blind channel estimation for OFDM systems", *IEEE Transactions on Signal Processing*, vol. 50, no. 7, 1699–712, 2002.

[Necker04] M. Necker and G. Stuber, "Totally blind channel estimation for OFDM on fast varying mobile radio channels", *IEEE Transactions on Wireless Communications*, vol. 3, no. 5, 1514–25, 2004.

[Negi98] R. Negi and J. Cioffi, "Pilot tone selection for channel estimation in a mobile OFDM system", in *IEEE Transactions on Consumer Electronics*, vol. 44, pp. 1122–8, 1998.

[Nilsson97] R. Nilsson, O. Edfors, M. Sandell, and P. Borjesson, "An analysis of two-dimensional pilot-symbol assisted modulation for OFDM", in *IEEE International Conference on Personal Wireless Communications (ICPWC)*, pp. 71–4, 1997.

[Ochandiano10] P. Ochandiano, I. Sobrón, L. Martínez, M. Mendicute, and J. Altuna, "Analysis of ICI compensation for DVB-T2", in *Proc. of the 7th International Symposium on Wireless Communication Systems (ISWCS)*, pp. 427–30, 2010.

[Ochandiano11a] P. Ochandiano, H. Wymeersch, M. Mendicute, L. Martínez, and I. Sobrón, "Iterative ICI cancellation based on factor graphs for large FFT sizes", in *European Signal Processing Conference (EUSIPCO)*, 2011.

[Ochandiano11b] P. Ochandiano, H. Wymeersch, I. Sobron, L. Martinez, and M. Mendicute, "Novel ICI Suppressing Receiver for High-mobility DVB-T2 Reception with Large FFT Modes", in *IEEE International Symposium on Broadband Multimedia Systems and Broadcasting (BMSB)*, 2011.

[Ochandiano12] P. Ochandiano, L. Martínez, I. Sobrón, and M. Mendicute, "Iterative Detection and Channel Estimation for Mobile Terrestrial TV with

Long OFDM Blocks", *Submitted to IEEE Transactions on Broadcasting*, 2012.

[Ozbek05] B. Ozbek, D. L. Ruyet, and C. Panazio, "Pilot-symbol-aided iterative channel estimation for OFDM systems", in *European Signal Processing Conference (EUSIPCO)*, 2005.

[Peng06] F. Peng and W. Ryan, "A low-complexity soft demapper for OFDM fading channels with ICI", in *IEEE Wireless Communications and Networking Conference (WCNC)*, pp. 1549–54, 2006.

[Poggioni09] M. Poggioni, L. Rugini, and P. Banelli, "DVB-T/H and T-DMB: physical layer performance comparison in fast mobile channels", *IEEE Transactions on Broadcasting*, vol. 55, no. 4, 719–30, 2009.

[Proakis95] J. Proakis, *Digital Communications*, third edition edn., 1995.

[Pätzold02] M. Pätzold, *Mobile Fading Channels*, 2002.

[Rappaport96] T. S. Rappaport, *Wireless Communications*, 1996.

[Robertson99] P. Robertson and S. Kaiser, "The effects of Doppler spreads in OFDM(A) mobile radio systems", in *Vehicular Technology Conference (VTC)*, vol. 1, pp. 329–33, 1999.

[Rom07] C. Rom, C. Navarro Manchón, L. Deneire, T. Bundgaard Sørensen, and P. Mogensen, "Unification of Frequency Direction PACE Algorithms for OFDM", in *In Proceedings of Wireless Personal Multimedia Communications (WPMC)*, 2007.

[Rom08] C. Rom, *Physical Layer Parameter and Algorithm Study in a Downlink OFDM-LTE Context*, Ph.D. thesis, Department of Electronic Systems, Aalborg University, 2008.

[Rousseaux04] O. Rousseaux and G. Leus, "An iterative method for improved training-based estimation of doubly selective channels", vol. vol.4, pp. 889–92, 2004.

[Roy02] S. Roy and C. Li, "A subspace blind channel estimation method for OFDM systems without cyclic prefix", *IEEE Transactions on Wireless Communications*, vol. 1, no. 4, 572–9, 2002.

[Rugini05a] L. Rugini, P. Banelli, and G. Leus, "Block DFE and windowing for Doppler-affected OFDM systems", in *IEEE International Workshop on*

Signal Processing Advances in Wireless Communications (SPAWC), pp. 470–4, 2005.

[Rugini05b] L. Rugini, P. Banelli, and G. Leus, "Simple equalization of time-varying channels for OFDM", *IEEE Communications Letters*, vol. 9, no. 7, 619–21, 2005.

[Rugini06] L. Rugini, P. Banelli, and G. Leus, "Low-complexity banded equalizers for OFDM systems in Doppler spread channels", *EURASIP Journal on Applied Signal Processing*, , no. 19, 13, 2006.

[Russell95] M. Russell and G. Stuber, "Interchannel interference analysis of OFDM in a mobile environment", in *Vehicular Technology Conference (VTC)*, vol. 2, pp. 820–4, 1995.

[Sanzi03] F. Sanzi, S. Jelting, and J. Speidel, "A Comparative Study of Iterative Channel Estimators forMobile OFDMSystems", *IEEE Transactions on Wireless Communications*, vol. 2, no. 5, 2003.

[Schafhuber01] D. Schafhuber, G. Matz, and F. Hlawatsch, "Simulation of wideband mobile radio channels using subsampled ARMA models and multistage interpolation", pp. 571–4, 2001.

[Schniter04] P. Schniter, "Low-complexity equalization of OFDM in doubly selective channels", *IEEE Transactions on Signal Processing*, vol. 52, no. 4, 1002–11, 2004.

[Schniter06] P. Schniter, "On doubly dispersive channel estimation for pilot-aided pulse-shaped multi-carrier modulation", in *Conference on Information Sciences and Systems (CISS)*, pp. 1296–1301, 2006.

[Sklar01] B. Sklar, *Digital Communications Fundamentals and Applications (2 edition)*, Prentice Hall, 2001.

[Slock04] D. Slock, "Signal processing challenges for wireless communications", in *IEEE International Symposium on Control, Communications and Signal Processing (ISCCSP)*, pp. 881–92, 2004.

[Speth99] M. Speth, S. Fechtel, G. Fock, and H. Meyr, "Optimum receiver design for wireless broad-band systems using OFDM. I", *IEEE Transactions on Communications*, vol. 47, no. 11, 1668–77, 1999.

[Stamoulis02] A. Stamoulis, S. N. Diggavi, and N. Al-Dhahir, "Inter-Carrier Interference in MIMO OFDM", *IEEE Transactions on Signal Processing*, vol. 50, no. 10, 2002.

[Tang07a] Z. Tang, R. Cannizzaro, G. Leus, and P. Banelli, "Pilot-assisted time-varying channel estimation for OFDM systems", *IEEE Transactions on Signal Processing*, vol. 55, no. 5, 2226–38, 2007.

[Tang07b] Z. Tang and G. Leus, "Pilot schemes for time-varying channel estimation in OFDM systems", in *IEEE Workshop on Signal Processing Advances in Wireless Communications (SPAWC)*, 2007.

[Tarokh98] V. Tarokh, N. Seshadri, and A. Calderbank, "Space-time codes for high data rate wireless communication: performance criterion and code construction", *IEEE Transactions on Information Theory*, vol. 44, no. 2, 744–65, 1998.

[Tarokh99] V. Tarokh, H. Jafarkhani, and A. Calderbank, "Space-time block codes from orthogonal designs", *IEEE Transactions on Information Theory*, vol. 45, no. 5, 1456–67, 1999.

[Tomasin05] S. Tomasin, A. Gorokhov, H. Yang, and J.-P. Linnartz, "Iterative interference cancellation and channel estimation for mobile OFDM", *IEEE Transactions on Wireless Communications*, vol. 4, no. 1, 238–45, 2005.

[Tong94] L. Tong, G. Xu, and T. Kailath, "Blind identification and equalization based on second-order statistics: a time domain approach", *IEEE Transactions on Information Theory*, vol. 40, no. 2, 340–9, 1994.

[Tong04] L. Tong, B. Sadler, and M. Dong, "Pilot-assisted wireless transmissions: general model, design criteria, and signal processing", *IEEE Signal Processing Magazine*, vol. 21, no. 6, 12–25, 2004.

[Tsatsanis96a] M. Tsatsanis and G. Giannakis, "Equalization of rapidly fading channels: self-recovering methods", *IEEE Transactions on Communications*, vol. 44, no. 5, 619–30, 1996.

[Tsatsanis96b] M. Tsatsanis and G. Giannakis, "Modelling and equalization of rapidly fading channels", *International Journal of Adaptive Control and Signal Processing*, vol. 10, no. 2-3, 159–76, 1996.

[Tuchler02] M. Tuchler, R. Koetter, and A. Singer, "Turbo equalization: principles and new results", *IEEE Transactions on Communications*, vol. 50, no. 5, 754–67, 2002.

[Tugnait02] J. Tugnait and W. Luo, "Linear prediction error method for blind identification of periodically time-varying channels", *IEEE Transactions on Signal Processing*, vol. 50, no. 12, 3070–82, 2002.

[Tureli98] U. Tureli and H. Liu, "Blind carrier synchronization and channel identification for OFDM communications", in *International Conference on Telecommunications (ICT)*, vol. 1, pp. 372–6, 1998.

[Turin01] W. Turin, R. Jana, C. Martin, and J. Winters, "Modeling wireless channel fading", vol. 3, pp. 1740–4, 2001.

[vandeBeek95] J.-J. van de Beek, O. Edfors, M. Sandell, S. Wilson, and P. Borjesson, "On channel estimation in OFDM systems", in *IEEE Vehicular Technology Conference (VTC)*, vol. 2, pp. 815–19, 1995.

[Vucetic03] B. Vucetic and J. Yuan, *Space-time coding*, 2003.

[Wilhelmsson07] L. Wilhelmsson, J. Svensson, A. Nevalainen, and M. Faulkner, "Some results on implementing low-complex ICI cancellation for DVB-H", in *Vehicular Technology Conference (VTC)*, pp. 2931–5, 2007.

[Wilson94] S. Wilson, R. Khayata, and J. Cioffi, "16 QAM modulation with orthogonal frequency division multiplexing in a Rayleigh-fading environment", in *IEEE Vehicular Technology Conference (VTC)*, vol. 3, pp. 1660–4, 1994.

[Wolniansky98] P. Wolniansky, G. Foschini, G. Golden, and R. Valenzuela, "V-BLAST: an architecture for realizing very high data rates over the rich-scattering wireless channel", in *International Symposium on Signals, Systems, and Electronics (ISSSE)*, pp. 295–300, 1998.

[Xiao06] C. Xiao, Y. Zheng, and N. Beaulieu, "Novel sum-of-sinusoids simulation models for Rayleigh and Rician fading channels", *IEEE Transactions on Wireless Communications*, vol. 5, no. 12, 3667–79, 2006.

[Yang01] B. Yang, K. Letaief, R. Cheng, and Z. Cao, "Channel estimation for OFDM transmission in multipath fading channels based on parametric channel modeling", *IEEE Transactions on Communications*, vol. 49, no. 3, 467–79, 2001.

[Zemen03a] T. Zemen and C. Mecklenbrauker, "Time-variant channel equalization via discrete prolate spheroidal sequences", in *Asilomar Conference on Signals, Systems and Computers (ACSSC)*, vol. 2, pp. 1288–92, 2003.

[Zemen03b] T. Zemen, C. F. Mecklenbräuker, and R. R. Müller, "Time Variant Channel Equaliztion for MC-CDMA via Fourier Basis Functions", in *International Workshop on Multi-Carrier Spread Spectrum (MC-SS)*, 2003.

[Zemen05] T. Zemen and C. Mecklenbrauker, "Time-variant channel estimation using discrete prolate spheroidal sequences", *IEEE Transactions on Signal Processing*, vol. 53, no. 9, 3597–607, 2005.

[Zheng93] F.-C. Zheng, S. McLaughlin, and B. Mulgrew, "Blind equalization of nonminimum phase channels: higher order cumulant based algorithm", *IEEE Transactions on Signal Processing*, vol. 41, no. 2, 681–91, 1993.

[Zheng03] Y. R. Zheng and C. Xiao, "Simulation models with correct statistical properties for Rayleigh fading channels", *IEEE Transactions on Communications*, vol. 51, no. 6, 920–8, 2003.